Mucins regulate virulence and colonization factors in *Streptococcus pneumoniae*

by

Jade Rose Bath

A.B. Biology
Bryn Mawr College, 2016

Submitted to the Microbiology Graduate Program
in partial fulfillment of the requirements for the degree of
Doctor of Philosophy

at the

Massachusetts Institute of Technology

May 2024

Signature of Author.....
Jade R. Bath
Microbiology Graduate Program
April 2, 2024

Certified by.....
Katharina Ribbeck
Thesis Supervisor
Professor of Biological Engineering

Accepted by.....
Jacquin C. Niles
Professor of Biological Engineering
Co-Director of the Microbiology Graduate Program

Mucin glycans regulate virulence and colonization factors in *Streptococcus pneumoniae*

by

Jade Rose Bath

Submitted to the Microbiology Graduate Program in partial fulfillment of the requirements for the degree of Doctor of Philosophy at the Massachusetts Institute of Technology

Abstract

Mucus covers all wet epithelia in the human body, creating a protective barrier for the underlying cell layer, and accommodating trillions of microbes that make up the microbiota. Mucin glycoproteins, the main gel-forming component of mucus, have emerged as multifaceted regulators of microbial physiology and microbial communities. Defects in mucus production or changes in mucin glycosylation are associated with microbial dysbiosis, where the outgrowth of opportunistic pathogens threatens human health. *Streptococcus pneumoniae* is a ubiquitous opportunistic pathogen, able to both asymptomatically colonize the microbiota of healthy children and adults and to cause invasive diseases. The mechanisms by which the body tolerates the presence of *S. pneumoniae* as part of the microbiota remain largely unknown. In this thesis, I fill this gap by exploring how *S. pneumoniae* senses and responds to the mucin environment. First, I identify that mucins downregulate a key virulence factor of *S. pneumoniae*, the cytolytic toxin pneumolysin (PLY). I show that through the regulation of PLY, mucin protects host cells from toxin-mediated killing and modulates inflammatory signals. Second, I identify that mucins downregulate colonization factors in *S. pneumoniae*, modulating microbe-microbe interactions between nasopharyngeal bacteria. Together, these results uncover novel mechanisms for how mucin tames opportunistic pathogens and provides insight for the development of novel therapeutics to treat *S. pneumoniae* infection.

Thesis supervisor: Katharina Ribbeck
Title: Professor of Biological Engineering

Acknowledgements

First and foremost, I would like to thank my thesis advisor Katharina Ribbeck. Thank you for sharing your enthusiasm for mucins and microbes, for your scientific mentorship, and for pushing me to do the best science possible. Your support has helped me grow into a more thoughtful and independent scientist, and I will use these skills in my future endeavors.

Thank you to my committee members, Jacquin Niles and Becky Lamason, for sharing your scientific contributions and advice over the course of my PhD. Thank you to my external committee member Richard Malley for sharing your expertise on pneumolysin and *S. pneumoniae* infection.

Thank you to my external collaborators, Elisabet Bjanes, Victor Nizet, Cengiz Gökeri, Geraldine Nouailles, Lindsey Burcham, and Kelly Doran. We worked with Elisabet and Victor on *in vivo* models of *S. pneumoniae* infection. Cengiz and Geraldines's technical expertise and general advice on neutrophil biology were hugely helpful. Lindsey's advice on working with *S. pneumoniae* was invaluable. Kelly encouraged me to present at the 2022 Streptococcal Gordon Conference which was a highlight of my PhD.

Thank you to past and present members of the Ribbeck lab. I am thankful to have done my PhD with a group that was so open and actively engaged in each other's research questions. Thank you to Gerardo Cárcamo-Oyarce, a master microbiologist, and Bradley Turner, an expert on mucus biology. Thank you to past lab members for the advice and many insightful discussions: Liubov Yakovlieva, Caroline Werlang, Chloe Wu, Michaela Gold, Alexa Gomberg, Abigail McShane, Nicole Bustos, Julie Takagi, and Ben Wang. A special thanks to Jeff Hsiao who was a wonderful resource on neutrophil biology and support during graduate school. Thank you to current lab members, Kerry Forristall, George Degen, Kelsey Wheeler, Daniel Sellers, Mei Yi You, Joseph Romeo, Deniz Uzun, Reuben Allen, and Sofia Vargas, for continuing to make the lab a great environment. I am excited to see where your mucus projects take you!

I am grateful for my fantastic scientific mentors throughout my life. Thank you to Aline Garcia-Rubio, Dan Griffith, Tamara Davis, and Joshua Shapiro who were inspiring biology teachers and professors throughout high school and college. Thank you to David Fidock for allowing me to join his lab at Columbia University Medical Center as a research technician and providing a supportive research environment. A special thanks to Fidock lab alumni Barbara Stokes and Kelly Rubiano. I am so thankful for your research mentorship and continued friendship throughout graduate school.

Thank you to the MIT community, especially the Microbiology program. Thank you to the 2018 Microbiology Cohort: Veda, Irene, Mandy, and Annika. I am so thankful for your friendship and support throughout graduate school—I especially enjoyed our time at the Muddy Charles.

Thank you to my friends both new and old. I always have something to look forward to!

Thank you to my family: to my parents, David and Ruth, my sister Jasmine, and her partner Michael, for their love, unwavering support, and encouragement. They talked me through so many challenges of my PhD journey.

Finally, thank you to my partner Andy Nelson. You make every day better and I could not have done this without your love and support!

Table of Contents

List of Figures

Chapter 1: Introduction

Sections of the text and figures presented in this chapter were adapted from:
McShane A*, Bath J*, Jaramillo AM*, Ridley C*, Walsh AA, Evans CM, Thornton DJ and Ribbeck K. Mucus. *Current Biology*. 31:15 (2021): R938-R945.
https://doi.org/10.1016/j.cub.2021.06.093
*these authors contributed equally to this work

Biochemistry and structure of the mucus barrier

Mucus is a complex hydrogel that forms a physical barrier and lines all non-keratinized epithelial surfaces that are exposed to the outside environment. These surfaces include the respiratory tract, the gastrointestinal tract, the reproductive tract, and the ocular cavity (Fig. 1.1a) (Wagner et al., 2018a). As a barrier, mucus performs many essential functions; mucus hydrates and lubricates surfaces, protecting cells from physical stress (Wagner et al., 2018a). As a selective barrier, mucus allows the passage of nutrients and gases while clearing pathogens and debris (Witten et al., 2018). Mucus also serves as the major ecological niche for the microbiota, accommodating trillions of microbes that form dynamic communities throughout the body (B. X. Wang, Wu, et al., 2021).

Mucus is mainly composed of water (90-95%), however other components such as salts (1%), lipids (1-2%), mucins (1-5%) and other proteins contribute to the structure and function of mucus (Bansil & Turner, 2018). Salts regulate the pH, hydration, and rheology of mucus (Allen & Flemström, 2005; Ambort et al., 2012; Cao et al., 1999; Snary et al., 1971; Verdugo, 2012), while lipids prevent evaporation and contribute to lubricating properties among other roles (Johnson & Murphy, 2004; Sarosiek et al., 1984). Many of the smaller proteins present in mucus such as defensins, enzymes, and immunoglobulins (including IgA and IgM), play important roles in the protective function of mucus by targeting invading microbes (Macpherson et al., 2001; Royle et al., 2003). The mucus composition varies by mucosal niche, reflecting the different functions of mucus throughout the body. For example, the mucus in the ocular cavity that enables blinking is much thinner than mucus in the gastrointestinal tract that protects the stomach lining from gastric acid (Bansil & Turner, 2018).

Mucins are large, heavily glycosylated proteins that are responsible for the viscoelastic

properties of the mucus gel. The MUC gene family encodes 21 different mucin-type glycoproteins in humans and are produced by specialized cells such as mucous and goblet cells depending on the mucin and tissue type. Within the MUC gene family, there are two subgroups: secreted mucins and tethered membrane-bound mucins. Each mucin varies by length and amino acid sequence but shares key structural features.

Within the secreted mucins, there are five oligomeric, gel-forming mucins (MUC2, MUC5AC, MUC5B, MUC6 and MUC19), as well as two non-oligomeric glycoproteins (MUC7 and MUC8) (Hattrup & Gendler, 2008; Thornton et al., 2008a). Mucins are differentially expressed depending on the tissue leading to heterogenous mucus gels throughout the body (Figure 1.1a). The protein backbone of all mucins includes regions that contain a variable number of tandem repeats (VNTR) that are rich in proline, threonine, and serine residues (PTS domains) (Figure 1.1b). PTS domains are densely modified with *O*-linked glycans that extend from the protein backbone giving mucins an elongated bottlebrush-like structure (Hattrup & Gendler, 2008; Thornton et al., 2008a). Secreted mucins also contain cysteine-rich regions interspersed between PTS domains, and at the amino- and carboxy-terminals. The cysteine rich regions create linear and branched polymers via end-to-end intermolecular disulfide bonds. The length, placement, and number of cysteine-rich segments between PTS domains differs between mucins (Thornton et al., 2008a). Together, the water binding capacity of mucin glycans and the mucin polymer structure enable mucins to entangle and form hydrogels (Thornton et al., 2008a).

The 11 membrane-bound mucins (MUC1, MUC3A, MUC3B, MUC4, MUC 12, MUC13, MUC15, MUC16, MUC17, MUC20, and MUC21) are typically monomeric and have short cytoplasmic tail domains that remain inside of the cell, as well as extensive extracellular domains that contain the VNTR and associated *O*-glycosylated PTS domains (Hattrup & Gendler, 2008). Membrane-bound mucins are a major component of the glycocalyx on the cell surface and serve important roles in cell signaling and preventing adhesion of invading particles (Rahn et al., 2004; Wesseling et al., 1995). The three remaining mucins include oviductal glycoprotein 1 (OVGP1), endomucin (EMCN), and MUC22.

In this thesis, I will focus on secreted mucins that form the mucosal niches that house the microbiota and comprise approximately 90% of mucin in the lung (Hattrup & Gendler, 2008; B. X. Wang, Wu, et al., 2021). Specifically, I will focus on the most abundant secreted gel-forming mucins MUC2, MUC5B, and MUC5AC that are located in the oral, respiratory, and gastro-

intestinal tracts. Secreted mucins present in these niches can be purified from human saliva and porcine sources that serve as models for human mucins (Turner et al., 1995, 1999). The mucus barrier in these regions provides a first line of defense against invading pathogens, while accommodating dynamic microbial communities that are critical for human health.

Mucin glycosylation

The *O*-glycans grafted on the mucin protein backbone are incredibly diverse; individual mucins can display >80 unique glycan structures that encode a wealth of biochemical information (Jin et al., 2017; Takagi et al., 2022). In fact, the glycan content of mucins accounts for approximately 80% of the mass of a mucin molecule. While the vast majority of mucin glycans are *O*-linked in the PTS domain, the Cys-rich domains also contain mannose-rich *N*-linked and *C*-linked glycans (Bansil & Turner, 2018).

O-glycan chains are built in a stepwise process where various glycosyltransferases coordinate their initiation, extension, and termination (Fig. 1.2). Initiation of the glycan chains occurs via the addition of N-acetylgalactosamine (GalNAc) to the hydroxyl group of serine or threonine residues by polypeptide GalNAc (ppGalNAc) transferases. Initiation forms the Tn antigen and is accomplished by a family of up to 20 homologous ppGalNAc transferases (Bennett et al., 2012; Brockhausen et al., 2022). After initiation, glycan chains are extended via the addition of galactose and N-acetylglucosamine (GlcNAc) residues to form one of eight common core structures designated Core 1-8. Cores 1-4 are most prevalent in mucins (Takagi et al., 2022), while Cores 5-8 occur less frequently and in restricted conditions. Glycans may be further extended by 30 additional glycosyltransferases to create linear and branched structures via the addition of additional sugars, or terminated with fucose, sialic acid and sulfate groups (Bennett et al., 2012). The negative charge of sialic acid and sulfate groups present in mucin glycans give the mucin polymer an overall negative charge. Common glycan structural motifs include ABO blood group antigens, Lewis antigens, sialyl Lewis antigens and poly-N-acetyl-lactosamine (LacNAc) repeats that make up longer chains (Corfield, 2015). The different monomers and linkages quickly build up combinatorial complexity to yield the diversity observed in mucin glycans.

The specific glycan structures that are formed depend on the expression patterns of glycosyltransfereases specific to the cell or tissue type. There is a high degree of functional

redundancy among glycotransferases and the process of building glycans is stochastic such that glycan content is dependent on glycosidase expression (Bennett et al., 2012; Yang et al., 1994). Thus, it is possible for the same mucin peptide to display different glycan structures when expressed in different tissues or at different times. For example, the glycosylation of cervical mucins change with the menstrual cycle as the specific combination and levels of glycosyltransferases are hormonally regulated (Andersch-Björkman et al., 2007; Argüeso, Spurr-Michaud, et al., 2002). In addition, changes in glycosidase expression and subsequent changes to mucin glycans are linked to cancer (Yang et al., 1994).

Beyond glycan identity, which sites are glycosylated can vary between individual mucin molecules, and there is a lack of understanding the potential contribution of the protein sequence. In addition, because mucin molecules can have the same mass, it has been difficult to resolve the structure and location of glycosylation. Recent studies have leveraged direct spatial imaging of individual glycoconjugate molecules to understand the structure of MUC1 fragments by combining soft-landing electrospray ion beam deposition with scanning tunneling microscopy (Anggara et al., 2023). The observed *O*-glycans were consistent with glycoprofiling analysis and revealed *O*-glycosylation patterns that depend on the underlying protein sequence. Extending this technology to other mucin isoforms may reveal differences in the *O*-glycosylation patterns and density of glycans. The tremendous structural heterogeneity of mucin glycans and complex regulation suggests that these complex sugars may play multifunctional roles in biological processes.

Mucus in health and disease

The mucus layer has multiple essential functions in human health. Mucus lubricates and hydrates the underlying epithelia, allows the passage of nutrients and gasses, accommodates trillions of microbes that comprise the microbiota, and traps invading pathogens and particles for mucociliary clearance.

Alterations in mucus production or mucin glycosylation leads to changes in the mucus barrier and associated pathologies (Fig. 1.3). Mucin expression is often differentially regulated in response to infection. For example, lung epithelial cells upregulated MUC2 and MUC5AC in response to a panel of Gram-negative and Gram-positive opportunistic pathogens including

Pseudomonas aeruginosa, Escherichia coli, *Staphylococcus aureus*, *Staphylococcus epidermidis* and *Streptococcus pyogenes* (Dohrman et al., 1998). In fact, lipopolysaccharides (LPS) alone, a surface component of Gram-negative bacteria, upregulates the expression and secretion of mucins in epithelial cells (Smirnova et al., 2003). The upregulation of mucins in response to infection may represent a defensive host response, thus changes to mucus regulation may weaken the response to infection.

In the healthy lung, mucus functions to maintain a relatively sterile environment by binding, trapping, and removing the vast majority of inhaled bacteria, viruses, and particles through mucociliary clearance (Fahy & Dickey, 2010; Knowles & Boucher, 2002). In cystic fibrosis (CF) and chronic obstructive pulmonary disease (COPD), mucus hypersecretion leads to decreased mucus permeability, impaired mucociliary clearance, and increased risk of opportunistic infection (Fig. 1.3a) (Fahy & Dickey, 2010; Henke et al., 2004; Innes et al., 2006). However, a lack of mucus production can also lead to infection. In a murine model, MUC5B is required for airway defense to maintain health. Deletion of *Muc5B*$^{-/-}$ led to chronic inflammation and bacterial infection of the mouse lung (Roy et al., 2014).

In the gut, mucus functions to separate the microbiota from the underlying epithelia, enabling the important digestive functions of the microbiome while reducing the potential for inflammation (Johansson et al., 2013; Johansson et al., 2008). Decreased mucus production and altered glycosylation leads to increased mucus permeability in inflammatory bowel diseases such as ulcerative colitis and Crohn's disease, and is associated with changes in microbiome composition and inflammation (Fig. 1.3b) (Corfield et al., 1996; M. E. V. Johansson et al., 2014; Larsson et al., 2011; Michail et al., 2012). Deletion of *Muc2* in a murine model leads to spontaneous development of colitis, colorectal cancer, and increased loads of bacteria in the colon, highlighting the protective roles of MUC2 (Van der Sluis et al., 2006; Wenzel et al., 2014).

In the oral cavity, mucins are important components of saliva and are responsible for lubricating and hydrating the oral mucosa. For example, patients with the autoimmune disease Sjögren's syndrome (SS) experience persistent dry mouth and dry eyes due to the impairment of salivary and lachrymal glands (Castro et al., 2013). In SS, the expression of MU5AC in tears is reduced, and the glyocosylation of MUC7 in saliva is altered, potentially contributing to the dryness (Fig. 1.3c) (Argüeso, Balaram, et al., 2002; Chaudhury et al., 2015, 2016). Changes to mucus secretion and mucin glycan content lead to dental caries, oral candidiasis, and changes to

the microbiome in multiple niches (De Paiva et al., 2016; Macfarlane & Mason, 1974). Thus, a common characteristic of mucus barrier disruption across niches is dysbiosis, or an altered microbiome, suggesting mucus plays an active role in supporting a healthy microbiome.

Mechanisms of mucin-microbe interactions

The interaction between mucins and the microbes embedded within mucus is complex. Each domain of the mucin molecule plays a role in forming the mucus barrier. Similarly, different properties of mucin are important for its interaction with microbes. Specifically, mucins create a three-dimensional selective barrier, provide a complex nutrient source, and display a wealth of biochemical signals (Fig. 1.4a-c).

Mucus is a selectively permeable 3D barrier that spatially organizes microbes

Mucins crosslink to form the mucus gel, enabling mucus to regulate the diffusion of microbes, particulates, and small molecules (Fig. 1.4a) (Witten et al., 2018). The heterogenous polymer network is formed through reversible, hydrophobic interactions, and disulfide bonds between mucin molecules, creating a mesh size ranging from 10-2000 nm depending on the niche (Lai et al., 2010; Wagner et al., 2018b; Witten et al., 2018). Large particles, such as eukaryotic microbes, are filtered based on size by the cross-linked mucus mesh. The passage of molecules smaller than the pore size, including many bacteria, is carefully controlled through physical binding interactions with charged and hydrophobic residues on mucin polymers (Lieleg et al., 2010).

Because many bacteria are smaller than the mucus mesh size, they may be able to diffuse through the mucus layer. However, secreted mucins display glycans that mimic those found on epithelial cell surfaces and are receptors for bacterial adhesins. Mucin glycans thus allow the polymer to act as a decoy molecule, binding invading microbes, leading to trapping and removal by mucociliary clearance. In some cases, membrane bound mucins act as a releasable decoy molecule whereby the extracellular glycosylated portion is cleaved. For example, *Helicobacter pylori* expresses two adhesins BabA and SabA that bind to the Lewis B and sialyl-Lewis X and A motifs on MUC5AC. Pretreatment of *H. pylori* with mucins protected gastric cells from bacterial killing (S. Lindén et al., 2002; S. K. Lindén et al., 2009; Skoog et al., 2012). In the gut, sialic acid

residues on mucins bind *Salmonella typhimurium* via the adhesin *SiiE* to protect host cells from infection (Bala Vimal et al., 2000; X. Li et al., 2019; McGuckin et al., 2023). Mucin glycans, especially sialylated glycans, can also bind viruses including influenza viruses, rotaviruses, and coronaviruses, preventing host cell infection (Cohen et al., 2013; Delaveris et al., 2020; Wardzala et al., 2022; Willoughby, 1993).

Mucins are also able to agglutinate microbes, enabling their clearance and preventing invasion. Salivary mucins agglutinate oral bacteria including multiple *Streptococcus* species to enable clearance through swallowing and salivary flow (Murray et al., 1992; Slomiany et al., 1996). Agglutination of oral commensal *Streptococcus gordonii* after incubation with human saliva extended the benefit of agglutination; increasing cell aggregate size also enhanced clearance through phagocytosis and bacterial killing by granulocytes (Itzek et al., 2017). MUC5B agglutinates vaginal opportunistic pathogen Group B *Streptococccus* (GBS; *Streptococcus agalactiae*), preventing ascension from the vaginal canal to the uterus in a murine model of infection (Burcham et al., 2022).

The 3D mucin matrix also spatially organizes microbial communities through binding interactions and the regulation of pore size. Creating a microscale spatial structure potentially balances the competition and positive interactions between microbes, stabilizing the community (Kim et al., 2008). While this has not been empirically proved in mucin, the microbial communities that colonize mucus throughout the body are biogeographically distinct (Lu et al., 2014; Mark Welch et al., 2016). Many of the community behaviors of microbes that impact community assembly and stability depend on the diffusion of small molecules such as nutrients and quorum sensing signals (Donaldson et al., 2015; Horswill et al., 2007). Due to the variety of binding and interaction possibilities, estimating the diffusion of a particle through a mucin network is difficult. Thus, while many binding interactions between microbes and the mucin barrier have been characterized, the impact of 3D mucin scaffolding on a community level remains an open question.

Mucins provide a nutrient source for metabolically diverse microbial communities

Mucin glycans serve as a nutrient source for the microbiota and may promote a stable and diverse microbiome by selecting for specific community members (Fig. 1.4b). The glycosidic linkages of mucin glycans are complex and require specific enzymes to break down and release

smaller subunits to be used as a microbial carbon source (Wardman et al., 2022). For example, *Bifidobacterium* spp. colonize the gastrointestinal (GI) tract microbiome of breast-fed infants and encode glycans to utilize human milk oligosaccharides (HMOs) that are prevalent in breast milk. *Lactobacillus* spp. metabolize broken down HMOs, synergizing with *Bifidobacterium* spp. (Koropatkin et al., 2012). In adults, the GI tract is commonly colonized by multiple mucin-degrading bacteria such as *Bacteroides* spp., *Bifidobacterium* spp., *Ruminococcus* spp., and *Akkermansia muciniphila* (Derrien et al., 2004; Martens et al., 2011; Roberton & Stanley, 1982; Ruas-Madiedo et al., 2008; Salyers et al., 1977; Wardman et al., 2022). Each organism encodes a subset of enzymes required for breaking down the variety of mucin glycans available in the gut, suggesting a high degree of cooperation between community members (Koropatkin et al., 2012). In the gut, opportunistic pathogens often do not encode mucin degrading tools (Pruss et al., 2021). Rather, mucin glycans seem to support the establishment of commensal bacteria in the gut that prevent pathogen growth by competitive exclusion through cross-feeding networks (Bergstrom & Xia, 2013; Pruss et al., 2021; Wardman et al., 2022). A healthy gut microbiome is critical to human digestion and nutrition as our microbiome generates nutrients from substrates that are unavailable to the host.

While less dense than the gut microbiome, mucus of the oral and respiratory niches also hosts a diverse microbiome where mucin represents a key carbon source. For example, microbial communities isolated from dental plaque and saliva were able to utilize mucin as a carbon source (Bradshaw et al., 1994; Wickstörm et al., 2009; Wu et al., 2023). In *ex vivo* salivary communities, the addition of mucin glycans enhanced community diversity by supporting a wide range of metabolic capabilities compared to glucose alone (Wu et al., 2023). In the respiratory tract, the lack of dietary sugars points to mucin and other host factors as an important nutrient source; however, the microbiome of the healthy respiratory tract is less well characterized than in other niches. In one study, multiple types of mucin degrading bacteria including *Streptococcus* spp., *Fusobacterium* spp., and *Prevotella* spp. were identified in the sinus mucus of healthy patients, although the prevalence of these species also increased in patients with chronic rhinosinusitis (Lucas et al., 2021). Mucin-degrading bacteria present in the sputum of CF patients potentiate the growth of opportunistic pathogen *P. aeruginosa*, but the role of mucin-degrading bacteria in healthy sputum was not characterized (Flynn et al., 2016). Thus, while mucin bolsters healthy communities as a nutritive substrate in the gut, this may not hold true in the oral niche. Mucin

modulates microbial communities through multiple mechanisms, and it follows that the function of mucus may differ between niches.

Mucins act as a signaling molecule to reduce virulence behaviors of opportunistic pathogens

The models of mucus as a physical barrier and nutrient source are well established, but recent work has shown that mucin can directly regulate microbial physiology through signaling (Fig. 1.4c). Microbes have evolved complex methods to sense and respond to their environment. For example, *Bacillus subtilis* and other Gram-positive bacteria employ a carbon catabolite repressor (CCR) system via CcpA to transcriptionally regulate the expression of genes involved in carbohydrate utilization depending on nutrient availability (Shelburne et al., 2008). Bacteria also encode quorum sensing systems that produce autoinducer molecules and primarily sense cell density but can also respond to pH and antibiotic stress (Moreno-Gámez et al., 2017). Lastly, bacteria sense and respond to a variety of signals through two component systems (TCS); highly conserved systems that are comprised of a membrane-bound histidine kinase and a corresponding response regulator that directs transcriptional changes (Capra & Laub, 2012; Gómez-Mejia et al., 2018). These highly conserved systems are examples of the many strategies bacteria employ to sense and respond to their environment.

Mucin is a major component of the mucosal environments colonized by our microbiome. Recent work has shown native mucin can attenuate virulence-associated traits of cross-kingdom opportunistic pathogens including *Candida albicans* (Kavanaugh et al., 2014; Takagi et al., 2022), *Pseudomonas aeruginosa* (Co et al., 2018; B. X. Wang, Wheeler, et al., 2021; Wheeler et al., 2019), *Vibrio cholerae* (B. X. Wang et al., 2023), *Streptococcus agalactiae* (Burcham et al., 2022) and *Streptococcus mutans* (Frenkel & Ribbeck, 2015; C. A. Werlang et al., 2021). There are several common signatures of mucin-regulation of virulence including the disruption of biofilms, host-microbe toxicity, and microbe-microbe interactions.

Biofilms are a community behavior of microbes and are characterized by aggregation or attachment to a surface, the production of an extracellular matrix, and a microbial population that is metabolically inactive (Lichtenberg et al., 2023; Sauer et al., 2022; Stewart & Franklin, 2008; Tolker-Nielsen, 2015). These features complicate antibiotic penetration and activity and make opportunistic biofilm infections particularly difficult to treat (C. W. Hall & Mah, 2017). Mucins

prevent biofilm formation in *C. albicans*, *P. aeruginosa*, and *S. mutans* by retaining cells in the planktonic state without impacting overall growth (Co et al., 2018; Frenkel & Ribbeck, 2015; Kavanaugh et al., 2014; Takagi et al., 2022; C. A. Werlang et al., 2021; Wheeler et al., 2019). In the case of *P. aeruginosa*, mucins even disassemble mature biofilms through a motility-dependent mechanism (Co et al., 2018). While the pathway involved in each case is distinct, mucin has evolved the capacity to reduce biofilm formation across multiple opportunistic pathogens.

Mucins downregulate the virulence of multiple opportunistic pathogens against the host both *in vitro* and *in vivo*. Mucins reduce the virulence of *P. aeruginosa* against HT-29 host intestinal epithelial cells in a dose-dependent manner *in vitro* (Wheeler et al., 2019) and reduce the virulence of both *P. aeruginosa* and *C. albicans* in *in vivo* wound models (Takagi et al., 2022; Wheeler et al., 2019). While the virulence factors responsible for cytotoxicity or infection are specific to each microbe, in each case, mucins reduce the damage to the host.

Mucins also reduce microbe-microbe competition in multiple opportunistic pathogens, suggesting an important role in regulating microbial communities. In *S. mutans*, mucins reduce the expression of bacteriocins that mediate microbe-microbe interactions, and mucins have been shown to mediate co-culture dynamics with commensal oral microbes (Frenkel & Ribbeck, 2017; C. A. Werlang et al., 2021). In other co-culture models, mucins similarly enhanced microbial co-existence of *C. albicans* and *P. aeruginosa* through multiple mechanisms (Takagi et al., 2022; Wang, Wheeler, et al., 2021). In an *ex vivo* oral community model, mucin and mucin glycans regulated microbial diversity through mechanisms not fully explained by nutritive contributions of glycans (Wu et al., 2023). Thus, mucins broadly regulate microbial dynamics in multiple dual species models and more complex *ex vivo* microbial communities, preventing the outgrowth of opportunistic pathogens. These findings highlight the potential of mucin as a therapeutic agent inspired by host defenses that reduce virulence without selecting for resistance in opportunistic pathogens.

Mucin glycans mediate many microbe-mucin signaling interactions

Recent work has demonstrated that in many cases, mucin glycans are sufficient for signaling. Mucin glycans can be chemically cleaved from the protein backbone via non-reductive, alkaline β-elimination (Y. Huang et al., 2001). This method leaves the reducing end of the glycan

intact and preserves the heterogeneity of the glycan structures, yielding a pool of mucin glycans that can be used for downstream analyses. Mass spectrometry identified >80 glycans released from MUC5AC, MUC5B and MUC2 isolated from human and porcine sources (Takagi et al., 2022; C. A. Werlang et al., 2021; Wheeler et al., 2019). These studies revealed similarities and differences between glycans displayed on different mucin isoforms. While many glycans were displayed on all three isoforms, the glycan pools differ in the relative abundances of core structures, glycan length, sialylation and fucosylation. Mucin glycan pools are sufficient for gene regulation in *P. aeruginosa*, *C. albicans*, *S. mutans*, and *V. cholerae*, and treatment with isolated glycans recapitulates many of the phenotypes observed with whole mucin (Takagi et al., 2022; B. X. Wang et al., 2023; C. A. Werlang et al., 2021; Wheeler et al., 2019). In many cases, the monosaccharides that make up mucin glycans were not sufficient for regulation, suggesting the complex structures of mucin glycans are important for activity.

While it is desirable to identify specific active mucin glycans, fractionating and recovering unlabeled glycans at preparatory scales is difficult (Z. Li & Chai, 2019). Recent studies have synthesized the most abundant mucin glycans *de novo* to address this challenge (Minzer & Hevey, 2023; Takagi et al., 2022; B. X. Wang et al., 2023). In both *C. albicans*, and *V. cholerae*, defined core mucin glycans with simple modifications of fucose, galactose, and sialic acid are sufficient to regulate gene expression (Takagi et al., 2022; B. X. Wang et al., 2023). In *C. albicans*, structures based on core 1 and core 2 had similar activity as the full mucin glycan pool (Takagi et al., 2022). Interestingly, in *V. cholerae*, core 2 glycans were much more effective than core 1 glycans at regulating gene expression (B. X. Wang et al., 2023). However, some microbes, such as *P. aeruginosa*, require more complex glycans for signaling effects and did not respond to simple core structures (B. X. Wang, Wheeler, et al., 2021).

Carbohydrate binding domains can be quite specific; lectins display preferences for specific *O*-glycan core structures even if the extended glycan motif is the same. In addition, many lectins and carbohydrate binding domains require multivalent binding or synergistic effects between distinct glycan structures (S. Wang et al., 2021). Continued efforts in *O*-glycan synthesis or mucin mimetic engineering will likely illuminate the effects of mucin that are not mediated by mucin glycan pools or individual core glycans. In addition, while mucin-microbe interactions have been explored in-depth in a handful of opportunistic pathogens, they represent only a subset of the trillions of microbes that make up our microbiota. Continued understanding of mucin-microbe

interactions will open new therapeutic strategies for treatment of infectious diseases and pathologies associated with dysbiosis.

Streptococcus pneumoniae is an opportunistic pathogen that colonizes the mucosa

Streptococcus pneumoniae is a Gram-positive diplococcus and one of the most common colonizers of mucosal surfaces of the human upper respiratory tract (URT). Colonization is most frequent in children and the elderly where up to 65% of children and 40% of the elderly are carriers of *S. pneumoniae* (Smith et al., 2020; Weiser et al., 2018). In healthy adults, up to 10% of people carry *S. pneumoniae* as part of their microbiota (Weiser et al., 2018). While colonization is usually asymptomatic, *S. pneumoniae* can migrate to other tissues and cause invasive diseases such as pneumonia, meningitis, septicemia, and otitis media (Weiser et al., 2018), leading to significant morbidity and mortality.

The molecular mechanisms of invasive disease have been the subject of decades of study. However, these investigations describe only one of the lifestyles of *S. pneumoniae*. As a mucosal pathogen and common resident of the microbiota, there is a lack of understanding how the body tolerates *S. pneumoniae* colonization and what host factors are involved. Studies on *S. pneumoniae* and mucus thus far have focused on mucus as a barrier and nutrient source. *S. pneumoniae* avoids entrapment in mucus through the production of a thick and negatively charged polysaccharide capsule (Nelson et al., 2007). In a mouse model, unencapsulated *S. pneumoniae* is easily trapped within mucus and is less able to reach the epithelial layer (Nelson et al., 2007). Over 90 serotypes of *S. pneumoniae* have been described, and the negative charge of the capsule type correlates with carriage prevalence, highlighting the potential role of the capsule in avoiding the mucus barrier (Y. Li et al., 2013). Certain strains of *S. pneumoniae* can also modify membrane-bound mucin MUC16 of the ocular surface through the expression of a metalloprotease *zmpC* (Govindarajan et al., 2012). Thus *S. pneumoniae* has multiple strategies to breach the mucus barrier.

The role of mucin as a carbon source has been of considerable interest as *S. pneumoniae* strictly ferments carbohydrates and devotes a large portion of its genome to carbohydrate metabolism. Over 30% of predicted transporters in the *S. pneumoniae* genome are predicted to be sugar transporters (Tettelin et al., 2001) and *S. pneumoniae* encodes more than 40 proteins predicted to break glycosidic bonds (Hobbs et al., 2018). Studies with commercially available

mucins as a carbon source have shown that *S. pneumoniae* upregulates glycosidsases in response to mucin (Paixão et al., 2015; Yesilkaya et al., 2008). Thus, while the metabolic and barrier properties of mucin have been investigated in relation to *S. pneumoniae*, this leaves a gap as to how *S. pneumoniae* may respond to mucin as a signaling molecule.

Research focus and approach

In this thesis, I focus on how *Streptococcus pneumoniae* senses and responds to mucin as a key signaling molecule in the mucus environment. In Chapter 2, I investigate the global transcriptional effects of native mucin and mucin glycans on *S. pneumoniae* and identify that mucins and their associated glycans potently downregulate key virulence factor, pneumolysin. I identify how mucin protects host cell survival, modulates immune cell activation, and immune cell activity. In Chapter 3, I explore how mucins reduce the expression of genes involved in competence and microbe-microbe interactions. I show that mucin enhances microbial co-existence during growth with *S. pneumoniae* and competing nasopharyngeal microbes. In Appendix A, I attempt to understand the mechanism behind mucin-regulation of virulence factor and therapeutic target, pneumolysin. While regulatory pathways of *ply* are not well defined, I explored the regulation of *ply* by generating and profiling mutants. In Appendix B, I identify that mucin alters the response to cell wall-targeting antibiotics through an unknown mechanism. Together, this thesis extends our understanding of host mucins as a regulator of opportunistic pathogens, including *S. pneumoniae*. For the first time, our data reveals how mucin may also modulate the innate immune response to microbes. Understanding native host defenses embedded within mucin may enable the development of mucin-inspired therapeutics that tame opportunistic pathogens.

Figures

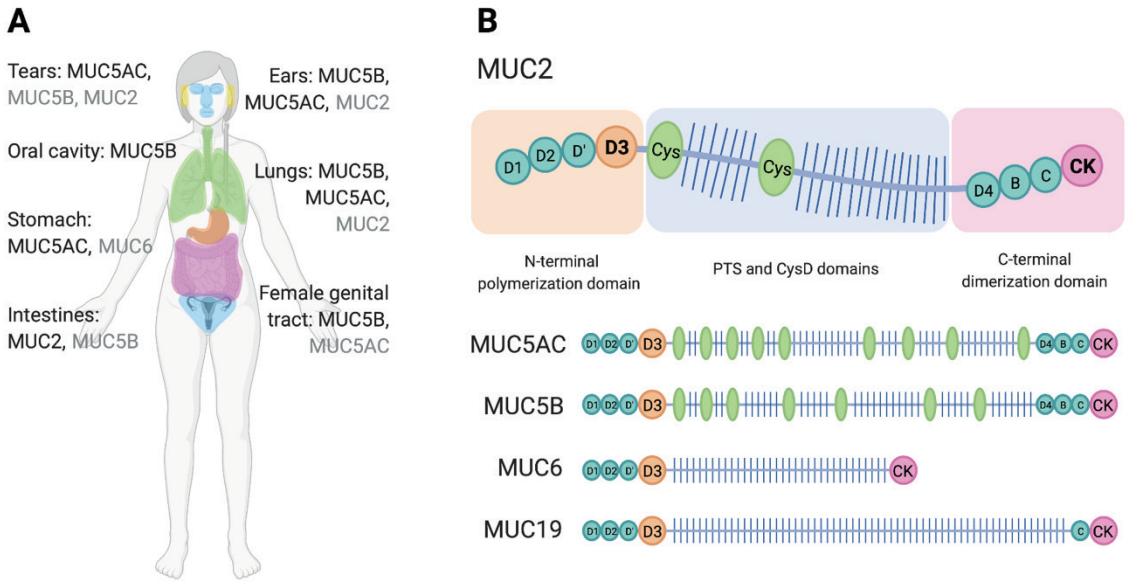

Figure 1.1 Locations of secreted mucins in the body and their structural diversity.
(A) Mucus coats all non-keratinized wet epithelial surfaces. Various *MUC* genes are expressed throughout the body to form mucin gels that are adapted to various physiological environments. For tissues expressing multiple mucin types, the dominant mucins are listed in black, with non-dominant mucin types in grey. **(B)** Summary of the features of the gel-forming mucin, MUC2. The cartoon illustrates the domain organization of MUC2 (not drawn to scale), highlighting the von Willebrand factor (vWF)-like cysteine-rich domains at the amino and carboxy termini (B, C, and D domains; teal circles), the centrally located, highly *O*-glycosylated PTS domains (glycans shown as lines), and the internal cysteine-rich domains (CysD; green ovals). The amino- and carboxy-terminal domains are essential for polymer formation. Mucin polymers are stabilized by tail-to-tail disulfide linkages between carboxy-terminal cysteine knot (CK) domains (pink) and head-to-head disulfide linkages between amino-terminal vWF-like D3 domains (orange circles).

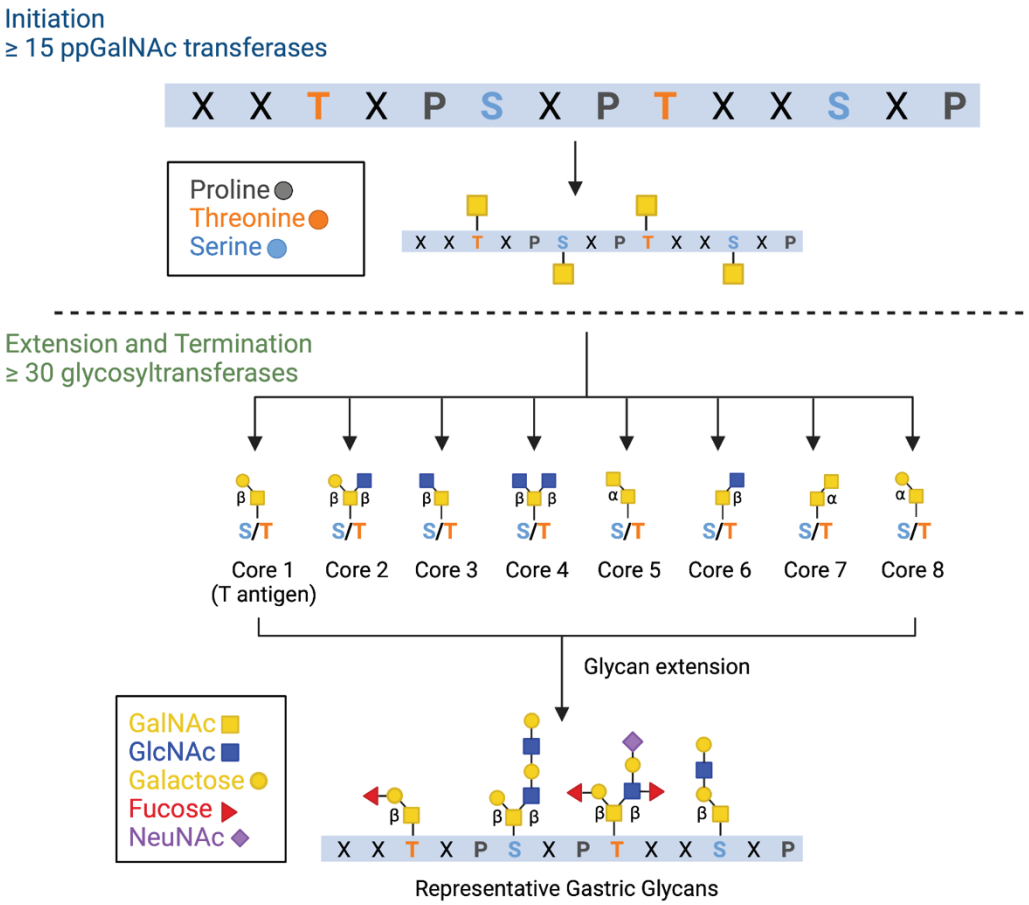

Figure 1.2 Multiple glycosyltransferases contribute to the generation of mucin-type *O*-glycan diversity.

Serine and threonine residues are potential sites of *O*-glycosylation within mucin PTS domains. Up to 20 ppGalNAc transferases initiate glycans by transferring a GalNAc to a serine or threonine residue. As the *O*-glycosylated mucin moves through the Golgi apparatus, glycans are further extended by at least 30 different additional glycosyltransferases with distinct donor and acceptor sugars using both α and β linkages. This combinatorial approach generates a plethora of diverse glycan structures based on eight core scaffolds, with cores 1–4 being the most common. Representative glycan structures present on human gastric mucin (MUC2) are shown.

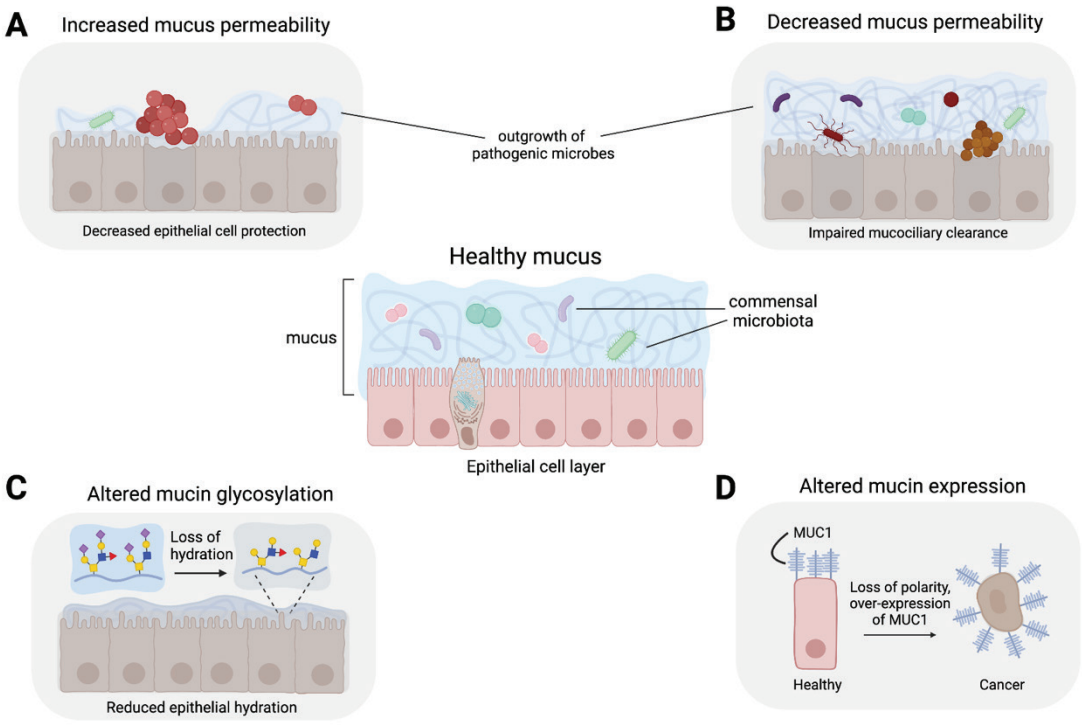

Figure 1.3 Healthy mucus protects against barrier dysfunction and disease.

Healthy mucus (center) protects epithelia by acting as a dynamic barrier that provides hydration, regulates diffusion and accommodates commensal microbes. Changes in mucin expression and identity are associated with disease. **(A)** Increased mucus permeability in various tissues potentially allows the outgrowth of pathogenic microbes. **(B)** Decreased mucus permeability impairs mucociliary clearance, leading to increased microbial colonization, as observed in cystic fibrosis and chronic obstructive pulmonary disease. **(C)** Altered mucin glycosylation is associated with various diseases, including Sjögren's syndrome, cancer, and cystic fibrosis. Loss of sialylated glycans in Sjögren's syndrome reduces the hydrophilicity of mucin glycans, causing dry mouth. **(D)** Altered mucin expression can lead to cancer. Membrane-associated MUC1 promotes the survival of epithelial cells, but MUC1 overexpression can lead to aberrant regulation of growth factor signaling.

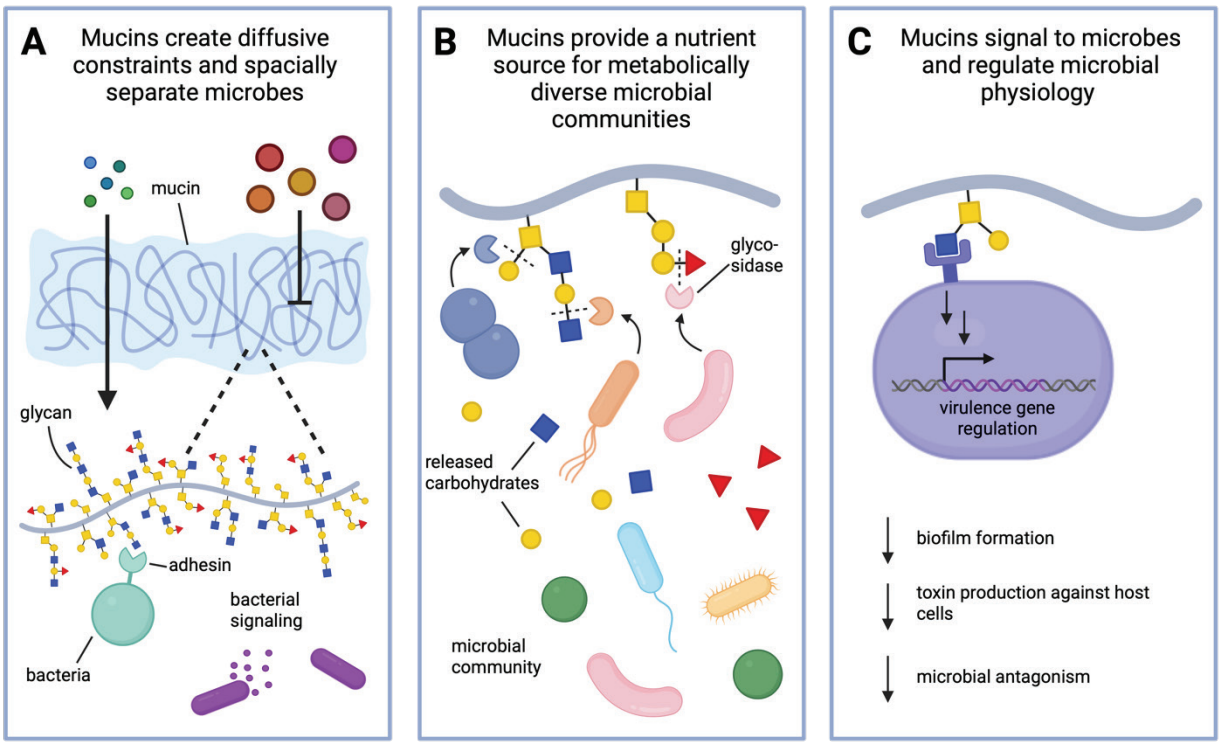

Figure 1.4 Mucins regulate microbial communities through multiple mechanisms.

(A) Mucins create a selectively permeable 3D polymer network. The mucin mesh size can regulate the diffusion of particles through steric constraints. Particles smaller than the mesh size such as bacteria may bind the variety of chemical moieties on mucins, such as through adhesins on the bacterial surface. **(B)** Mucin glycans provide a variety of metabolic substrates. Mucin glycans may select for bacteria that express glycosidases and metabolic pathways to utilize these carbohydrates, in addition to bacteria that can metabolize components of glycans through cross-feeding effects. **(C)** Mucins and mucin glycans act as signaling molecules to reduce virulence phenotypes of multiple microbes. Signatures of mucin include the reduction of biofilm formation, toxin production, and microbial competition.

References

Allen, A., & Flemström, G. (2005). Gastroduodenal mucus bicarbonate barrier: protection against acid and pepsin. *Am J Physiol Cell Physiol*, *288*, 1–19. https://doi.org/10.1152/ajpcell.00102.2004.-Secretion

Ambort, D., Johansson, M. E. V., Gustafsson, J. K., Nilsson, H. E., Ermund, A., Johansson, B. R., Koeck, P. J. B., Hebert, H., & Hansson, G. C. (2012). Calcium and pH-dependent packing and release of the gel-forming MUC2 mucin. *Proceedings of the National Academy of Sciences of the United States of America*, *109*(15), 5645–5650. https://doi.org/10.1073/pnas.1120269109

Andersch-Björkman, Y., Thomsson, K. A., Holmén Larsson, J. M., Ekerhovd, E., & Hansson, G. C. (2007). Large scale identification of proteins, mucins and their O-glycosylation in the endocervical mucus during the menstrual cycle. *Molecular and Cellular Proteomics*, *6*(4), 708–716. https://doi.org/10.1074/mcp.M600439-MCP200

Anggara, K., Sršan, L., Jaroentomeechai, T., Wu, X., Rauschenbach, S., Narimatsu, Y., Clausen, H., Ziegler, T., Miller, R. L., & Kern, K. (2023). Direct observation of glycans bonded to proteins and lipids at the single-molecule level. *Science*, *382*. https://www.science.org

Argüeso, P., Balaram, M., Spurr-Michaud, S., Keutmann, H. T., Dana, M. R., & Gipson, I. K. (2002). Decreased Levels of the Goblet Cell Mucin MUC5AC in Tears of Patients with Sjögren Syndrome. *Investigative Ophthalmology & Visual Science*, *43*(4). http://www.ncbi.nlm.nih.gov/

Argüeso, P., Spurr-Michaud, S., Tisdale, A., & Gipson, I. K. (2002). Variation in the amount of T antigen and N-acetyllactosamine oligosaccharides in human cervical mucus secretions with the menstrual cycle. *Journal of Clinical Endocrinology and Metabolism*, *87*(12), 5641–5648. https://doi.org/10.1210/jc.2002-020766

Bala Vimal, D., Khullar, M., Gupta, S., & Kumar Ganguly, N. (2000). Intestinal mucins: The binding sites for Salmonella typhimurium. In *Molecular and Cellular Biochemistry* (Vol. 204).

Bansil, R., & Turner, B. S. (2018). The biology of mucus: Composition, synthesis, and organization ☆. *Advanced Drug Delivery Reviews*, *124*, 3–15. https://doi.org/10.1016/j.addr.2017.09.023

Bennett, E. P., Mandel, U., Clausen, H., Gerken, T. A., Fritz, T. A., & Tabak, L. A. (2012). Control of mucin-type O-glycosylation: A classification of the polypeptide GalNAc-transferase gene family. In *Glycobiology* (Vol. 22, Issue 6, pp. 736–756). https://doi.org/10.1093/glycob/cwr182

Bergstrom, K. S. B., & Xia, L. (2013). Mucin-type O-glycans and their roles in intestinal homeostasis. In *Glycobiology* (Vol. 23, Issue 9, pp. 1026–1037). https://doi.org/10.1093/glycob/cwt045

Bradshaw, D. J., Homer, K. A., Marsh', P. D., & Beighton2, D. (1994). Metabolic cooperation in oral microbial communities during growth on mucin. In *Microbiology* (Vol. 140).

Brockhausen, I., Wandall, H. H., Hagen, K. G. Ten, & Stanley, P. (2022). O-GalNAc Glycans. In A. Varki, R. Cummings, & Esko JD (Eds.), *Essentials of Glycobiology [Internet]* (4th ed.). Cold Spring Harbor Laboratory Press.

Burcham, L. R., Bath, J. R., Werlang, C. A., Lyon, L. M., Liu, N., Evans, C., Ribbeck, K., & Doran, K. S. (2022). Role of MUC5B during Group B Streptococcal Vaginal Colonization. *MBio*, *13*(2). https://doi.org/10.1128/mbio.00039-22

Cao, X., Bansil, R., Bhaskar, K. R., Turner, B. S., LaMont, J. T., Niu, N., & Afdhal, N. H. (1999). pH-dependent conformational change of gastric mucin leads to sol-gel transition. *Biophysical Journal*, *76*(3), 1250–1258. https://doi.org/10.1016/S0006-3495(99)77288-7

Capra, E. J., & Laub, M. T. (2012). Evolution of two-component signal transduction systems. In *Annual Review of Microbiology* (Vol. 66, pp. 325–347). https://doi.org/10.1146/annurev-micro-092611-150039

Castro, I., Sepúlveda, D., Cortés, J., Quest, A. F. G., Barrera, M. J., Bahamondes, V., Aguilera, S., Urzúa, U., Alliende, C., Molina, C., González, S., Hermoso, M. A., Leyton, C., & González, M. J. (2013). Oral dryness in Sjögren's syndrome patients. Not just a question of water. In *Autoimmunity Reviews* (Vol. 12, Issue 5, pp. 567–574). https://doi.org/10.1016/j.autrev.2012.10.018

Chaudhury, N. M. A., Proctor, G. B., Karlsson, N. G., Carpenter, G. H., & Flowers, S. A. (2016). Reduced mucin-7 (MUC7) sialylation and altered saliva rheology in Sjögren's syndrome associated oral dryness. *Molecular and Cellular Proteomics*, *15*(3), 1048–1059. https://doi.org/10.1074/mcp.M115.052993

Chaudhury, N. M. A., Shirlaw, P., Pramanik, R., Carpenter, G. H., & Proctor, G. B. (2015). Changes in Saliva Rheological Properties and Mucin Glycosylation in Dry Mouth. *Journal of Dental Research*, *94*(12), 1660–1667. https://doi.org/10.1177/0022034515609070

Co, J. Y., Cárcamo-Oyarce, G., Billings, N., Wheeler, K. M., Grindy, S. C., Holten-Andersen, N., & Ribbeck, K. (2018). Mucins trigger dispersal of Pseudomonas aeruginosa biofilms. *Npj Biofilms and Microbiomes*, *4*(1). https://doi.org/10.1038/s41522-018-0067-0

Cohen, M., Zhang, X. Q., Senaati, H. P., Chen, H. W., Varki, N. M., Schooley, R. T., & Gagneux, P. (2013). Influenza A penetrates host mucus by cleaving sialic acids with neuraminidase. *Virology Journal*, *10*. https://doi.org/10.1186/1743-422X-10-321

Corfield, A. P. (2015). Mucins: A biologically relevant glycan barrier in mucosal protection. In *Biochimica et Biophysica Acta - General Subjects* (Vol. 1850, Issue 1, pp. 236–252). Elsevier B.V. https://doi.org/10.1016/j.bbagen.2014.05.003

Corfield, A. P., Myerscough, N., Bradfield, N., Corfield, C. D. A., Gough, M., Clamp, J. R., Durdey, P., Warren, B. F., Bartolo, D. C., King, K. R., & Williams, J. M. (1996). Colonic mucins in ulcerative colitis: evidence for loss of sulfation. *Glycoconjugate Journal*, *13*, 809–822.

De Paiva, C. S., Jones, D. B., Stern, M. E., Bian, F., Moore, Q. L., Corbiere, S., Streckfus, C. F., Hutchinson, D. S., Ajami, N. J., Petrosino, J. F., & Pflugfelder, S. C. (2016). Altered Mucosal Microbiome Diversity and Disease Severity in Sjögren Syndrome. *Scientific Reports*, *6*. https://doi.org/10.1038/srep23561

Delaveris, C. S., Webster, E. R., Banik, S. M., Boxer, S. G., & Bertozzi, C. R. (2020). Membrane-tethered mucin-like polypeptides sterically inhibit binding and slow fusion kinetics of influenza A virus. *PNAS*, *117*(23), 12643–12650. https://doi.org/10.1073/pnas.1921962117/-/DCSupplemental

Derrien, M., Vaughan, E. E., Plugge, C. M., & de Vos, W. M. (2004). Akkermansia municiphila gen. nov., sp. nov., a human intestinal mucin-degrading bacterium. *International Journal of Systematic and Evolutionary Microbiology*, *54*(5), 1469–1476. https://doi.org/10.1099/ijs.0.02873-0

Dohrman, A., Miyata, S., Gallup, M., Li, J.-D., Chapelin, C., Coste, A., Escudier, E., Nadel, J., & Basbaum, C. (1998). Mucin gene MUC 2 and MUC 5AC upregulation by Gram-positive and Gram-negative bacteria. In *Biochimica et Biophysica Acta* (Vol. 1406).

Donaldson, G. P., Lee, S. M., & Mazmanian, S. K. (2015). Gut biogeography of the bacterial microbiota. In *Nature Reviews Microbiology* (Vol. 14, Issue 1, pp. 20–32). Nature Publishing Group. https://doi.org/10.1038/nrmicro3552

Fahy, J. V, & Dickey, B. F. (2010). Airway Mucus Function and Dysfunction. In *N Engl J Med* (Vol. 363).

Flynn, J. M., Niccum, D., Dunitz, J. M., & Hunter, R. C. (2016). Evidence and Role for Bacterial Mucin Degradation in Cystic Fibrosis Airway Disease. *PLoS Pathogens*, *12*(8). https://doi.org/10.1371/journal.ppat.1005846

Frenkel, E. S., & Ribbeck, K. (2015). Salivary mucins protect surfaces from colonization by cariogenic bacteria. *Applied and Environmental Microbiology*, *81*(1), 332–338. https://doi.org/10.1128/AEM.02573-14

Frenkel, E. S., & Ribbeck, K. (2017). Salivary mucins promote the coexistence of competing oral bacterial species. *ISME Journal*, *11*(5), 1286–1290. https://doi.org/10.1038/ismej.2016.200

Gómez-Mejia, A., Gámez, G., & Hammerschmidt, S. (2018). Streptococcus pneumoniae two-component regulatory systems: The interplay of the pneumococcus with its environment. In *International Journal of Medical Microbiology* (Vol. 308, Issue 6, pp. 722–737). Elsevier GmbH. https://doi.org/10.1016/j.ijmm.2017.11.012

Govindarajan, B., Menon, B. B., Spurr-Michaud, S., Rastogi, K., Gilmore, M. S., Argüeso, P., & Gipson, I. K. (2012). A metalloproteinase secreted by Streptococcus pneumoniae removes membrane mucin MUC16 from the epithelial glycocalyx barrier. *PLoS ONE*, *7*(3). https://doi.org/10.1371/journal.pone.0032418

Hall, C. W., & Mah, T. F. (2017). Molecular mechanisms of biofilm-based antibiotic resistance and tolerance in pathogenic bacteria. In *FEMS Microbiology Reviews* (Vol. 41, Issue 3, pp. 276–301). Oxford University Press. https://doi.org/10.1093/femsre/fux010

Hattrup, C. L., & Gendler, S. J. (2008). Structure and function of the cell surface (tethered) mucins. In *Annual Review of Physiology* (Vol. 70, pp. 431–457). https://doi.org/10.1146/annurev.physiol.70.113006.100659

Henke, M. O., Renner, A., Huber, R. M., Seeds, M. C., & Rubin, B. K. (2004). MUC5AC and MUC5B mucins are decreased in cystic fibrosis airway secretions. *American Journal of*

Respiratory Cell and Molecular Biology, *31*(1), 86–91. https://doi.org/10.1165/rcmb.2003-0345OC

Hobbs, J. K., Pluvinage, B., & Boraston, A. B. (2018). Glycan-metabolizing enzymes in microbe–host interactions: the Streptococcus pneumoniae paradigm. In *FEBS Letters* (Vol. 592, Issue 23, pp. 3865–3897). Wiley Blackwell. https://doi.org/10.1002/1873-3468.13045

Horswill, A. R., Stoodley, P., Stewart, P. S., & Parsek, M. R. (2007). The effect of the chemical, biological, and physical environment on quorum sensing in structured microbial communities. *Analytical and Bioanalytical Chemistry*, *387*(2), 371–380. https://doi.org/10.1007/s00216-006-0720-y

Huang, Y., Mechref, Y., & Novotny, M. V. (2001). Microscale Nonreductive Release of O-Linked Glycans for Subsequent Analysis through MALDI Mass Spectrometry and Capillary Electrophoresis. *Analytical Chemistry*, *73*(24), 6063–6069. https://doi.org/10.1021/ac015534c

Innes, A. L., Woodruff, P. G., Ferrando, R. E., Donnelly, S., Dolganov, G. M., Lazarus, S. C., & Fahy, J. V. (2006). Epithelial mucin stores are increased in the large airways of smokers with airflow obstruction. *Chest*, *130*(4), 1102–1108. https://doi.org/10.1378/chest.130.4.1102

Itzek, A., Chen, Z., Merritt, J., & Kreth, J. (2017). Effect of salivary agglutination on oral streptococcal clearance by human polymorphonuclear neutrophil granulocytes. *Molecular Oral Microbiology*, *32*(3), 197–210. https://doi.org/10.1111/omi.12164

Jin, C., Kenny, D. T., Skoog, E. C., Padra, M., Adamczyk, B., Vitizeva, V., Thorell, A., Venkatakrishnan, V., Lindén, S. K., & Karlsson, N. G. (2017). Structural diversity of human gastric mucin glycans. *Molecular and Cellular Proteomics*, *16*(5), 743–758. https://doi.org/10.1074/mcp.M117.067983

Johansson, M. E. V., Gustafsson, J. K., Holmen-Larsson, J., Jabbar, K. S., Xia, L., Xu, H., Ghishan, F. K., Carvalho, F. A., Gewirtz, A. T., Sjovall, H., & Hansson, G. C. (2014). Bacteria penetrate the normally impenetrable inner colon mucus layer in both murine colitis models and patients with ulcerative colitis. *Gut*, *63*(2), 281–291. https://doi.org/10.1136/gutjnl-2012-303207

Johansson, M. E. V., Sjövall, H., & Hansson, G. C. (2013). The gastrointestinal mucus system in health and disease. In *Nature Reviews Gastroenterology and Hepatology* (Vol. 10, Issue 6, pp. 352–361). https://doi.org/10.1038/nrgastro.2013.35

Johansson, M. E. V, Phillipson, M., Petersson, J., Velcich, A., Holm, L., Hansson, G. C., & Greenberg, E. P. (2008). The inner of the two Muc2 mucin-dependent mucus layers in colon is devoid of bacteria. *PNAS*, *105*(39), 15064–15069. www.pnas.orgcgidoi10.1073pnas.0803124105

Johnson, M. E., & Murphy, P. J. (2004). Changes in the tear film and ocular surface from dry eye syndrome. In *Progress in Retinal and Eye Research* (Vol. 23, Issue 4, pp. 449–474). https://doi.org/10.1016/j.preteyeres.2004.04.003

Kavanaugh, N. L., Zhang, A. Q., Nobile, C. J., Johnson, A. D., & Ribbeck, K. (2014). Mucins suppress virulence traits of Candida albicans. *MBio*, *5*(6), e01911-14. https://doi.org/10.1128/mBio.01911-14

Kim, H. J., Boedicker, J. Q., Choi, J. W., Ismagilov, R. F., Designed, R. F. I., & Performed, J. W. C. (2008). Defined spatial structure stabilizes a synthetic multispecies bacterial community. *PNAS*, *105*(47), 18188–18193.

Knowles, M. R., & Boucher, R. C. (2002). Mucus clearance as a primary innate defense mechanism for mammalian airways. *Journal of Clinical Investigation*, *109*(5), 571–577. https://doi.org/10.1172/jci15217

Koropatkin, N. M., Cameron, E. A., & Martens, E. C. (2012). How glycan metabolism shapes the human gut microbiota. In *Nature Reviews Microbiology* (Vol. 10, Issue 5, pp. 323–335). https://doi.org/10.1038/nrmicro2746

Lai, S. K., Wang, Y. Y., Hida, K., Cone, R., & Hanes, J. (2010). Nanoparticles reveal that human cervicovaginal mucus is riddled with pores larger than viruses. *Proceedings of the National Academy of Sciences of the United States of America*, *107*(2), 598–603. https://doi.org/10.1073/pnas.0911748107

Larsson, J. M. H., Karlsson, H., Crespo, J. G., Johansson, M. E. V, Eklund, L., Sjövall, H., & Hansson, G. C. (2011). Altered O-glycosylation profile of MUC2 mucin occurs in active ulcerative colitis and is associated with increased inflammation. *Inflammatory Bowel Diseases*, *17*(11), 2299–2307. https://doi.org/10.1002/ibd.21625

Li, X., Bleumink-Pluym, N. M. C., Luijkx, Y. M. C. A., Wubbolts, R. W., van Putten, J. P. M., & Strijbis, K. (2019). MUC1 is a receptor for the Salmonella SiiE adhesin that enables apical invasion into enterocytes. *PLoS Pathogens*, *15*(2). https://doi.org/10.1371/journal.ppat.1007566

Li, Y., Weinberger, D. M., Thompson, C. M., Trzciński, K., & Lipsitch, M. (2013). Surface charge of Streptococcus pneumoniae predicts serotype distribution. *Infection and Immunity*, IAI.00724-13. https://doi.org/10.1128/IAI.00724-13

Li, Z., & Chai, W. (2019). Mucin O-glycan microarrays. *Current Opinion in Structural Biology*, *56*, 187–197. https://doi.org/10.1016/j.sbi.2019.03.032

Lichtenberg, M., Coenye, T., Parsek, M. R., Bjarnsholt, T., & Jakobsen, T. H. (2023). What's in a name? Characteristics of clinical biofilms. *FEMS Microbiology Reviews*, *47*(5). https://doi.org/10.1093/femsre/fuad050

Lieleg, O., Vladescu, I., & Ribbeck, K. (2010). Characterization of particle translocation through mucin hydrogels. *Biophysical Journal*, *98*(9), 1782–1789. https://doi.org/10.1016/j.bpj.2010.01.012

Lindén, S. K., Sheng, Y. H., Every, A. L., Miles, K. M., Skoog, E. C., Florin, T. H. J., Sutton, P., & McGuckin, M. A. (2009). MUC1 limits Helicobacter pylori infection both by steric hindrance and by acting as a releasable decoy. *PLoS Pathogens*, *5*(10). https://doi.org/10.1371/journal.ppat.1000617

Lindén, S., Nordman, H., Hedenbro, J., Hurtig, M., Borén, T., & Carlstedt, I. (2002). Strain- and blood group-dependent binding of Helicobacter pylori to human gastric MUC5AC glycoforms. *Gastroenterology*, *123*(6), 1923–1930. https://doi.org/10.1053/gast.2002.37076

Lu, H. P., Lai, Y. C., Huang, S. W., Chen, H. C., Hsieh, C. H., & Yu, H. T. (2014). Spatial heterogeneity of gut microbiota reveals multiple bacterial communities with distinct characteristics. *Scientific Reports*, *4*. https://doi.org/10.1038/srep06185

Lucas, S. K., Villarreal, A. R., Ahmad, M. M., Itabiyi, A., Feddema, E., Boyer, H. C., & Hunter, R. C. (2021). Anaerobic microbiota derived from the upper airways impact staphylococcus aureus physiology. *Infection and Immunity*, *89*(9). https://doi.org/10.1128/IAI.00153-21

Macfarlane, T. W., & Mason, D. K. (1974). Changes in the oral flora in Sjogren's syndrome. In *J. clin. Path* (Vol. 27).

Macpherson, A. J., Hunziker, L., Mccoy, K., & Lamarre, A. (2001). *IgA responses in the intestinal mucosa against pathogenic and non-pathogenic microorganisms*.

Mark Welch, J. L., Rossetti, B. J., Rieken, C. W., Dewhirst, F. E., & Borisy, G. G. (2016). Biogeography of a human oral microbiome at the micron scale. *Proceedings of the National Academy of Sciences of the United States of America*, *113*(6), E791–E800. https://doi.org/10.1073/pnas.1522149113

Martens, E. C., Lowe, E. C., Chiang, H., Pudlo, N. A., Wu, M., McNulty, N. P., Abbott, D. W., Henrissat, B., Gilbert, H. J., Bolam, D. N., & Gordon, J. I. (2011). Recognition and degradation of plant cell wall polysaccharides by two human gut symbionts. *PLoS Biology*, *9*(12). https://doi.org/10.1371/journal.pbio.1001221

McGuckin, M. A., Davies, J. M., Felgner, P., Wong, K. Y., Giri, R., He, Y., Moniruzzaman, M., Kryza, T., Sajiir, H., Hooper, J. D., Florin, T. H., Begun, J., Oussalah, A., Hasnain, S. Z., Hensel, M., & Sheng, Y. H. (2023). MUC13 Cell Surface Mucin Limits Salmonella Typhimurium Infection by Protecting the Mucosal Epithelial Barrier. *Cellular and Molecular Gastroenterology and Hepatology*. https://doi.org/10.1016/j.jcmgh.2023.08.011

Michail, S., Durbin, M., Turner, D., Griffiths, A. M., Mack, D. R., Hyams, J., Leleiko, N., Kenche, H., Stolfi, A., & Wine, E. (2012). Alterations in the gut microbiome of children with severe ulcerative colitis. *Inflammatory Bowel Diseases*, *18*(10), 1799–1808. https://doi.org/10.1002/ibd.22860

Minzer, G., & Hevey, R. (2023). Synthesis of Mucin O-Glycans Associated with Attenuation of Pathogen Virulence. *ChemistryOpen*, *12*(5). https://doi.org/10.1002/open.202200134

Moreno-Gámez, S., Sorg, R. A., Domenech, A., Kjos, M., Weissing, F. J., Van Doorn, G. S., & Veening, J. W. (2017). Quorum sensing integrates environmental cues, cell density and cell history to control bacterial competence. *Nature Communications*, *8*(1). https://doi.org/10.1038/s41467-017-00903-y

Murray, P. A., Prakobphol, A., Lee, T., Hoover, C. I., & Fisher, S. J. (1992). Adherence of Oral Streptococci to Salivary Glycoproteins. *Infection and Immunity*, *60*(1), 31–38. https://journals.asm.org/journal/iai

Nelson, A. L., Roche, A. M., Gould, J. M., Chim, K., Ratner, A. J., & Weiser, J. N. (2007). Capsule enhances pneumococcal colonization by limiting mucus-mediated clearance. *Infection and Immunity*, *75*(1), 83–90. https://doi.org/10.1128/IAI.01475-06

Paixão, L., Oliveira, J., Veríssimo, A., Vinga, S., Lourenço, E. C., Ventura, M. R., Kjos, M., Veening, J. W., Fernandes, V. E., Andrew, P. W., Yesilkaya, H., & Neves, A. R. (2015). Host glycan sugar-specific pathways in streptococcus pneumonia: Galactose as a key sugar in colonisation and infection. *PLoS ONE*, *10*(3). https://doi.org/10.1371/journal.pone.0121042

Pruss, K. M., Marcobal, A., Southwick, A. M., Dahan, D., Smits, S. A., Ferreyra, J. A., Higginbottom, S. K., Sonnenburg, E. D., Kashyap, P. C., Choudhury, B., Bode, L., & Sonnenburg, J. L. (2021). Mucin-derived O-glycans supplemented to diet mitigate diverse microbiota perturbations. *ISME Journal*, *15*(2), 577–591. https://doi.org/10.1038/s41396-020-00798-6

Rahn, J. J., Shen, Q., Mah, B. K., & Hugh, J. C. (2004). MUC1 initiates a calcium signal after ligation by intercellular adhesion molecule-1. *Journal of Biological Chemistry*, *279*(28), 29386–29390. https://doi.org/10.1074/jbc.C400010200

Roberton, A. M., & Stanley, R. A. (1982). In Vitro Utilization of Mucin by Bacteroides fragilis. *Applied and Environmental Microbiology*, *43*(2), 325–330.

Roy, M. G., Livraghi-Butrico, A., Fletcher, A. A., McElwee, M. M., Evans, S. E., Boerner, R. M., Alexander, S. N., Bellinghausen, L. K., Song, A. S., Petrova, Y. M., Tuvim, M. J., Adachi, R., Romo, I., Bordt, A. S., Bowden, M. G., Sisson, J. H., Woodruff, P. G., Thornton, D. J., Rousseau, K., … Evans, C. M. (2014). Muc5b is required for airway defence. *Nature*, *505*(7483), 412–416. https://doi.org/10.1038/nature12807

Royle, L., Roos, A., Harvey, D. J., Wormald, M. R., Van Gijlswijk-Janssen, D., Redwan, E. R. M., Wilson, I. A., Daha, M. R., Dwek, R. A., & Rudd, P. M. (2003). Secretory IgA N- and O-glycans provide a link between the innate and adaptive immune systems. *Journal of Biological Chemistry*, *278*(22), 20140–20153. https://doi.org/10.1074/jbc.M301436200

Ruas-Madiedo, P., Gueimonde, M., Fernández-García, M., De Los Reyes-Gavilán, C. G., & Margolles, A. (2008). Mucin degradation by Bifidobacterium strains isolated from the human intestinal microbiota. *Applied and Environmental Microbiology*, *74*(6), 1936–1940. https://doi.org/10.1128/AEM.02509-07

Salyers, A. A., West, S. E. H., Vercellotii,' And, J. R., & Wilkins', T. D. (1977). Fermentation of Mucins and Plant Polysaccharides by Anaerobic Bacteria from the Human Colon. *Applied and Environmental Microbiology*, 529–533.

Sarosiek, V. L. N., Slomiany, A., & Slomiany, B. L. (1984). Effect of lipids and proteins on the viscosity of gastric mucus glycoprotein. *Biochemical and Biophysical Research Communications*, *121*(2), 521–529.

Sauer, K., Stoodley, P., Goeres, D. M., Hall-Stoodley, L., Burmølle, M., Stewart, P. S., & Bjarnsholt, T. (2022). The biofilm life cycle: expanding the conceptual model of biofilm formation. In *Nature Reviews Microbiology* (Vol. 20, Issue 10, pp. 608–620). Nature Research. https://doi.org/10.1038/s41579-022-00767-0

Shelburne, S. A., Davenport, M. T., Keith, D. B., & Musser, J. M. (2008). The role of complex carbohydrate catabolism in the pathogenesis of invasive streptococci. In *Trends in Microbiology* (Vol. 16, Issue 7, pp. 318–325). https://doi.org/10.1016/j.tim.2008.04.002

Skoog, E. C., Sjöling, Å., Navabi, N., Holgersson, J., Lundin, S. B., & Lindén, S. K. (2012). Human gastric mucins differently regulate helicobacter pylori proliferation, gene expression and interactions with host cells. *PLoS ONE*, *7*(5). https://doi.org/10.1371/journal.pone.0036378

Slomiany, B. L., Murty, V. L. N., Piotrowski, J., & Slomiany, A. (1996). Salivary Mucins in Oral Mucosal Defense. In *Gen. Pharmac* (Vol. 27, Issue 5).

Smirnova, M. G., Guo, L., Birchall, J. P., & Pearson, J. P. (2003). LPS up-regulates mucin and cytokine mRNA expression and stimulates mucin and cytokine secretion in goblet cells. *Cellular Immunology*, *221*(1), 42–49. https://doi.org/10.1016/S0008-8749(03)00059-5

Smith, E. L., Wheeler, I., Adler, H., Ferreira, D. M., Sá-Leão, R., Abdullahi, O., Adetifa, I., Becker-Dreps, S., Esposito, S., Farida, H., Kandasamy, R., Mackenzie, G. A., Nuorti, J. P., Nzenze, S., Madhi, S. A., Ortega, O., Roca, A., Safari, D., Schaumburg, F., … Rylance, J. (2020). Upper airways colonisation of Streptococcus pneumoniae in adults aged 60 years and older: A systematic review of prevalence and individual participant data meta-analysis of risk factors. *Journal of Infection*, *81*(4), 540–548. https://doi.org/10.1016/j.jinf.2020.06.028

Snary, D., Allen, A., & Pain, R. H. (1971). The Structure of Pig Gastric Mucus Conformational Transitions Induced by Salt. *European Journal of Biochemistry*, *24*(1), 183–189. https://doi.org/10.1111/j.1432-1033.1971.tb19669.x

Stewart, P. S., & Franklin, M. J. (2008). Physiological heterogeneity in biofilms. In *Nature Reviews Microbiology* (Vol. 6, Issue 3, pp. 199–210). https://doi.org/10.1038/nrmicro1838

Takagi, J., Aoki, K., Turner, B. S., Lamont, S., Lehoux, S., Kavanaugh, N., Gulati, M., Valle Arevalo, A., Lawrence, T. J., Kim, C. Y., Bakshi, B., Ishihara, M., Nobile, C. J., Cummings, R. D., Wozniak, D. J., Tiemeyer, M., Hevey, R., & Ribbeck, K. (2022). Mucin O-glycans are natural inhibitors of Candida albicans pathogenicity. *Nature Chemical Biology*, *18*(7), 762–773. https://doi.org/10.1038/s41589-022-01035-1

Tettelin, H., Nelson, K., Paulsen, I. T., Eisen, J. A., Read, T. D., Haft, D. H., Dodson, R. J., Durkin, A. S., Gwinn, M., Kolonay, J. F., Nelson, W. C., Peterson, J. D., Umayam, L. A., White, O., Salzberg, S. L., Lewis, M. R., Radune, D., Holtzapple, E., Khouri, H., … Fraser, C. M. (2001). Complete genome sequence of a virulent isolate of Streptococcus pneumoniae. *Science*, *293*(5529), 498–506. https://doi.org/10.1126/science.1061217

Thornton, D. J., Rousseau, K., & McGuckin, M. A. (2008). Structure and function of the polymeric mucins in airways mucus. In *Annual Review of Physiology* (Vol. 70, pp. 459–486). https://doi.org/10.1146/annurev.physiol.70.113006.100702

Tolker-Nielsen, T. (2015). Biofilm Development. *Microbiology Spectrum*, *3*(2). https://doi.org/10.1128/microbiolspec.mb-0001-2014

Turner, B. S., Bhaskar, K. R., Hadzopoulou-Cladaras, M., & Lamont, J. T. (1999). Cysteine-rich regions of pig gastric mucin contain von Willebrand factor and cystine knot domains at the carboxyl terminal. *Biochimica et Biophysica Acta*, *1447*, 77–92. www.elsevier.com/locate/bba

Turner, B. S., Bhaskar, R. K., Hadzopoulou-Cladaras, M., Specian, R. D., & Lamont, J. T. (1995). Isolation and characterization of cDNA clones encoding pig gastric mucin. In *Biochem. J* (Vol. 308).

Van der Sluis, M., De Koning, B. A. E., De Bruijn, A. C. J. M., Velcich, A., Meijerink, J. P. P., Van Goudoever, J. B., Büller, H. A., Dekker, J., Van Seuningen, I., Renes, I. B., & Einerhand, A. W. C. (2006). Muc2-Deficient Mice Spontaneously Develop Colitis, Indicating That MUC2 Is Critical for Colonic Protection. *Gastroenterology*, *131*(1), 117–129. https://doi.org/10.1053/j.gastro.2006.04.020

Verdugo, P. (2012). Supramolecular dynamics of mucus. *Cold Spring Harbor Perspectives in Medicine*, *2*(11). https://doi.org/10.1101/cshperspect.a009597

Wagner, C. E., Wheeler, K. M., & Ribbeck, K. (2018a). Mucins and Their Role in Shaping the Functions of Mucus Barriers. *Annu. Rev. Cell Dev. Biol*, *34*, 189–215. https://doi.org/10.1146/annurev-cellbio-100617

Wagner, C. E., Wheeler, K. M., & Ribbeck, K. (2018b). Mucins and Their Role in Shaping the Functions of Mucus Barriers. *Annual Review of Cell and Developmental Biology*, *34*(1), 189–215. https://doi.org/10.1146/annurev-cellbio-100617-062818

Wang, B. X., Takagi, J., McShane, A., Park, J. H., Aoki, K., Griffin, C., Teschler, J., Kitts, G., Minzer, G., Tiemeyer, M., Hevey, R., Yildiz, F., & Ribbeck, K. (2023). Host-derived O -glycans inhibit toxigenic conversion by a virulence-encoding phage in Vibrio cholerae. *The EMBO Journal*, *42*(3). https://doi.org/10.15252/embj.2022111562

Wang, B. X., Wheeler, K. M., Cady, K. C., Lehoux, S., Cummings, R. D., Laub, M. T., & Ribbeck, K. (2021). Mucin Glycans Signal through the Sensor Kinase RetS to Inhibit Virulence-Associated Traits in Pseudomonas aeruginosa. *Current Biology*, *31*(1), 90-102.e7. https://doi.org/10.1016/j.cub.2020.09.088

Wang, B. X., Wu, C. M., & Ribbeck, K. (2021). Home, sweet home: how mucus accommodates our microbiota. In *FEBS Journal* (Vol. 288, Issue 6, pp. 1789–1799). Blackwell Publishing Ltd. https://doi.org/10.1111/febs.15504

Wang, S., Chen, C., Gadi, M. R., Saikam, V., Liu, D., Zhu, H., Bollag, R., Liu, K., Chen, X., Wang, F., Wang, P. G., Ling, P., Guan, W., & Li, L. (2021). Chemoenzymatic modular assembly of O-GalNAc glycans for functional glycomics. *Nature Communications*, *12*(1). https://doi.org/10.1038/s41467-021-23428-x

Wardman, J. F., Bains, R. K., Rahfeld, P., & Withers, S. G. (2022). Carbohydrate-active enzymes (CAZymes) in the gut microbiome. In *Nature Reviews Microbiology* (Vol. 20, Issue 9, pp. 542–556). Nature Research. https://doi.org/10.1038/s41579-022-00712-1

Wardzala, C. L., Wood, A. M., Belnap, D. M., & Kramer, J. R. (2022). Mucins Inhibit Coronavirus Infection in a Glycan-Dependent Manner. *ACS Central Science*, *8*(3), 351–360. https://doi.org/10.1021/acscentsci.1c01369

Weiser, J. N., Ferreira, D. M., & Paton, J. C. (2018). Streptococcus pneumoniae: Transmission, colonization and invasion. In *Nature Reviews Microbiology* (Vol. 16, Issue 6, pp. 355–367). Nature Publishing Group. https://doi.org/10.1038/s41579-018-0001-8

Wenzel, U. A., Magnusson, M. K., Rydström, A., Jonstrand, C., Hengst, J., Johansson, M. E. V., Velcich, A., Öhman, L., Strid, H., Sjövall, H., Hansson, G. C., & Wick, M. J. (2014). Spontaneous colitis in Muc2-deficient mice reflects clinical and cellular features of active ulcerative colitis. *PLoS ONE*, *9*(6). https://doi.org/10.1371/journal.pone.0100217

Werlang, C. A., Chen, W. G., Aoki, K., Wheeler, K. M., Tymm, C., Mileti, C. J., Burgos, A. C., Kim, K., Tiemeyer, M., & Ribbeck, K. (2021). Mucin O-glycans suppress quorum-sensing pathways and genetic transformation in Streptococcus mutans. *Nature Microbiology*. https://doi.org/10.1038/s41564-021-00876-1

Wesseling, J., van der Valk, S. W., Vos, H. L., Sonnenberg, A., & I-lilkens, J. (1995). Episialin (MUC1) Overexpression Inhibits Integrin-mediated Cell Adhesion to Extracellular Matrix Components. *The Journal of Cell Biology*, *129*(1), 255–265. http://rupress.org/jcb/article-pdf/129/1/255/1478558/255.pdf

Wheeler, K. M., Cárcamo-Oyarce, G., Turner, B. S., Dellos-Nolan, S., Co, J. Y., Lehoux, S., Cummings, R. D., Wozniak, D. J., & Ribbeck, K. (2019). Mucin glycans attenuate the virulence of Pseudomonas aeruginosa in infection. In *Nature Microbiology* (Vol. 4, Issue 12, pp. 2146–2154). Nature Research. https://doi.org/10.1038/s41564-019-0581-8

Wickstörm, C., Herzberg, M. C., Beighton, D., & Svensäter, G. (2009). Proteolytic degradation of human salivary MUC5B by dental biofilms. *Microbiology*, *155*(9), 2866–2872. https://doi.org/10.1099/mic.0.030536-0

Willoughby, R. E. (1993). Rotaviruses preferentially bind O-linked sialylglycoconjugates and sialomucins. In *Glycobiology* (Vol. 3, Issue 5). http://glycob.oxfordjournals.org/

Witten, J., Samad, T., & Ribbeck, K. (2018). Selective permeability of mucus barriers. *Current Opinion in Biotechnology*, *52*, 124–133. https://doi.org/10.1016/j.copbio.2018.03.010

Wu, C. M., Wheeler, K. M., Cárcamo-Oyarce, G., Aoki, K., McShane, A., Datta, S. S., Mark Welch, J. L., Tiemeyer, M., Griffen, A. L., & Ribbeck, K. (2023). Mucin glycans drive oral microbial community composition and function. *Npj Biofilms and Microbiomes*, *9*(1). https://doi.org/10.1038/s41522-023-00378-4

Yang, J.-M., Cbyrd, J., Siddiki, B. B., Chung, Y.-S., Okuno, M., Sowa, M., Kim, Y. S., Matta, K. L., & Brockhausen, I. (1994). Alterations of O-glycan biosynthesis in human colon cancer tissues. In *Glycobiology* (Vol. 4, Issue 6). http://glycob.oxfordjournals.org/

Yesilkaya, H., Manco, S., Kadioglu, A., Terra, V. S., & Andrew, P. W. (2008). The ability to utilize mucin affects the regulation of virulence gene expression in Streptococcus pneumoniae. *FEMS Microbiology Letters*, *278*(2), 231–235. https://doi.org/10.1111/j.1574-6968.2007.01003.x

Chapter 2: Mucin *O*-glycans protect host cells by tempering pneumolysin expression in *Streptococcus pneumoniae*

Work presented in this chapter has been submitted for publication.

Bath JR, Bjanes E, Goekeri C, Hsiao J, Uzun D, Nouailles G, Nizet V, and Ribbeck K. Mucin *O*-glycans protect host cells by tempering pneumolysin expression in *Streptococcus pneumoniae*.

Abstract

The ability of the body to sustain asymptomatic colonization by pathogens such as *Streptococcus pneumoniae*, which colonizes mucus-rich epithelial surfaces, remains a significant and unresolved scientific question. This study sheds light on this issue, revealing that mucins, the main gel-forming elements of mucus, and their associated glycans, suppress the expression of pneumolysin, a toxin produced by *S. pneumoniae* that causes mucosal tissue injury and triggers accompanying inflammatory responses. These results highlight a unique protective function of mucins, offering insights into potential therapeutic strategies that disarm pathogens without compromising host defenses.

Introduction

Streptococcus pneumoniae is a common member of the microflora of the human nasopharyngeal mucosa, asymptomatically colonizing 20 to 60% of school-age children, and approximately 5 to 10% of adults (Gierke et al., 2021). Yet this very same bacterium is responsible for almost 1.2 million deaths each year across the globe from lower respiratory infection (Troeger et al., 2018). The host-pathogen dynamics of pneumococcal carriage, and why it only rarely leads to severe illness, remain a great enigma in the study of human infectious disease.

One of the primary molecular barriers that *S. pneumoniae* encounters upon colonization of the nasopharyngeal mucosa are mucins, the extensive glycoprotein polymers that are integral to the host's innate immune defense (Thornton et al., 2008; Weiser et al., 2018) (Fig. 2.1a). Mucins form a robust physical barrier and play a decisive regulatory role by mediating interactions with and responses to pathogenic microbes (Takagi et al., 2022; Wang et al., 2021; C. A. Werlang et al., 2021; Wheeler et al., 2019). Despite the central role of mucins in the innate immune system, the extent to which they influence the behavior of *S. pneumoniae* remains largely unknown.

Results

In order to understand how mucins may modulate *S. pneumoniae*, this study utilized a well-established source of mucin that replicates essential structural and functional attributes of human airway mucin MUC5AC. The chosen analog, natively purified porcine gastric MUC5AC, is recognized for its similarity to human mucins and has undergone extensive validation for its relevance in deciphering mucin-bacteria interactions, with clear implications for understanding human respiratory pathophysiology (Celli et al., 2007; Co et al., 2018; Wagner et al., 2018; C. Werlang et al., 2019).

The bacterial strain under investigation is *S. pneumoniae* TIGR4, selected for its high clinical relevance as a well-characterized invasive human disease isolate that displays reproducible virulence phenotypes in tissue culture and small animal models of pneumococcal infection. *S. pneumoniae* TIGR4 was exposed to mucin, and its gene expression was measured by RNA-sequencing analysis. The data revealed that both MUC5AC and its isolated glycans induced widespread alterations in *S. pneumoniae* gene expression (Fig. 2.1b-c). The most pronounced effect was the downregulation of the operon encoding pneumolysin (*ply*), a virulence factor

implicated in tissue damage, transmission enhancement, and inflammatory response (Berry et al., 1989; Witzenrath et al., 2011; Zafar et al., 2017). In fact, the increased pathogenicity of serotype 1 pneumococcal isolates is driven primarily by increased expression of PLY (Jacques et al., 2020).

Analysis of *ply* expression by RT-qPCR indicated that MUC5AC, along with mucins from other mucosal surfaces, MUC5B (human salivary mucin) and MUC2 (porcine intestinal mucin), consistently reduced *ply* expression despite their different structures and glycan profiles (Takagi et al., 2022; Thornton et al., 2008), indicating a shared role among mucins as regulatory signals (Fig. 2.2a). This effect was specific to native mucins, as a control gel-forming polymer carboxymethyl cellulose (van der Reijden et al., 1994) (CMC) and commercial porcine gastric mucin, which has altered rheological properties (Wagner et al., 2018) failed to suppress *ply* expression (Fig. 2.2a). The downregulation of *ply* was consistent across different *S. pneumoniae* serotypes (Fig. 2.2b), carbon sources (Fig. 2.2c), growth stages (Fig. 2.2d), and after short exposure times (Fig. 2.2e), indicating a robust and rapid transcriptional response. This emphasizes the broad and significant impact of mucins in curtailing *ply* expression in *S. pneumoniae*. The decrease in PLY was confirmed by western blot analysis, demonstrating decreased PLY protein after mucin exposure (Fig. 2.2f).

S. pneumoniae encodes numerous glycosidases and carbohydrate transport machinery with the potential to metabolize mucin (Tettelin et al., 2001; Yesilkaya et al., 2008), leading to the hypothesis that growth with mucin may lead to changes in growth dynamics. However, we found that the decrease in PLY did not correlate with changes in bacterial growth when exposed to mucins or mucin glycans (Fig 2.3a-b). In addition, despite previous reports that *S. pneumoniae* can metabolize mucins, we found *S. pneumoniae* cannot utilize mucins as a sole carbon source (Fig. 2.3c-d). Together, our analysis of transcriptional changes and growth patterns implicate a targeted transcriptional response to a mucin-rich environment rather than broad changes in metabolism.

Given that PLY can inflict tissue damage and provoke inflammation, we expected that its downregulation by mucins should result in the protection of host tissues. To test this hypothesis, *S. pneumoniae* was grown in the presence of mucins, and the supernatant containing released toxin was collected, exposed to cells, and cell viability was quantified. Indeed, when grown in the presence of mucins and mucin glycans, the *S. pneumoniae* supernatant exhibited reduced activity against red blood cells in a standard hemolysis assay (Fig 2.4a-b), compared to bacteria grown in the absence of mucins. This protective effect was strictly PLY-dependent, as the TIGR4Δ*ply*

mutant, which does not express PLY, showed no hemolytic activity (Fig. 2.4a). Furthermore, the protective effect extended to MUC2, MUC5B, and mucin glycans, but not to the control polymer CMC or monosaccharides.

Given the strong results, we next tested two cell types relevant at the site of infection: A549 lung epithelial cells and primary human neutrophils. PLY-induced lung epithelial barrier disruption is a hallmark of pneumococcal disease, and PLY induces an inflammatory response in epithelial cells (Rubins et al., 1993; Witzenrath et al., 2006; Yoo et al., 2010). Similarly, PLY is a pro-inflammatory signal to neutrophils, integral cells of the innate immune response, and phagocytic defense against *S. pneumoniae* (Domon & Terao, 2021; Garvy & Harmsen, 1996). Mucins protected both lung epithelial cells and neutrophils from *S. pneumoniae*-induced killing after exposure to PLY-containing supernatant (Fig. 2.5a-d). Again, this protective effect was PLY-dependent, as the TIGR4Δ*ply* mutant showed no cytotoxic activity against either cell type. This finding emphasizes the specificity of mucins in mitigating PLY-mediated cellular damage.

Secreted PLY is just one of many virulence factors produced by *S. pneumoniae*, thus we also assessed the viability of neutrophils during co-culture with live *S. pneumoniae*. The results revealed that mucins protected neutrophils from killing when co-cultured with mucin-preexposed *S. pneumoniae* or TIGR4Δ*ply* (Fig. 2.6a). Collectively, these findings highlight the crucial role of mucins in suppressing PLY and the accompanying pneumococcal cytotoxicity, suggesting a potent and conserved defensive mechanism within the mucosal barrier.

The dampening of PLY expression by mucins adds an intriguing dimension, especially considering PLY's role in modulating the immune response (Cockeran et al., 2002; Houldsworth et al., 1994; Subramanian et al., 2019). To investigate this, we employed a co-culture model to examine the impact of PLY expression on neutrophil activation. Myeloperoxidase (MPO), released from azurophilic granules upon neutrophil activation, plays a key defensive role against *S. pneumoniae* (Xiang et al., 2017). We observed a reduction in MPO release from neutrophils when co-cultured with mucin-preexposed *S. pneumoniae*, approaching levels observed with the TIGR4Δ*ply* mutant (Fig. 2.6b). This suggests a mucin-mediated modulation of the neutrophil's antimicrobial response. Moreover, PLY is known to induce the release of pro-inflammatory interleukin-1β (IL-1β) (McNeela et al., 2010; Witzenrath et al., 2011), a critical cytokine in immune cell activation and differentiation. We observed that neutrophil secretion of IL-1β was diminished following incubation with mucin-treated *S. pneumoniae* compared to the wild-type

TIGR4 strain (Fig. 2.6c). Collectively, these data suggest that the mucosal regulation of PLY not only preserves neutrophil viability but also modulates their activation state, potentially mitigating excessive inflammatory responses during infection.

The observed reduction cytokine production prompted by mucins could suggest a state of cellular inactivity, raising the question of whether neutrophil phagocytosis is compromised. To address this, we examined whether mucin-altered *S. pneumoniae* impacts neutrophil microbicidal function by measuring their ability to engulf and kill bacteria. Employing GFP-tagged *S. pneumoniae* (Kjos et al., 2015), we co-cultured these bacteria with primary human neutrophils and deployed flow cytometry to track phagocytosis, complemented by a gentamicin protection assay to discern bacterial killing capabilities (Goekeri et al., 2023). We found that neutrophil phagocytosis remained robust even in the presence of mucins, maintaining high efficiency even at elevated bacterial densities (Fig. 2.6d-e). This resilience suggests that mucins do not impair the inherent phagocytic capacity of neutrophils. For comparison, the TIGR4Δ*ply* mutant, lacking PLY, exhibited a stark reduction in phagocytosis, underscoring the protein's pivotal role in activating this critical immune response (Fig. 2.6d-e).

Further evidence of neutrophil functionality was observed in their ability to kill internalized bacteria, with no significant difference between mucin-exposed and non-exposed conditions (Fig. 2.6f). These observations confirm that mucin's modulation of PLY expression does not impair neutrophil phagocytosis or bacterial killing efficiency. However, the observation that mucins only partially suppress PLY, as evidenced by western blot analysis showing low but detectable levels of the toxin (Fig. 2.2f), implies that even this reduced amount of PLY is sufficient to trigger phagocytosis. Thus, mucins tune PLY to maintain neutrophil activation, while protecting neutrophils from toxin-mediated killing.

Given that PLY is a key streptococcal virulence factor, we next assessed whether exposure to mucin and mucin glycans was sufficient to reduce virulence *in vivo*. We conducted a pilot study in which we pre-exposed *Spn* to mucin or mucin glycans before infecting mice intratracheally. In one group, we delivered an additional dose of mucin or mucin glycans 8 hours post infection. After 24 hours, we analyzed the bacteria recovered from the lung and blood and observed a trend indicating that pre-treatment with mucin or mucin glycans reduced the virulence of *Spn* (Fig. 2.7a-b). Further optimization of mucin or mucin glycan treatment dosage and timing will likely reveal the potential impact of mucin on attenuating *Spn* infection *in vivo*.

Discussion

Here, we report that mucins and mucin glycans strongly downregulate the key toxin and virulence factor in *S. pneumoniae*, PLY. We show the suppression of PLY by mucin leads to protection of host cells and modulates the neutrophil response to *S. pneumoniae*. This nuanced regulation of PLY by mucins may reflect a balanced host-pathogen interaction, wherein host defense mechanisms remain engaged in pathogen eradication without overactivation that could lead to excessive inflammation and tissue damage. Our results add to the growing body of work that describe mucus as a critical regulator of the microbiota, and for the first time show how mucins modulate interactions between microbes and the host immune system.

Beyond the regulation of PLY, our RNA-seq results identified many mucin-regulated genes that warrant further exploration. For example, mucins strongly downregulated the fatty acid biosynthesis operon. *S. pneumoniae* encodes multiple fatty acid scavenging proteins and this regulation may reflect a defense mechanism due to the availability of fatty acids from the host at the mucosal surface (Gullett et al., 2019). Further explorations of mucin-regulated genes may reveal other adaptations of *S. pneumoniae* to the mucosal environment.

The molecular mechanism by which mucins regulate *ply* remains an open question. In general, regulatory mechanisms of *ply* and the mechanism of *ply* export have not been well characterized (Price et al., 2012; Stevens et al., 2022). One possibility is that mucin and mucin glycans may shift the metabolism of *S. pneumoniae*, without impacting growth dynamics. *S. pneumoniae* expresses glycosidases with the potential to breakdown mucin (Mathew et al., 2023; Yesilkaya et al., 2008), and carbohydrate transportation systems to transport glycan components (Buckwalter & King, 2012). Our RNA-seq indicated that while mucin did not strongly regulate glycosidase expression, carbohydrate transportation machinery was upregulated, leaving open the possibility of a metabolic shift that could direct changes in gene expression. We explore this question further in Appendix A of this thesis, but the mechanism of *ply* regulation remains unclear. Identifying the mechanism of mucin regulation may reveal other mechanisms of *ply* regulation in *S. pneumoniae* and opens avenues for novel therapeutic interventions designed to mitigate the virulence mechanisms of this preeminent human bacterial pathogen.

Materials and methods

Strains and reagents

This study used the *Streptococcus pneumoniae* strain TIGR4, generously provided by Marc Lipsitch (Harvard T.H. Chan School of Public Health) and Rick Malley (Harvard Medical School). This strain, originally isolated from an adult male patient's blood, exhibits high virulence in murine infection models. The TIGR4Δ*ply* mutant was obtained from Justin Thornton (Mississippi State University) (Bryant et al., 2016). Strains D39V and JWV500 were gifts from Jan-Willem Veening (University of Lausanne) (Kjos et al., 2015). A comprehensive list of strains is detailed in Supplementary Table 2.1. For routine growth and preservation, we cultured the bacteria on tryptic soy agar with 5% sheep blood (TSB) at 37 °C in a 5% CO_2 atmosphere. Cultures for experiments were grown in THY broth, BHI broth, or CDM (Van De Rijn & Kessler, 1980) supplemented with 0.1% choline. When required, media were supplemented with erythromycin (Ery; 0.5 μg/mL) or chloramphenicol (Cam; 4.5 μg/mL) for antibiotic-resistant strains. Growth kinetics were monitored in THY broth with additives like CMC or mucin at 37 °C with 5% CO_2, measuring optical density (OD) at 30-minute intervals using a Synergy H1 microplate reader (BioTek).

Mutant strain construction

Primer sequences used for strain construction are listed in Supplementary Table 2.2. To generate TIGR4-*hlpA*-GFP and TIGR4Δ*ply*-*hlpA*-GFP strains, we amplified the GFP-tagged *hlpA* region from strain JWV50016 using PCR with Roche KAPA HiFi HotStart ReadyMix. This segment, carrying a chloramphenicol resistance cassette for selection, was then purified. *Streptococcus pneumoniae* transformation was initiated with 100 ng of CSP-2 (AnaSpec) followed by the addition of the purified DNA. Resultant mutants were selected on TSB agar plates containing chloramphenicol.

Collection of human saliva

Submandibular saliva was collected from healthy volunteers using a specialized vacuum pump system. Post-collection, the saliva was diluted with 5.5 M NaCl to achieve a final concentration of 0.16 M. To inhibit microbial growth and proteolytic degradation, we treated the saliva with a combination of antimicrobial agents and protease inhibitors: sodium azide (0.04 wt%), benzamidine HCl (5 mM), dibromoacetophenone (1 mM), phenylmethylsulfonyl fluoride (1 mM),

EDTA (5 mM at pH 7), Triton-X-100 (TX100; 0.5%), and tri-n-butyl phosphate (15%). The treated saliva was then flash-frozen in liquid nitrogen and stored at -80 °C. To remove TX100, we used SDR HyperD resin (Sartorius). Collection of saliva samples was conducted with informed consent from participants, under the approval of the institutional review board and the Massachusetts Institute of Technology's Committee on the Use of Humans as Experimental Subjects, protocol number 1312006096.

Mucin purification

Native porcine gastric mucins (MUC5AC), porcine intestinal mucins (MUC2), and human salivary mucins (MUC5B) were isolated following previously established methods (Wheeler et al., 2019). Briefly, mucus was harvested from pig stomachs and intestines, dissolved in a NaCl buffer with protease inhibitors and sodium azide, and clarified by centrifugation first at low speed (8,000g for 30 min) and then by ultracentrifugation (190,000g for 1 h at 4 °C using a Beckman 50.2 Ti rotor). Residual fat and particulates were filtered out using Whatman 3 paper. Human submandibular saliva was collected, and mucins purified as outlined earlier. Mucins were fractionated by size-exclusion chromatography on Sepharose CL-2B columns, desalted, concentrated, and dissolved in water. To eliminate potential phage or viral contaminants, MUC2 and MUC5AC preparations were treated with 0.5% Triton X-100 (TX100) and 0.15% tri-N-butyl phosphate after mucin purification. TX100 was subsequently removed using SDR HyperD resin (Sartorius). The mucins were then lyophilized, rehydrated by overnight shaking at 4 °C in water or appropriate media, and checked for purity using mass spectrometry (MS). MS analysis typically reveals that mucin extracts from porcine stomach predominantly contain MUC5AC, with minor components like MUC2, MUC5B, MUC6, histones, actin, and albumin.

Isolation of mucin glycans from mucins

We dissociated non-reduced glycans from mucins using non-reductive alkaline β-elimination ammonolysis as previously detailed (Takagi et al., 2022; Wang et al., 2021; C. A. Werlang et al., 2021; Wheeler et al., 2019). Commercial porcine gastric mucin (Sigma) was cleaned by ethanol precipitation, redissolved in PBS, then desalted and lyophilized after ethanol removal. The mucins were treated with ammonium hydroxide and ammonium carbonate, incubated at 60 °C for 50-60 hours, resulting in glycosylamines and partially deglycosylated mucins. Volatile compounds were

evaporated by centrifugation. Glycosylamines were separated from residual mucins using 10-kDa cut-off centrifugal filters (Amicon Ultracel), then converted to oligosaccharide hemiacetals with boric acid, and purified with Hypercarb minicolumns (Thermo Fisher Scientific).

Mass spectrometry of glycans

Glycan samples were permethylated using dimethyl sulfoxide (DMSO)/sodium hydroxide (NaOH) base and iodomethane. Briefly, samples were resuspended in DMSO, and DMSO/NaOH base and iodomethane were added and mixed for 20 mins. This process was repeated one more time. Following the second incubation, the reaction was quenched with LC-MS grade water, and dichloromethane was used to extract the glycans. The DCM layer was then transferred to a clean tube and dried under N_2. Samples were resuspended in 200 µL of MeOH and 1mM NaOH and analyzed by nanoLC-MSMS system. MS and MS^2 data were analyzed using GlycoWorkbench 2.0, GRITS software, and manual interpretation. Relative abundances were retrieved from MS^1 level using m/z's for multiple charge states. FreeStyle 1.8 was used to pull out the peaks.

RNA preparation for gene expression analysis

S. pneumoniae was initially cultured on TSB agar plates overnight. The resulting colonies were then used to start pre-cultures in THY broth. Once these cultures reached an optical density (OD) of approximately 0.4, they were diluted to an OD of 0.01, equivalent to 10^7 CFU/mL, in THY broth enriched with either 0.5% CMC, 0.5% mucin, 0.1% monosaccharides, or 0.1% glycans. After 5 hours of incubation at 37 °C in a 5% CO_2 atmosphere, the bacteria were harvested at mid-log phase by centrifugation at 16,000g. The supernatant was discarded, and the bacterial pellets were rapidly frozen in liquid nitrogen and stored at -80 °C. For RNA extraction, the frozen pellets were thawed on ice, resuspended in 25µL of lysozyme buffer, treated with Ready-Lyse Lysozyme for 15 minutes at room temperature, and then processed using the MasterPure RNA Purification kit. Any contaminating genomic DNA was eliminated with the Turbo DNA-free kit and the RNA samples were preserved at -20 °C.

RNA-seq analysis

For the RNA-seq analysis, we used three biological replicates per experimental condition. The RNA libraries were prepared with the Ribo-Zero Magnetic Kit (for bacteria) from Epicentre and

the KAPA RNA HyperPrep kit from Kapa Biosystems. Sequencing of these libraries was carried out on the Illumina NextSeq platform, utilizing a single-end protocol with 92 nucleotide read lengths.

The sequencing reads were aligned to the TIGR4 genome (NC_003028.3) via Burrows–Wheeler aligner, with expression quantified using featureCounts on the Galaxy platform. We determined differential gene expression and statistical significance using the DESeq2 package within the R Bioconductor suite, applying the Benjamini-Hochberg procedure to adjust *P*-values.

To understand the biological implications of gene expression changes, we conducted Gene Ontology (GO) analysis to pinpoint biological processes overrepresented among the significantly regulated genes. This analysis was performed using the BioCyc database, with Fisher's exact test evaluating the enrichment significance, and again applying the Benjamini-Hochberg method to adjust P-values for multiple hypothesis testing.

RT–qPCR analysis

A list of the primers used for RT-qPCR is provided in Supplementary Table 2.2. Complementary DNA (cDNA) was synthesized using the Protoscript II First-Strand cDNA Synthesis kit (New England Biolabs). The elimination of genomic DNA was confirmed by qPCR amplification on negative control samples that did not have reverse transcriptase during cDNA synthesis. 8 ng of cDNA was used as a template for RT-qPCR using the SYBR Green Master Mix (Thermo Fisher Scientific) and performed in a Cycler 480 II Real-time PCR Machine (Roche). Forward and reverse primers were added at 3 μM each. Melting-curve analyses verified amplification of a single product. Gene expression changes were calculated based on mean change in the qPCR cycle threshold compared to *gyrB* or *16S* (ΔC_t) and are reported as $\log_2[\text{FC}] = \Delta C_t\_\text{CM} - \Delta C_t\_\text{sample}$. Each sample was analyzed with at least three technical replicates.

Western blot

For western blot analysis, we processed *S. pneumoniae* cell lysates and culture supernatants separately. For cell lysates, bacteria were cultured in THY broth with 0.1% CMC or mucin for 5 hours, washed, flash-frozen, and stored at -80 °C. Upon thawing, cells were lysed using B-PER Reagent (ThermoFisher) with a Halt Protease Inhibitor Cocktail added. Protein concentrations were determined with the Pierce BCA Protein Assay. For supernatant analysis, bacteria were

incubated overnight in THY with 0.1% CMC or mucin. The supernatant was collected and treated with protease inhibitor.

For blotting, 5 µg of lysate or 35 µL of supernatant were mixed with Laemmli buffer, heated, then separated on a 10% TGX gel, and electro-transferred to nitrocellulose membranes. Post-transfer, we used No-Stain Protein Labeling Reagent for total protein visualization as a loading control. Membranes were blocked in milk/PBS-Tween, incubated with an anti-PLY antibody (Abcam ab71811), washed, then incubated with a horseradish peroxidase-conjugated secondary antibody. After a final wash, we applied the Super Signal West Femto substrate for band detection, visualized with a ChemiDoc imager.

Hemolysis assay

The relative amount of pneumolysin (PLY) released into the culture supernatant was determined using a hemolytic assay. We isolated supernatants from *S. pneumoniae* cultures that had been grown for 5 hours with and without mucin and performed serial dilutions in PBS with 0.1% dithiothreitol. To these dilutions, we added a 1% solution of sheep red blood cells in PBS and incubated the mixture at 37 °C for one hour. For controls, we used water for complete hemolysis (100%) and PBS for no hemolysis (0%). Post-incubation, the red cells were centrifuged down, the supernatant carefully removed, and its absorbance measured at 540 nm to quantify the extent of hemolysis.

Human cell culture

We used certified mycoplasma-free A549 cells (ATCC, CCL-184), a human lung epithelial carcinoma cell line, sourced from the American Type Culture Collection (ATCC). We regularly checked the cells' morphology to ensure authenticity and conducted PCR tests to rule out contamination. The A549 cells were cultured in F-12K medium with 10% FBS at 37 °C in a 5% CO_2 environment, passaged at a 1:12 ratio upon reaching confluency. For bacterial co-culture experiments, the cells were seeded in glass-bottom 96-well plates until confluent.

Human neutrophils were isolated from blood obtained from healthy donors through Research Blood Components. The blood was treated with HetaSep in a 1:5 ratio, incubated at 37 °C for 30 minutes to separate leukocytes from erythrocytes. The leukocyte-rich fraction was then transferred to a new tube, erythrocytes lysed with lysis buffer, and the cell mixture was washed in PBS.

Neutrophils were subsequently isolated using the EasySep Direct Human Neutrophil Isolation kit, following the provided protocol. The isolated neutrophils were suspended in either PBS or R10 medium for subsequent assays.

Human cell visualization

S. pneumoniae was inoculated at 10^8 CFU/mL and grown for 3 hours with and without mucin. We isolated and purified the supernatant by passing it through 0.22 μm filters to eliminate any bacterial cells. This filtered supernatant, along with a THY medium control, was then applied in triplicate to A549 cell monolayers and neutrophils seeded in glass-bottom 96-well plates. The plates were incubated at 37 °C with 5% CO_2 for 60 minutes. Subsequently, we added the LIVE/DEAD Cell Imaging reagent and allowed a further incubation at room temperature for 15 minutes. We captured images using a Zeiss LSM 800 confocal microscope with a 63× oil immersion lens and analyzed them with Zeiss ZEN software version 2.1. The images provided are representative of the observed results.

Human cell cytotoxicity assay

S. pneumoniae was inoculated at 10^8 CFU/mL and grown for 3 hours with and without mucin. Following incubation, supernatants were separated and passed through 0.22 μm filters to remove bacterial cells. These filtered supernatants, along with THY medium controls, were added to A549 cells or neutrophils, which were suspended at 10^5 cells per well in a 96-well plate in triplicate. To assess cell viability, we added alamarBlue reagent and incubated the plates at 37 °C with 5% CO_2. After two hours, we measured fluorescence at 560/590 nm (excitation/emission) using a plate reader. Cell viability percentages were calculated relative to the medium control and adjusted for background fluorescence.

In assays using live bacteria, we suspended 4×10^5 neutrophils in 400 μL of R10 medium with or without 0.1% MUC5AC. We then added *S. pneumoniae* TIGR4 or its *ply*-deficient variant at multiple multiplicities of infection (MOI of 0.1, 1, 10, and 100), and the mixtures were incubated overnight for 16 hours at 37 °C with 5% CO_2. The next day, supernatants were collected, and lactate dehydrogenase (LDH) release was quantified using the LDH release assay kit (ab65393; Abcam) as per the manufacturer's protocol.

Neutrophil viability and phagocytosis

To assess neutrophil phagocytosis and bactericidal activity, we prepared a suspension of 5×10^5 neutrophils in Hank's balanced salt solution fortified with calcium and magnesium (HBSS++; Thermo Fisher Scientific), with or without 0.1% MUC5AC. We treated GFP-tagged *S. pneumoniae* TIGR4 and its ply-deficient variant (TIGR4Δ*ply*) with 50% human serum in HBSS++ to opsonize the bacteria, then incubated this mixture at 37 °C with 5% CO_2 for 30 minutes. The neutrophils were then exposed to the opsonized bacteria at multiplicities of infection (MOIs) of 10 and 100 and incubated for one hour under the same conditions to allow phagocytosis. Following phagocytosis, we applied gentamicin at 100 μg/mL for five minutes at room temperature to eliminate any bacteria not internalized by the neutrophils. After two washes with PBS, the neutrophils underwent further incubation for one and two hours, after which we analyzed the neutrophils and internalized GFP-positive *S. pneumoniae* by flow cytometry.

Flow cytometry

For flow cytometry, neutrophils were labeled with CD66b-PerCP/Cy5.5 (BioLegend) at a 1:100 dilution and Fixable Viability Dye (eBioscience) at a 1:1,000 dilution in FACS buffer, a solution of PBS supplemented with 0.1% bovine serum albumin. This staining process was carried out for 25 minutes at 4 °C in the dark. Following staining, cells were washed in PBS, centrifuged, and fixed in a 1% formaldehyde solution in PBS overnight at 4 °C. The next day, we washed the samples again in PBS, centrifuged them, resuspended them in 200 μL of FACS buffer, and filtered through a 35μm strainer. The prepared cells were then analyzed on a FACS Celesta flow cytometer (BD Biosciences). For data analysis, we used FlowJo software version 10.

ELISA

Cytokine production by neutrophils was assessed by resuspending 4×10^5 cells in 400 μL of R10 medium, with or without 0.1% MUC5AC. We then introduced *S. pneumoniae* TIGR4 or its ply-deficient variant (TIGR4Δ*ply*) at multiplicities of infection (MOI) of 1 and 0.1. After incubating the co-cultures overnight for 16 hours at 37 °C with 5% CO_2, we harvested the supernatants. Concentrations of myeloperoxidase (MPO) and IL-1β in the supernatants were measured using ELISA kits from BioLegend according to the manufacturer's instructions.

In vivo *intratracheal infection model*

All animal studies were conducted in accordance with federal regulations set forth in the Animal Welfare Act. All experiments were performed based on UCSD Institution Animal Care and Use Committee (IACUC) approved protocols (#S00227M) and recommendations by the guide for the care and use of laboratory animals. Mice were housed in specific pathogen-free facility with a 12-hour light/dark cycle on pre-bedded corn cob disposable cages (Innovive). Mice received acidified water and 2020X chow (Envigo). For intratracheal infections, mice were anesthetized with 100 mg/kg ketamine and 10 mg/kg xylazine prior to visualization of the vocal cords using an otolaryngoscope (Welch Allyn). 8-10 week old C57BL/6 mice (Jackson Labs) were infected with ~$5*10^6$ CFUs TIGR4 WT grown in the presence of THY, 0.1% MUC5AC or 0.1% MUC5AC glycans. In one of two experiments pooled, 8 hours post infection, mice received intratracheal treatment of 40 μL THY, 0.1% MUC5AC, or MUC5AC after brief anesthesia with isoflurane. Mice were monitored for full recovery. At 24 hours post infection, mice were humanely euthanized according to approved protocols. Blood was harvested by cardiac puncture and lungs were homogenized. Blood and lungs were serially diluted and plated on TSA + 5% sheep's blood for enumeration.

Statistics and reproducibility

All experiments were conducted with a minimum of three biological replicates. Data are reported as the mean ± standard error of the mean (s.e.m.). Where applicable, we employed the Mann-Whitney U-test or the Wilcoxon signed-rank test for statistical analysis. The microscopy images provided are representative of consistent observations across multiple fields. Source data for the raw measurements can be accessed upon request. We have verified that MUC2, MUC5AC, MUC5B, and their glycans show reproducible results across various purification batches.

Data availability

RNA-sequencing data will be made available in the Gene Expression Omnibus (GEO) upon publication. Until then, all data that support the findings of this study are available from the author upon reasonable request.

References

Berry, A. M., Lock, R. A., Hansman, D., & Paton, J. C. (1989). Contribution of Autolysin to Virulence of Streptococcus pneumoniae. *Infection and Immunity*, 2324–2330. https://journals.asm.org/journal/iai

Bryant, J. C., Dabbs, R. C., Oswalt, K. L., Brown, L. R., Rosch, J. W., Seo, K. S., Donaldson, J. R., McDaniel, L. S., & Thornton, J. A. (2016). Pyruvate oxidase of Streptococcus pneumoniae contributes to pneumolysin release. *BMC Microbiology*, *16*(1), 1–12. https://doi.org/10.1186/s12866-016-0881-6

Buckwalter, C. M., & King, S. J. (2012). Pneumococcal carbohydrate transport: Food for thought. In *Trends in Microbiology* (Vol. 20, Issue 11, pp. 517–522). https://doi.org/10.1016/j.tim.2012.08.008

Celli, J. P., Turner, B. S., Afdhal, N. H., Ewoldt, R. H., McKinley, G. H., Bansil, R., & Erramilli, S. (2007). Rheology of gastric mucin exhibits a pH-dependent sol-gel transition. *Biomacromolecules*, *8*(5), 1580–1586. https://doi.org/10.1021/bm0609691

Co, J. Y., Cárcamo-Oyarce, G., Billings, N., Wheeler, K. M., Grindy, S. C., Holten-Andersen, N., & Ribbeck, K. (2018). Mucins trigger dispersal of Pseudomonas aeruginosa biofilms. *Npj Biofilms and Microbiomes*, *4*(1). https://doi.org/10.1038/s41522-018-0067-0

Cockeran, R., Durandt, C., Feldman, C., Mitchell, T. J., Anderson, R., & Anderson, R. (2002). Pneumolysin Activates the Synthesis and Release of Interleukin-8 by Human Neutrophils In Vitro. In *The Journal of Infectious Diseases* (Vol. 186). https://academic.oup.com/jid/article/186/4/562/807202

Domon, H., & Terao, Y. (2021). The Role of Neutrophils and Neutrophil Elastase in Pneumococcal Pneumonia. In *Frontiers in Cellular and Infection Microbiology* (Vol. 11). Frontiers Media S.A. https://doi.org/10.3389/fcimb.2021.615959

Garvy, B. A., & Harmsen, A. G. (1996). The importance of neutrophils resistance to pneumococcal pneumonia in adult and neonatal mice. *Inflammation*, *20*(5).

Gierke, R., Wodi, A. P., & Kobayashi, M. (2021). Pneumococcal Disease. In E. Hall, A. P. Wodi, J. Hamborsky, V. Morelli, & S. Schillie (Eds.), *Epidemiology and Prevention of Vaccine-Preventable Diseases* (14th ed., pp. 255–274). Public Health Foundation.

Goekeri, C., Pennitz, P., Groenewald, W., Behrendt, U., Kirsten, H., Zobel, C. M., Berger, S., Heinz, G. A., Mashreghi, M. F., Wienhold, S. M., Dietert, K., Dorhoi, A., Gruber, A. D.,

Scholz, M., Rohde, G., Suttorp, N., Witzenrath, M., & Nouailles, G. (2023). MicroRNA-223 Dampens Pulmonary Inflammation during Pneumococcal Pneumonia. *Cells*, *12*(6). https://doi.org/10.3390/cells12060959

Gullett, J. M., Cuypers, M. G., Frank, M. W., White, S. W., & Rock, C. O. (2019). A fatty acid-binding protein of Streptococcus pneumoniae facilitates the acquisition of host polyunsaturated fatty acids. *Journal of Biological Chemistry*, *294*(44), 16416–16428. https://doi.org/10.1074/jbc.RA119.010659

Houldsworth, S., Andrew, P. W., & Mitchell, T. J. (1994). *Pneumolysin Stimulates Production of Tumor Necrosis Factor Alpha and Interleukin-13 by Human Mononuclear Phagocytes* (Vol. 62, Issue 4). https://journals.asm.org/journal/iai

Jacques, L. C., Panagiotou, S., Baltazar, M., Senghore, M., Khandaker, S., Xu, R., Bricio-Moreno, L., Yang, M., Dowson, C. G., Everett, D. B., Neill, D. R., & Kadioglu, A. (2020). Increased pathogenicity of pneumococcal serotype 1 is driven by rapid autolysis and release of pneumolysin. *Nature Communications*, *11*(1). https://doi.org/10.1038/s41467-020-15751-6

Jim, K. K., Aprianto, R., Koning, R., Domenech, A., Kurushima, J., van de Beek, D., Vandenbroucke-Grauls, C. M. J. E., Bitter, W., & Veening, J. W. (2022). Pneumolysin promotes host cell necroptosis and bacterial competence during pneumococcal meningitis as shown by whole-animal dual RNA-seq. *Cell Reports*, *41*(12). https://doi.org/10.1016/j.celrep.2022.111851

Kjos, M., Aprianto, R., Fernandes, V. E., Andrew, P. W., Van Strijp, J. A. G., Nijland, R., & Veening, J. W. (2015). Bright fluorescent Streptococcus pneumoniae for live-cell imaging of host-pathogen interactions. *Journal of Bacteriology*, *197*(5), 807–818. https://doi.org/10.1128/JB.02221-14

Mathew, B. J., Gupta, P., Naaz, T., Rai, R., Gupta, S., Gupta, S., Chaurasiya, S. K., Purwar, S., Biswas, D., Vyas, A. K., & Singh, A. K. (2023). Role of Streptococcus pneumoniae extracellular glycosidases in immune evasion. In *Frontiers in Cellular and Infection Microbiology* (Vol. 13). Frontiers Media S.A. https://doi.org/10.3389/fcimb.2023.1109449

McNeela, E. A., Burke, Á., Neill, D. R., Baxter, C., Fernandes, V. E., Ferreira, D., Smeaton, S., El-Rachkidy, R., McLoughlin, R. M., Mori, A., Moran, B., Fitzgerald, K. A., Tschopp, J., Pétrilli, V., Andrew, P. W., Kadioglu, A., & Lavelle, E. C. (2010). Pneumolysin Activates

the NLRP3 Inflammasome and Promotes Proinflammatory Cytokines Independently of TLR4. *PLOS Pathogens*, *6*(11), e1001191. https://doi.org/10.1371/journal.ppat.1001191

Price, K. E., Greene, N. G., & Camilli, A. (2012). Export requirements of pneumolysin in Streptococcus pneumoniae. *Journal of Bacteriology*, *194*(14), 3651–3660. https://doi.org/10.1128/JB.00114-12

Rubins, J. B., Duane, P. G., Clawson, D., Charboneau,', D., Young,' And, J., & Niewoehner, D. E. (1993). Toxicity of Pneumolysin to Pulmonary Alveolar Epithelial Cells. In *INFECTION AND IMMUNITY*. https://journals.asm.org/journal/iai

Stevens, E. J., Morse, D. J., Bonini, D., Duggan, S., Brignoli, T., Recker, M., Lees, J. A., Croucher, N. J., Bentley, S., Wilson, D. J., Earle, S. G., Dixon, R., Nobbs, A., Jenkinson, H., van Opijnen, T., Thibault, D., Wilkinson, O. J., Dillingham, M. S., Carlile, S., … Massey, R. C. (2022). Targeted control of pneumolysin production by a mobile genetic element in Streptococcus pneumoniae. *Microbial Genomics*, *8*(4). https://doi.org/10.1099/mgen.0.000784

Subramanian, K., Neill, D. R., Malak, H. A., Spelmink, L., Khandaker, S., Dalla Libera Marchiori, G., Dearing, E., Kirby, A., Yang, M., Achour, A., Nilvebrant, J., Nygren, P. Å., Plant, L., Kadioglu, A., & Henriques-Normark, B. (2019). Pneumolysin binds to the mannose receptor C type 1 (MRC-1) leading to anti-inflammatory responses and enhanced pneumococcal survival. In *Nature Microbiology* (Vol. 4, Issue 1, pp. 62–70). Nature Publishing Group. https://doi.org/10.1038/s41564-018-0280-x

Takagi, J., Aoki, K., Turner, B. S., Lamont, S., Lehoux, S., Kavanaugh, N., Gulati, M., Valle Arevalo, A., Lawrence, T. J., Kim, C. Y., Bakshi, B., Ishihara, M., Nobile, C. J., Cummings, R. D., Wozniak, D. J., Tiemeyer, M., Hevey, R., & Ribbeck, K. (2022). Mucin O-glycans are natural inhibitors of Candida albicans pathogenicity. *Nature Chemical Biology*, *18*(7), 762–773. https://doi.org/10.1038/s41589-022-01035-1

Tettelin, H., Nelson, K., Paulsen, I. T., Eisen, J. A., Read, T. D., Haft, D. H., Dodson, R. J., Durkin, A. S., Gwinn, M., Kolonay, J. F., Nelson, W. C., Peterson, J. D., Umayam, L. A., White, O., Salzberg, S. L., Lewis, M. R., Radune, D., Holtzapple, E., Khouri, H., … Fraser, C. M. (2001). Complete genome sequence of a virulent isolate of Streptococcus pneumoniae. *Science*, *293*(5529), 498–506. https://doi.org/10.1126/science.1061217

Thornton, D. J., Rousseau, K., & McGuckin, M. A. (2008). Structure and Function of the Polymeric Mucins in Airways Mucus. *Annual Review of Physiology*, *70*(1), 459–486. https://doi.org/10.1146/annurev.physiol.70.113006.100702

Troeger, C., Blacker, B., Khalil, I. A., Rao, P. C., Cao, J., Zimsen, S. R. M., Albertson, S. B., Deshpande, A., Farag, T., Abebe, Z., Adetifa, I. M. O., Adhikari, T. B., Akibu, M., Al Lami, F. H., Al-Eyadhy, A., Alvis-Guzman, N., Amare, A. T., Amoako, Y. A., Antonio, C. A. T., … Reiner, R. C. (2018). Estimates of the global, regional, and national morbidity, mortality, and aetiologies of lower respiratory infections in 195 countries, 1990–2016: a systematic analysis for the Global Burden of Disease Study 2016. *The Lancet Infectious Diseases*, *18*(11), 1191–1210. https://doi.org/10.1016/S1473-3099(18)30310-4

Van De Rijn, I., & Kessler, R. E. (1980). Growth Characteristics of Group A Streptococci in a New Chemically Defined Medium. *Infection and Immunity*, *27*(2), 444–448. https://journals.asm.org/journal/iai

van der Reijden, W. A., Veerman, E. C. I., & Nieuw Amerongen, A. V. (1994). Rheological properties of commercially available polysaccharides with potential use in saliva substitutes. *Biorheology*, *31*, 631–642. https://doi.org/10.3233/BIR-1994-31604

Wagner, C. E., Wheeler, K. M., & Ribbeck, K. (2018). Mucins and Their Role in Shaping the Functions of Mucus Barriers. *Annual Review of Cell and Developmental Biology*, *34*(1), 189–215. https://doi.org/10.1146/annurev-cellbio-100617-062818

Wang, B. X., Wheeler, K. M., Cady, K. C., Lehoux, S., Cummings, R. D., Laub, M. T., & Ribbeck, K. (2021). Mucin Glycans Signal through the Sensor Kinase RetS to Inhibit Virulence-Associated Traits in Pseudomonas aeruginosa. *Current Biology*, *31*(1), 90-102.e7. https://doi.org/10.1016/j.cub.2020.09.088

Weiser, J. N., Ferreira, D. M., & Paton, J. C. (2018). Streptococcus pneumoniae: Transmission, colonization and invasion. In *Nature Reviews Microbiology* (Vol. 16, Issue 6, pp. 355–367). Nature Publishing Group. https://doi.org/10.1038/s41579-018-0001-8

Werlang, C. A., Chen, W. G., Aoki, K., Wheeler, K. M., Tymm, C., Mileti, C. J., Burgos, A. C., Kim, K., Tiemeyer, M., & Ribbeck, K. (2021). Mucin O-glycans suppress quorum-sensing pathways and genetic transformation in Streptococcus mutans. *Nature Microbiology*. https://doi.org/10.1038/s41564-021-00876-1

Werlang, C., Cárcarmo-Oyarce, G., & Ribbeck, K. (2019). Engineering mucus to study and influence the microbiome. *Nature Reviews Materials*, *4*(February). https://doi.org/10.1038/s41578-018-0079-7

Wheeler, K. M., Cárcamo-Oyarce, G., Turner, B. S., Dellos-Nolan, S., Co, J. Y., Lehoux, S., Cummings, R. D., Wozniak, D. J., & Ribbeck, K. (2019). Mucin glycans attenuate the virulence of Pseudomonas aeruginosa in infection. In *Nature Microbiology* (Vol. 4, Issue 12, pp. 2146–2154). Nature Research. https://doi.org/10.1038/s41564-019-0581-8

Witzenrath, M., Gutbier, B., Hocke, A. C., Schmeck, B., Hippenstiel, S., Berger, K., Mitchell, T. J., De Los Toyos, J. R., Rosseau, S., Suttorp, N., & Schütte, H. (2006). Role of pneumolysin for the development of acute lung injury in pneumococcal pneumonia. *Critical Care Medicine*, *34*(7), 1947–1954. https://doi.org/10.1097/01.CCM.0000220496.48295.A9

Witzenrath, M., Pache, F., Lorenz, D., Koppe, U., Gutbier, B., Tabeling, C., Reppe, K., Meixenberger, K., Dorhoi, A., Ma, J., Holmes, A., Trendelenburg, G., Heimesaat, M. M., Bereswill, S., van der Linden, M., Tschopp, J., Mitchell, T. J., Suttorp, N., & Opitz, B. (2011). The NLRP3 Inflammasome Is differentially activated by pneumolysin variants and contributes to host defense in pneumococcal pneumonia. *The Journal of Immunology*, *187*(1), 434 LP – 440. https://doi.org/10.4049/jimmunol.1003143

Xiang, Y., Jin, C., Wang, W., Wang, Z., Huang, Y., Fan, F., Ma, Y., Zhang, X., Xu, W., Yin, Y., & He, Y. (2017). The critical role of myeloperoxidase in Streptococcus pneumoniae clearance and tissue damage during mouse acute otitis media. *Innate Immunity*, *23*(3), 296–306. https://doi.org/10.1177/1753425917693907

Yesilkaya, H., Manco, S., Kadioglu, A., Terra, V. S., & Andrew, P. W. (2008). The ability to utilize mucin affects the regulation of virulence gene expression in Streptococcus pneumoniae. *FEMS Microbiology Letters*, *278*(2), 231–235. https://doi.org/10.1111/j.1574-6968.2007.01003.x

Yoo, I. H., Shin, H. S., Kim, Y. J., Kim, H. B., Jin, S., & Ha, U. H. (2010). Role of pneumococcal pneumolysin in the induction of an inflammatory response in human epithelial cells. *FEMS Immunology and Medical Microbiology*, *60*(1), 28–35. https://doi.org/10.1111/j.1574-695X.2010.00699.x

Zafar, M. A., Wang, Y., Hamaguchi, S., & Weiser, J. N. (2017). Host-to-Host Transmission of Streptococcus pneumoniae Is Driven by Its Inflammatory Toxin, Pneumolysin. *Cell Host and Microbe*, *21*(1), 73–83. https://doi.org/10.1016/j.chom.2016.12.005

Acknowledgements

We thank K. Hatch, A. Walsh, and C. Werlang for comments on the manuscript. This research was supported by the NIH NIAID award R21AI167289 (K.R.), R01AI176554 (V.N.), the Deutsche Forschungsgemeinschaft grant SFB 1449-431232613 sub-project B02 (GN, CG), the National Science Foundation MIM grant EF-2125118 (K.R.), the US Army Research Office under cooperative agreement W911NF1920026 for the Institute for Collaborative Biotechnologies (K.R.), the Toxicology Training Grant support T32-ES007020 (J.B.), the A.P. Giannini Foundation Postdoctoral Fellowship (E.B.), and ARO MURI award W911NF2210185 (K.R.). We acknowledge additional support from the MIT BioMicro Center and the National Institute of Environmental Health Sciences of the NIH Center grant P30ES002109. Biorender was used to create Figure 1a.

Figures

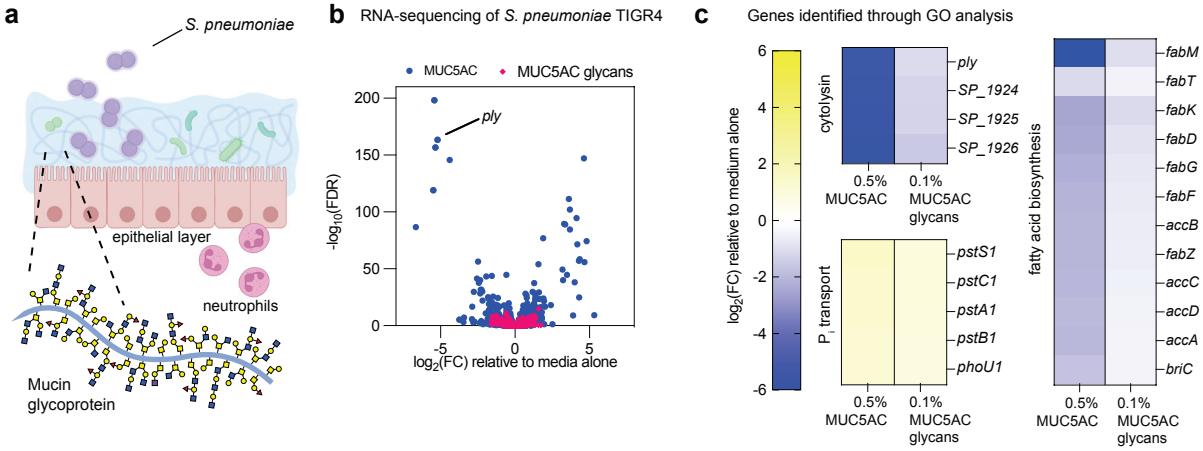

Figure 2.1: Gene expression analysis reveals mucins and mucin glycans downregulate pneumolysin.

(A) Mucus coats the epithelial layer, creating an ecological niche and barrier against microbes including *S. pneumoniae*. **(B)** MUC5AC and mucin glycans elicit global transcriptional responses in *S. pneumoniae* TIGR4 at 5 h. Fold change (FC) data are average measurements for $n = 4$ biological replicates. FDR-adjusted *P* values were determined using the Benjamini-Hochberg *P*-value adjustment method. **(C)** Heatmap shows RNA-seq FC values for selected genes representing pathways regulated by mucins and mucin glycans.

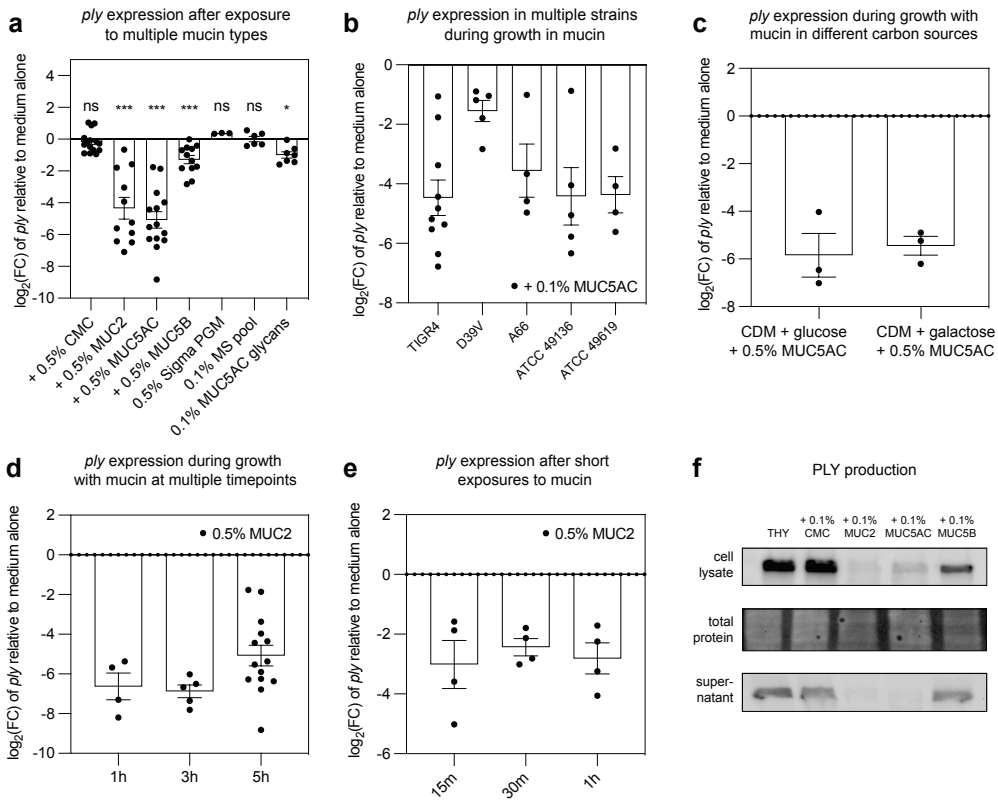

Figure 2.2: Gene and protein expression analysis reveals robust regulation of *ply* after exposure to mucin.

(A) *Ply* expression was measured after exposure to multiple mucin types after 5 h growth by RT-qPCR and normalized to *gyrB* expression. Significance was assessed using the Wilcoxon signed-rank test. **(B)** *Ply* expression in multiple strains was measured by RT-qPCR after 5 h and normalized to *16S* expression. **(C)** *Ply* expression was measured by RT-qPCR after 5 h growth in CDM supplemented with glucose or galactose and normalized to a control gene (*gyrB*). **(D)** *Ply* expression was measured after 1, 3 or 5 h of growth with mucins by RT-qPCR and normalized to *gyrB*. **(E)** *Ply* expression was measured after 15 min, 30 min, and 1 hour of exposure to mucin after 5 h total growth by RT-qPCR and normalized to *gyrB*. **(F)** Representative western blot of PLY in cell lysate (5 h) or culture supernatant (24 h) of *S. pneumoniae* treated with mucins or CMC. **(A-E)** Bars indicate mean ± s.e.m. with biological replicates shown. ns: not significant; * $P < 0.05$; ** $P < 0.01$; *** $P < 0.001$; **** $P<0.0001$.

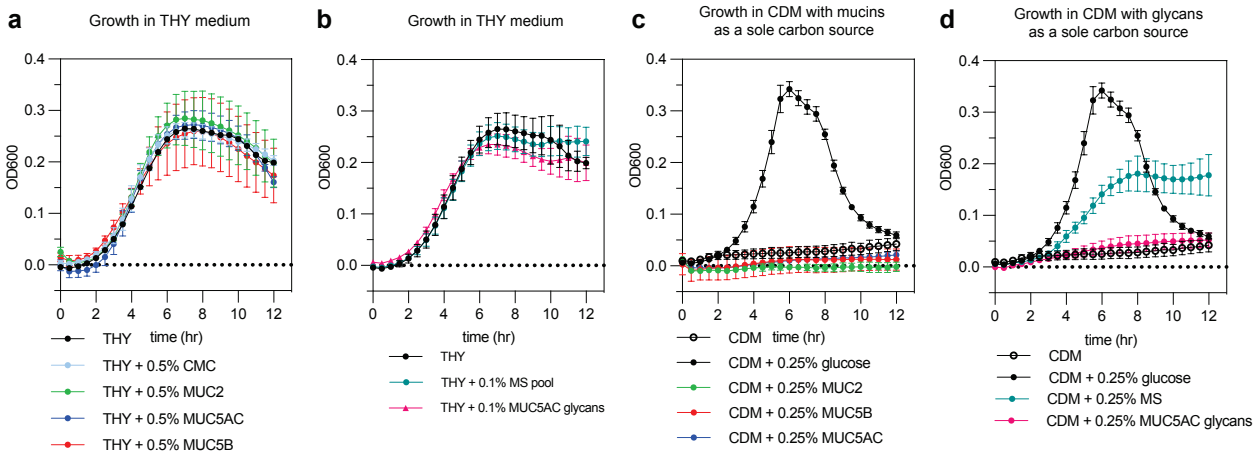

Figure 2.3: Gene expression analysis reveals mucins and mucin glycans downregulate pneumolysin.

(A) *S. pneumoniae* growth in THY supplemented with mucins or CMC. **(B)** *S. pneumoniae* growth in THY supplemented with mucin glycans or a pool of monosaccharides. **(C)** *S. pneumoniae* growth in CDM supplemented with glucose, mucins, or CMC as a sole carbon source. **(D)** *S. pneumoniae* growth in CDM supplemented with glucose, mucin glycans, or a pool of monosaccharides as a sole carbon source. **(A-D)** Data are the mean OD value at 600 nm ± s.e.m. for $n \geq 3$ biological replicates**.**

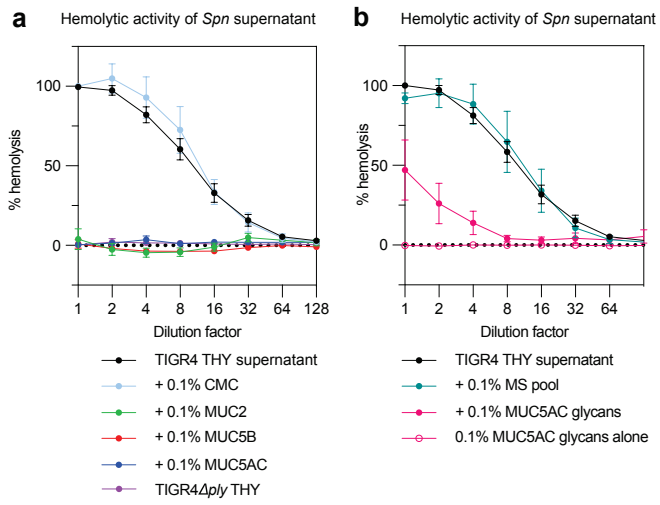

Figure 2.4: Mucins and mucin glycans suppress hemolysis.

(A) and **(B)** Hemolytic activity of *S. pneumoniae* culture supernatant (5 h) was assessed by absorbance of serially diluted supernatants at 540 nm relative to the WT and a PBS control. Data are mean % hemolysis ± s.e.m. for $n \geq 3$ biological replicates.

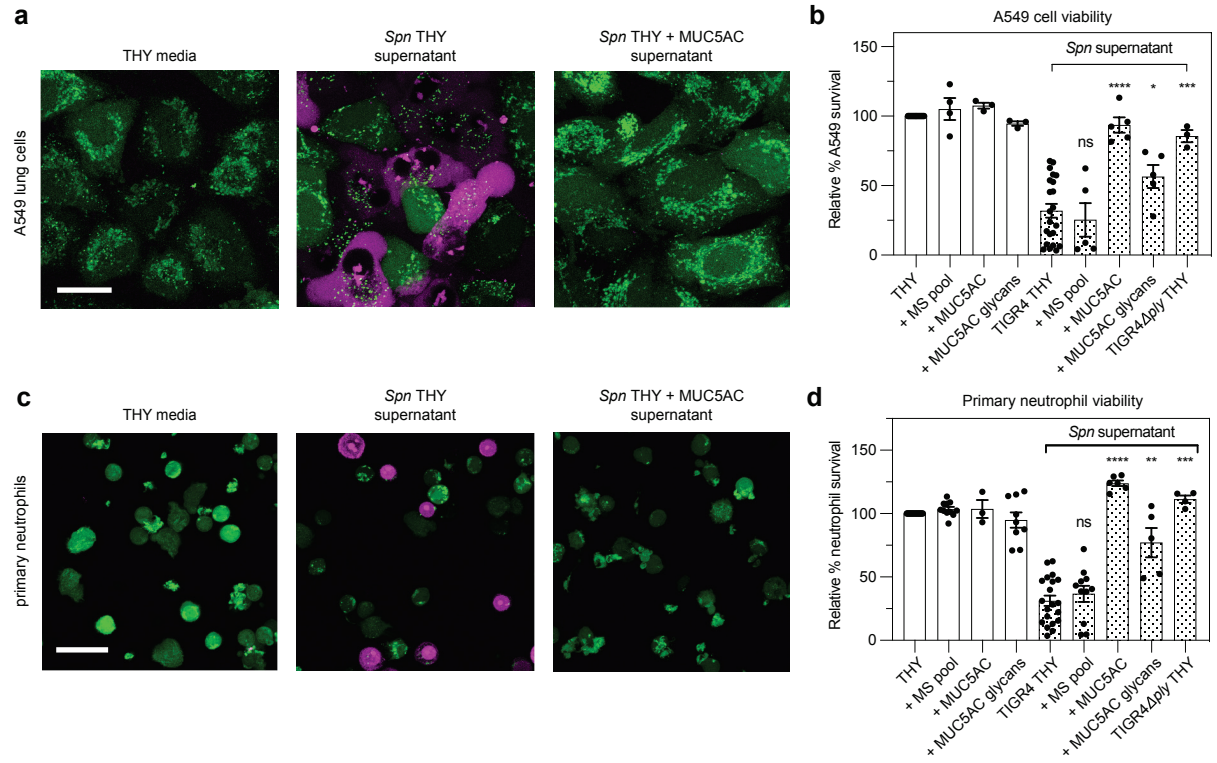

Figure 2.5: Mucins protect host cells from PLY-dependent killing and modulate neutrophil activity.

(A, C) Representative confocal microscopy of lung epithelial cells (**A**) and neutrophils (**C**) treated with LIVE/DEAD stain shows cell viability after treatment with medium, *S. pneumoniae* culture supernatant, or supernatant from MUC5AC-treated cultures. Scale bar, 20 μm. **(B, D)** Cell viability of lung epithelial cells (**B**) and neutrophils (**D**) was measured using alamarBlue after treatment with medium or *S. pneumoniae* culture supernatant relative to a medium control. **(B, D)** Bars indicate mean ± s.e.m. with biological replicates shown and the Mann-Whitney U test was used to assess significance. ns: not significant; * $P < 0.05$; ** $P < 0.01$; *** $P < 0.001$; **** $P<0.0001$.

.

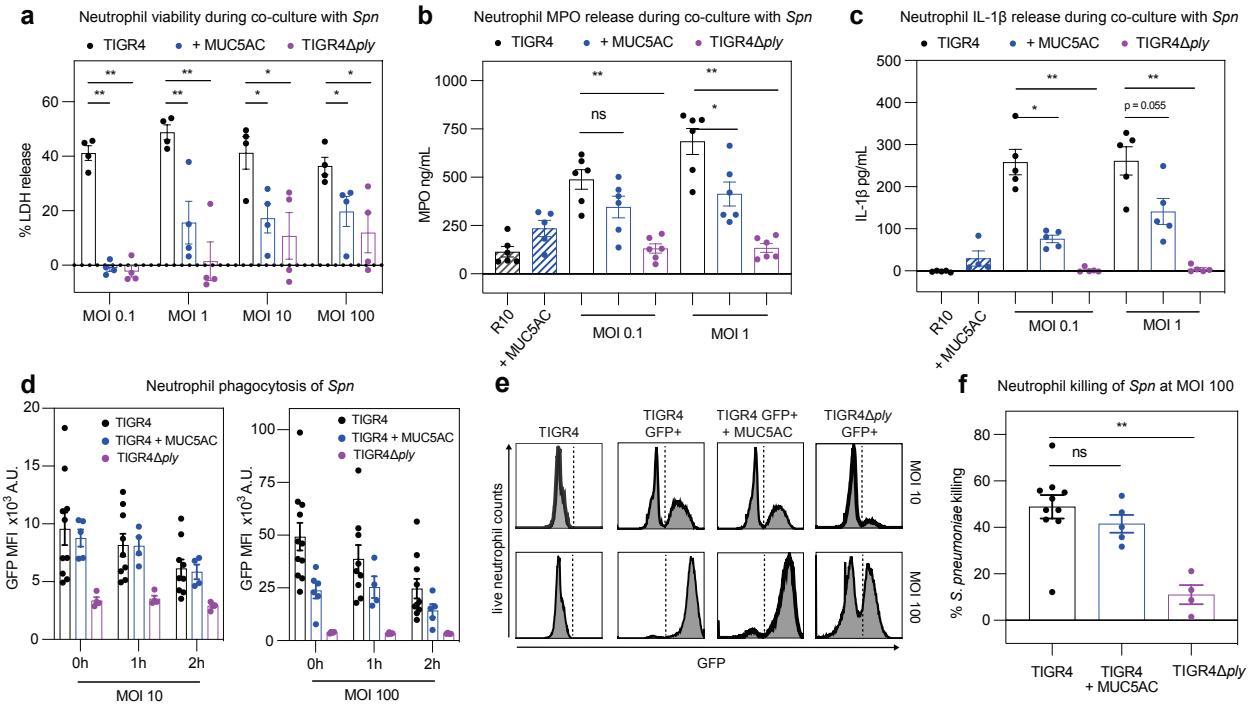

Figure 2.6: Mucins modulate neutrophil viability and activity during co-culture with *S. pneumoniae*.

(A) Neutrophil viability was measured after 16 h by LDH release assay during co-culture with *S. pneumoniae* TIGR4, TIGR4 + 0.1% MUC5AC, or TIGR4Δ*ply* at multiple MOIs. **(B-C)** Neutrophil secretion of MPO **(B)** and IL-1β **(C)** was measured by ELISA after stimulation with TIGR4, TIGR4 + 0.1% MUC5AC, or TIGR4Δ*ply*. **(D)** Phagocytosis was measured by flow cytometry with GFP-expressing *S. pneumoniae* TIGR4, TIGR4 + 0.1% MUC5AC or TIGR4Δ*ply*. Neutrophil GFP mean fluorescence intensity (MFI) at multiple timepoints shows phagocytosis and bacterial killing. The gating strategy for this experiment is available in Supplementary Fig. 2.1. **(E)** Representative histograms of neutrophil and GFP signal during neutrophil co-culture with *S. pneumoniae.* The dashed line separates GFP^+ and GFP^- populations. **(F)** Bacterial killing was quantified by comparing the GFP MFI at 2 h versus 0 h. **(A-D, F)** Bars show mean ± s.e.m. with individual biological replicates shown. A.U.: arbitrary units; Significance was assessed with the Mann-Whitney U test. ns: not significant; * $P < 0.05$; ** $P < 0.01$; *** $P < 0.001$; **** $P<0.0001$.

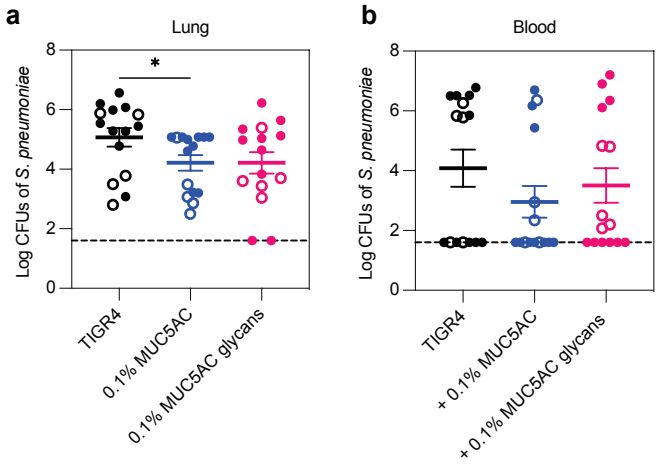

Figure 2.7: Pre-treatment with mucins reduces bacterial burden in the mouse lung.

(A, B) Mice were infected intratracheally with 10^6 CFUs TIGR4 grown in the presence of THY, MUC5AC or MUC5AC glycans. Lungs **(A)** and blood **(B)** were harvested 24 h post infection and plated to enumerate bacterial survival. Data show two experiments pooled, *n*=15/group. In one experiment (*n*=10, closed circles), mice received an additional dose of MUC5AC, or MUC5AC glycans 8 h post infection. Data are depicted as mean ± s.e.m. with individual biological replicates shown. Kruskal-Wallis test with Dunn's correction: ns (not significant), * ($P < 0.05$).

Supplementary Figures

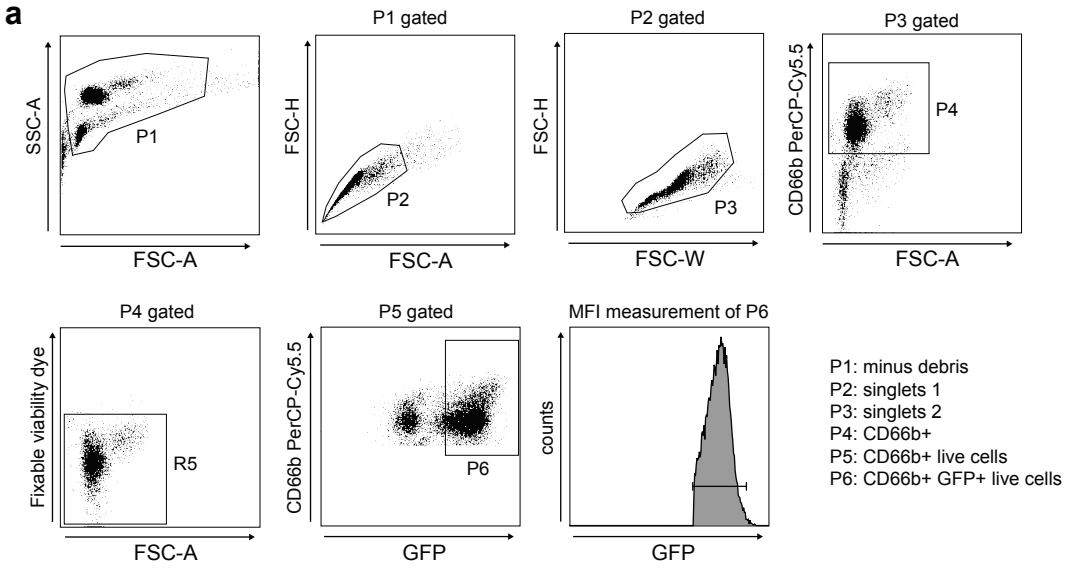

Supplementary Figure 2.1: Flow cytometry gating strategy.

(A) Dot plots and gating strategy used to identify neutrophils that have engulfed *S. pneumoniae* (CD66+ GFP+) via flow cytometry. The MFI was analyzed for each sample. FSC: forward scatter; SSC: side scatter.

Supplementary Tables

Strain	Species	Description	Source
TIGR4	*S. pneumoniae*	Serotype 4, WT	Tettelin et al. 2001
TIGR4-GFP	*S. pneumoniae*	PhlpA-hlpA-gfp_CamR	This study
TIGR4Δ*spxB*	*S. pneumoniae*	ΔspxB-EryR	Bryant et al. 2016
TIGR4Δ*ply*	*S. pneumoniae*	Δply-EryR	Bryant et al. 2016
TIGR4Δ*ply*-GFP	*S. pneumoniae*	Δply-EryR; PhlpA-hlpA-gfp_CamR	This study
D39V	*S. pneumoniae*	Serotype 2, WT	Kjos et al. 2015
JWV500	*S. pneumoniae*	D39V PhlpA-hlpA-gfp_CamR	Kjos et al. 2015
PN36	*S. pneumoniae*	Serotype 3, WT	NCTC 7978
ATCC 49136	*S. pneumoniae*	Serotype 17, WT	ATCC 49136
ATCC 49619	*S. pneumoniae*	Serotype 19F, WT	ATCC 49619

Supplementary Table 2.1: Strains of bacteria used in the study presented in Chapter 2.

Primer name	Purpose	Primer Sequence 5'>3'
hlpA-F	Generation of GFP+ strain	AACAAGTCAGCCACCTGTAG
hlpA-R	Generation of GFP+ strain	CGTGGCTGACGATAATGAGG
ply_up-F	Replace *ply* with ermB casette	CTCAATCCAGCTACCTGTCGC
ply_up_R_ermB	Replace *ply* with ermB casette	GTTTGCTTCTAAGTCTTATTTCC CTTCTACCTCCTAATAAG
ermB-F	Replace *ply* with ermB casette	GGAAATAAGACTTAGAAGCAAAC
ermB-R	Replace *ply* with ermB casette	CCAAATTTACAAAAGCGACTC
ply_down_F_ermB	Replace *ply* with ermB casette	GAGTCGCTTTTGTAAATTTGG GAGAGGAGAATGCTTGCG
ply_down-R	Replace *ply* with ermB casette	GCTTGTTTAGCACGGTCGATAACG
blpJ-F	RT-qPCR blpJ	ATGCTTGCGAAAGTTGAAGGG
blpJ-R	RT-qPCR blpJ	CTGCTCCAGTTCCACCAGTT
blpX-F	RT-qPCR blpX	ACAGTGGTTTGTTTGAAGCAGG
blpX-R	RT-qPCR blpX	GCGATTTCGAATATCTACTTCCTTG
ciaR-F	RT-qPCR ciaR	TGACTGCCAAGGAAAGTTTG
ciaR-R	RT-qPCR ciaR	GTTTGAGAAGGGCCTGAATC
comE-F	RT-qPCR comE	CATTCGTCATTACAATCCTTACG
comE-R	RT-qPCR comE	CAAAATCTAGGGCTGATACCTGG
ply-F	RT-qPCR ply	GAGAGGAATTTCTGCAGAGC
ply-R	RT-qPCR ply	CTTCATCACTCTTACTCGTGG
16S-F	RT-qPCR 16S	CTGCGTTGTATTAGCTAGTTGGTG
16S-R	RT-qPCR 16S	TCCGTCCATTGCCGAAGATTC
gyrB-F	RT-qPCR gyrB	CCAATCCTAGAAGCTGGTTATGT
gyrB-R	RT-qPCR gyrB	CACCCGGCTGGATATATTCTTT

Supplementary Table 2.2: Primers used in the study presented in Chapter 2.

Chapter 3: Mucins suppress bacteriocin expression and reduce antagonism of *S. pneumoniae* against nasopharyngeal microbes

Work presented in this chapter was performed by
Jade Bath, Rachel Hevey, and Katharina Ribbeck

Abstract

Mucus hosts diverse microbial communities throughout the body, including on the surface of the nasopharynx. Mucins, the main gel-forming component of mucus, regulate microbial communities through multiple mechanisms, including by acting as a signaling molecule. In this study, we show that mucins downregulate the competence and bacteriocin systems that drive competitive behaviors in *S. pneumoniae*, a habitual resident of the nasopharyngeal microbiota. We show that mucins reduce the antagonism of *S. pneumoniae* against multiple nasopharyngeal pathogens independently of H_2O_2 production, a major competitive strategy of *S. pneumoniae*. Lastly, we show that a pool of mucin glycans, monosaccharides, and individual mucin glycans regulate genes responsible for bacteriocin production. Together, these findings suggest mucins suppress the ability of *S. pneumoniae* to compete within a microbial community, highlighting the potential for leveraging mucins and mucin glycans to bolster bacterial communities against opportunistic pathogens

Introduction

When *S. pneumoniae* invades the nasopharynx, the bacterium must compete with the existing microbiota of the upper respiratory tract (URT) to establish itself. Colonization always precedes invasive disease; thus, the establishment of colonization is a critical step for pneumococcal pathogenesis. One method *S. pneumoniae* utilizes to compete is the secretion of bacteriocins, short peptides that disrupt cell membrane integrity or cell wall formation kill closely related neighboring microbes. Bacteriocin production represents an important strategy for promoting the survival of *S. pneumoniae* in microbial communities and enhancing nasopharyngeal colonization (Dawid et al., 2007; Son et al., 2011). *S. pneumoniae* employs the *com* quorum sensing (QS) system to regulate competitive behaviors, including the production of *blp* bacteriocins (also called pneumocins) (Slager et al., 2019a; Wholey et al., 2016) (Fig. 3.1a). While the exact genes and arrangement of the *blp* locus differs between strains, all sequenced strains contain this locus (Wholey et al., 2016), highlighting its importance.

Both the *com* QS system and the *blp* bacteriocin system encode two component systems made up of a sensor kinase and reponse regulator to regulate their own expression. The two-component system of the *com* QS system, *comDE*, is activated in response to multiple environmental inputs and positively regulates the expression of the *blp* locus (Slager et al., 2019a). Other genes regulated by *comDE* include the transporter *comAB* which is thought to transport environmental signals required to activate the *blp* locus in TIGR4 (C. Y. Wang et al., 2018).

Our RNA-seq presented in Chapter 2 of this thesis revealed that the *com* QS system and the *blp* bacteriocin locus were strongly downregulated during growth in MUC5AC (Fig 3.1b). Notably, this regulation is potentially conserved in other bacteria, as mucins also suppress the *com* QS system in the related oral pathogen *Streptococcus mutans* (C. A. Werlang et al., 2021). Given the importance of bacteriocins as a competitive strategy for *S. pneumoniae* colonization, we further characterized the regulation of the *com* and *blp* systems by mucins. Next, we show that mucins reduce *S. pneumoniae* antagonism through co-culture analysis with other nasopharyngeal microbes. Lastly, we find that individual mucin glycans and monosaccharides are sufficient to downregulate genes in the *blp* locus. The ability of mucin to disrupt the competitive strategies of *S. pneumoniae* is a desirable feature for the development of therapeutics to bolster the healthy microbiota against opportunistic pathogens.

Results

In order to validate our RNA-seq results and further understand whether MUC5AC regulates the *com* and *blp* systems in *S. pneumoniae*, we exposed TIGR4 to multiple mucin types a gel-forming polymer carboxymethyl cellulose (CMC) and measured gene expression by RT-qPCR. We found that *comE* (QS response regulator), *blpJ* (putative bacteriocin) and *blpX* (putative immunity gene) were downregulated by MUC5AC and MUC2, however MUC5B was less effective (Fig. 3.2a). Although QS depends on cell-density, we did not observe differential regulation of *blpJ*, *blpX* or *comE* after exposure to gel-forming polymer CMC, suggesting that specific properties of mucins are responsible for this regulation. We found that the regulation of *blpJ* in response to MUC5AC was dose-dependent (Fig. 3.2b). The concentration of mucin in mucosal sites reaches 1-5% (Bansil & Turner, 2018), suggesting strong suppression of *blp* at mucosal sites in the body based on mucin concentration.

S. pneumoniae has been shown to produce active bacteriocins against other Gram-positive bacteria (Lux et al., 2007; Wholey et al., 2019), thus we hypothesized that suppression of the *blp* system by mucins might modulate interactions between *S. pneumoniae* and other competing microbes. To assess this hypothesis, we examined the ability of *S. pneumoniae* TIGR4 to compete in a co-culture model with other nasopharyngeal microbes including *S. pneumoniae* D39, *Staphylococcus aureus*, *Streptococcus oralis*, and *Streptococcus salivarius*. In order to include mucins in our model, we grew co-cultures in liquid culture medium rather than on solid medium and leveraged selective plating to measure growth of competing strains. In a 1:1 co-culture in medium alone, *S. pneumoniae* TIGR4 significantly kills or prevents growth of *S. pneumoniae* D39, *S. aureus*, *S. oralis*, and *S. salivarius*. However, when co-cultured in the presence of MUC5AC, each competing microbe shows increased survival against *S. pneumoniae* by a factor of 3 to 100 fold. MUC5AC does not alter the growth of the competing microbes in monoculture (Fig 3.3a-d).

In addition to competing with other microbes through bacteriocin production, *S. pneumoniae* also kills its neighbors, including *S. aureus* (Regev-Yochay et al., 2006), through the secretion of hydrogen peroxide (H_2O_2). H_2O_2 is a biproduct of the *S. pneumoniae* lactose metabolism, and *S. pneumoniae* itself is highly resistant to H_2O_2 (Pericone et al., 2003). To determine whether H_2O_2 contributes to the co-culture phenotypes, we tested the H_2O_2 concentration during *S. pneumoniae* growth with mucins, and during co-culture with *S. aureus* (Fig. 3.4a). We found that there was no difference in H_2O_2 production with and without mucins in

either condition. We next generated an Δ*spxB* strain that does not produce H_2O_2 and tested the survival of *S. aureus* during co-culture with TIGR4Δ*spxB* (Fig. 3.4b). We again found that *S. aureus* survived better against TIGR4Δ*spxB* than TIGR4; however, mucins still enhanced the survival of *S. aureus* against TIGR4Δ*spxB* (Fig. 3.4c). These data show that *S. pneumoniae* TIGR4 employs strategies beyond H_2O_2 production, such as bacteriocin production, to compete in inter- and intra-species bacterial competition. Thus, mucin reduces *S. pneumoniae* antagonism against competing microbes and may reduce the ability of *S. pneumoniae* to colonize an existing microbial community.

Considering the effects of mucin on microbial competition in *S. pneumoniae*, we next sought to characterize whether mucin glycans were the active component of mucin governing these effects. We utilized RT-qPCR to investigate whether mucin glycans direct *blp* gene expression changes in *S. pneumoniae*. We found that at a 5 hour timepoint, 0.1% MUC5AC glycans significantly downregulated *blpJ* and *blpX*. The mucin glycan pool is dominated by core 1 and core 2 structures with simple modifications (Wagner et al., 2018b; B. X. Wang, Wheeler, et al., 2021). We synthesized individual structures that together make up >50% of the mucin glycan pool to evaluate individual mucin glycans (Fig. 3.4) (Minzer & Hevey, 2023; Takagi et al., 2022; B. X. Wang et al., 2023). We found that unmodified core 1 glycans downregulated *blpJ*, while modifications with sialic acid or fucose reversed this effect (Fig. 3.5a). Core 2 modified with fucose was also able to downregulate *blpJ*, while unmodified core 2 was not. In each case, it is possible modifications with sialic acid or fucose orient the glycan to preserve or block activity.

Given the effectiveness of mucin glycans and individual core structures, we next investigated the regulatory function of individual monosaccharides that make up mucin glycans. We also included *N*-acetyllactosamine (LacNAc), a disaccharide unit found in poly-LacNAc chains of extended glycans. We found that galactose and LacNAc significantly downregulated *blpJ*, while GalNAc and GlcNAc demonstrated a trend towards regulating *blpX* (Fig. 3.5b). Thus, simple mono and disaccharides regulate multiple genes in the *blp* region. The activity of individual monosaccharides may illuminate why some synthetic glycans were active, but others were not. For example, neither fucose or sialic acid regulate *blpJ* expression and core 1 glycans modified with these sugars block the terminal galactose residue, potentially blocking its regulatory activity on *blpJ*.

Considering the transcriptional effects of the mucin glycan pool, we assessed whether glycans were sufficient to regulate co-culture dynamics. We found that in the case of *S. aureus*, mucin glycans trended towards enhancing survival during co-culture with *S. pneumoniae*, although this result was not significant (Fig. 3.5c). Overall, these data show that mucins, isolated mucin glycans, and individual monosaccharides are regulators of the *blp* bacteriocin locus, and potentially mediate co-culture dynamics between *S. pneumoniae* and nasopharyngeal competitors.

Discussion

Together these results show that mucins and mucin glycans downregulate the *com* and *blp* systems in *S. pneumoniae* TIGR4, and modulate co-culture dynamics with nasopharyngeal microbes including *S. aureus, S. salivarius*, and *S. oralis*. Although we did not characterize the precise bacteriocins involved in this effect as there are several putative bacteriocin pairs, we demonstrated the effect of mucins on nasopharyngeal co-cultures was independent of changes in H_2O_2 production. We also did not explore how mucin may impact the physiology of the competing microbes.

The ability of mucin to support the survival of nasopharyngeal microbes during co-culture with *S. pneumoniae* lends itself to the hypothesis that mucin may be important for bolstering healthy microbial communities in the URT. Resisting the colonization of *S. pneumoniae* is of clinical relevance, as the presence of *S. pneumoniae* in the URT is associated with less stable microbial communities leading to health issues such as otitis media (Van Den Broek et al., 2019). The impact of mucin on *S. salivarius* and *S. oralis* survival during co-culture with *S. pneumoniae* is especially notable as these competing bacteria have been investigated as promising probiotics in the treatment of recurrent otitis media infections (La Mantia et al., 2017; Van Den Broek et al., 2019). Mucin glycans or associated monosaccharides could be explored as adjuvants to probiotic therapies due to their impact on bacteriocin expression.

In this work we further explored the regulation of the *blp* locus, one of many regulated by the *com* QS system (Slager et al., 2019a). The competence system also encodes machinery that allows *S. pneumoniae* to uptake foreign DNA, and regulates genes involved in DNA repair and stress-responses. Interestingly, while the master regulators were downregulated by MUC5AC, not all downstream genes annotated as *com* QS regulons were regulated by MUC5AC. The *com* QS

system is tightly temporally regulated, with *comE* controlling "early" competence genes, including the *blp* system, and *comX* controlling "late" competence genes. We did not observe strong regulation of late competence genes, suggesting mucin regulation either does not impact *comX*, or that testing *com* QS specific genes at multiple timepoints may illuminate additional genes regulated by mucin. Generation of a reporter strain that details maximum expression of competence-activating genes such as *comC* or *comE* may also reveal optimal timepoints to test the impact of mucin on the *com* QS system. Additional experiments to further define mucin regulation of the *com* QS system could leverage exposing *S. pneumoniae* to the competence stimulating peptide (CSP) during growth in mucin and profiling transcriptional responses.

Materials and methods

Strains and reagents

This study used the *Streptococcus pneumoniae* strain TIGR4, generously provided by Marc Lipsitch from the Harvard T.H. Chan School of Public Health. This strain, originally isolated from an adult male patient's blood, exhibits high virulence in murine infection models. Strain D39-GFP (D39V) was a gift from Jan-Willem Veening (University of Lausanne) (Kjos et al., 2015). Other strains were sourced from sourced from the American Type Culture Collection (ATCC). A comprehensive list of strains is detailed in Supplementary Table 3.1. For routine growth and preservation, we cultured the bacteria on tryptic soy agar with 5% sheep blood (TSB) at 37 °C in a 5% CO_2 atmosphere. Cultures for experiments were grown in THY broth. When required, media was supplemented with chloramphenicol (Cam; 4.5 μg/mL) for antibiotic-resistant strains.

Collection of human saliva

Submandibular saliva was collected from healthy human volunteers using a custom vacuum pump and was pooled and centrifuged at 2,500*g* for 5 min, and 1 mM phenylmethylsulfonylfluoride was added. Saliva was treated with protease inhibitors, 0.5% Triton-X-1000 (TX100), and 15% Tri-N-butyl phosphate to preserve saliva and remove contaminating virus or phage particles. Saliva was flash frozen in liquid nitrogen and stored a -80ºC. TX100 was removed by treatment with SDR HyperD resin (Sartorius). Samples of human saliva were collected obtaining informed consent and receiving approval from the institutional review board and Massachusetts Institute of Technology's Committee on the Use of Humans as Experimental Subjects under protocol number 1312006096.

Mucin purification

This study used native porcine gastric mucins (MUC5AC), porcine intestinal mucins (MUC2) and human salivary mucins (MUC5B), which differ from industrially purified mucins in their rheological properties and bioactivities. Native mucins were purified as described previously. In brief, mucus was scraped from fresh pig stomachs and intestines and solubilized in sodium chloride buffer containing protease inhibitors and sodium azide. Insoluble material was removed via low-speed centrifugation at 8,000*g* for 30 min and ultracentrifugation at 190,000*g* for 1 h at 4 °C (Beckman 50.2 Ti rotor with polycarbonate bottles). Fat and smaller particles were removed

through filtration with Whatman 3 filter paper. Submandibular saliva was collected from human volunteers as described above using a custom vacuum pump, pooled and centrifuged, and protease inhibitors were added. Mucins were purified using size-exclusion chromatography on separate Sepharose CL-2B columns. Mucin fractions were then desalted, concentrated, and resuspended in water. To remove contaminating phage or virus particles from MUC2 and MUC5AC, mucin was treated with 0.5% TX100 and 0.15% Tri-N-butyl phosphate. TX100 was removed by treatment with SDR HyperD resin (Sartorius). Lyophilized mucins were rehydrated by shaking them gently at 4 °C overnight in the desired medium. MS is routinely used to monitor the composition of purified mucin extracts. This type of analysis has shown that mucin extracts purified from porcine stomach mucus, for example, are composed predominantly of MUC5AC, with small quantities of MUC2, MUC5B and MUC6 as well as histones, actin, and albumin.

Isolation of mucin oligosaccharides

We used non-reductive alkaline β-elimination ammonolysis to dissociate non-reduced glycans from mucins as described previously. Commercial porcine gastric mucin (Sigma) was cleaned up by ethanol precipitation. Mucin was solubilized in PBS and ethanol was added. The mucin pellet was collected and resolubilized in water, desalted and lyophilized. Mucins were then dissolved in ammonium hydroxide saturated with ammonium carbonate and incubated at 60 °C for 50-60 h, creating oligosaccharide glycosylamines and partially deglycosylated mucins. Volatile salts were removed using repeated centrifugal evaporation. The oligosaccharide glycosylamines were separated from residual deglycosylated mucins via centrifugal filtration through 10 kDa molecular weight cutoff membranes (Amicon Ultracel) in accordance with the manufacturer's instructions. The resulting oligosaccharide glycosylamines were converted to reducing oligosaccharide hemiacetals via treatment with 0.5 M boric acid at 37 °C for 1 h. The samples were washed with methanol, and residual solvents were removed via repeated centrifugal evaporation. Oligosaccharides were further purified using solid-phase extraction using Hypercarb minicolumns (Thermo Fisher), and residual solvents were removed through centrifugal evaporation.

RNA preparation for gene expression analysis

In brief, *S. pneumoniae* was grown on TSB agar overnight and liquid pre-cultures were inoculated in THY broth. After growth to OD ~0.4, cultures were diluted to OD 0.01 (approximately 10^7

CFU/mL) into THY supplemented with 0.5% CMC, 0.5% mucin, or 0.1% monosaccharides and other glycan compounds. After 5 h (unless otherwise noted) of growth at 37 °C with 5% CO_2, the samples were collected mid-log phase and pelleted at 3,000*g*, supernatant was removed, and the pellets were flash-cooled in liquid nitrogen and stored at −80 °C. Pellets were thawed on ice and resuspended in 25uL lysozyme buffer. Ready-Lyse Lysozyme (Lucigen) was added and the samples were incubated at room temperature for 15 m. Total RNA was then extracted using the MasterPure Complete RNA Purification kit (Lucigen). Genomic DNA was removed using the Turbo DNA-free kit (Ambion). Total RNA was measured using an Agilent 2100 Bioanalyzer (Agilent Technologies). The samples were stored at −20 °C.

RT–qPCR analysis

A list of the primers used in this study is provided in Supplementary Table 3.2. First-strand cDNA was synthesized using the Protoscript II First-Strand cDNA Synthesis kit (New England Biolabs). The elimination of genomic DNA was confirmed by qPCR amplification on negative control samples that did not have reverse transcriptase during cDNA synthesis. 5 ng of cDNA was used as a template for qPCR using SYBR Green Master Mix (Thermo Fisher Scientific) performed using the Cycler 480 II Real-time PCR Machine (Roche). Forward and reverse primers were added at 3 μM each. Melting-curve analyses verified amplification of a single product. Gene expression changes were calculated based on mean change in qPCR cycle threshold compared to *gyrB* (ΔC_t) and are reported as $\log_2$[fold change] = ΔC_t_CM − ΔC_t_sample. Each sample was analyzed with at least three technical replicates.

H_2O_2 measurement

The hydrogen peroxide concentration was measured using the Pierce Quantitative Peroxide Kit (Thermo Fisher Scientific) which generates a colorimetric assay. Standard curves were generated in THY broth ± 0.25% MUC5AC with added hydrogen peroxide. Absorbance at 595 nm was measured using a Synergy H1 plate reader and the data were analyzed using Prism GraphPad.

Co-culture assay

S. pneumoniae TIGR4, *S. pneumoniae* D39-GFP, *S. aureus*, *S. oralis,* and *S. salivarius* were streaked out on the appropriate agar and grown overnight at 37 °C. Pre-cultures were grown in

THY broth for 3 h to mid-log phase. The co-culture was inoculated at 1:1 ratio with 10^7 cells into 200 µL THY broth with or without 0.25% MUC5AC and incubated at 37 °C with 5% CO_2. At 0 h, 4 h, and 24 h, the co-cultures were plated for CFU on TSA supplemented with catalase and chloramphenicol selective for *S. pneumoniae* D39-GFP, mannitol-salt agar selective for *S. aureus,* or Mitis-Salivarius agar selective for *S. oralis,* and *S. salivarius.* Plates were incubated at 37 °C overnight and CFU counts were assessed the following day.

Mucin glycan synthesis and analysis

The Core 1, Core 1+fucose Core 1+sialic acid, Core 2, Core 2+fucose, and Core 2+galactose glycans were prepared as previously described (Minzer & Hevey, 2023; Takagi et al., 2022; B. X. Wang et al., 2023). All commercial reagents were used as supplied unless otherwise stated, and anhydrous solvents were either commercially acquired or prepared using standard techniques. Organic solutions were concentrated and/or evaporated to dryness under vacuum in a water bath (<50 °C). Molecular sieves were dried at 400 °C under vacuum for 20–30 min prior to use. Amberlite IR-120H resin was washed extensively with methanol and dried under vacuum prior to use. Purification of compounds was performed through medium-pressure liquid chromatography using a CombiFlash Companion (Teledyne ISCO) with either RediSep normal-phase flash columns (Teledyne ISCO) or self-packed reversed-phase C18 columns (LiChroprep RP-18 resin, 25–40lm). High-pressure liquid chromatography (HPLC) analysis was used to assess final purity and was performed using an Agilent 1100LC equipped with an Atlantis T3 (3 mm, 2.1×100 mm) C18 column and an evaporative light scattering detector.

Statistics and reproducibility

Unless otherwise noted, experiments were performed with at least three biological replicates, and we have presented the results as mean ± standard error of the mean (s.e.m.). Raw data are available upon request.

References

Bansil, R., & Turner, B. S. (2018). The biology of mucus: Composition, synthesis, and organization ☆. *Advanced Drug Delivery Reviews*, *124*, 3–15. https://doi.org/10.1016/j.addr.2017.09.023

Bryant, J. C., Dabbs, R. C., Oswalt, K. L., Brown, L. R., Rosch, J. W., Seo, K. S., Donaldson, J. R., McDaniel, L. S., & Thornton, J. A. (2016). Pyruvate oxidase of Streptococcus pneumoniae contributes to pneumolysin release. *BMC Microbiology*, *16*(1), 1–12. https://doi.org/10.1186/s12866-016-0881-6

Dawid, S., Roche, A. M., & Weiser, J. N. (2007). The blp bacteriocins of Streptococcus pneumoniae mediate intraspecies competition both in vitro and in vivo. *Infection and Immunity*, *75*(1), 443–451. https://doi.org/10.1128/IAI.01775-05

La Mantia, I., Varricchio, A., & Ciprandi, G. (2017). Bacteriotherapy with Streptococcus salivarius 24SMB and Streptococcus oralis 89a nasal spray for preventing recurrent acute otitis media in children: A real-life clinical experience. *International Journal of General Medicine*, *10*, 171–175. https://doi.org/10.2147/IJGM.S137614

Lux, T., Nuhn, M., Hakenbeck, R., & Reichmann, P. (2007). Diversity of bacteriocins and activity spectrum in Streptococcus pneumoniae. *Journal of Bacteriology*, *189*(21), 7741–7751. https://doi.org/10.1128/JB.00474-07

Minzer, G., & Hevey, R. (2023). Synthesis of Mucin O-Glycans Associated with Attenuation of Pathogen Virulence. *ChemistryOpen*, *12*(5). https://doi.org/10.1002/open.202200134

Pericone, C. D., Park, S., Imlay, J. A., & Weiser, J. N. (2003). Factors Contributing to Hydrogen Peroxide Resistance in Streptococcus pneumoniae Include Pyruvate Oxidase (SpxB) and Avoidance of the Toxic Effects of the Fenton Reaction. *Journal of Bacteriology*, *185*(23), 6815–6825. https://doi.org/10.1128/JB.185.23.6815-6825.2003

Regev-Yochay, G., Trzciński, K., Thompson, C. M., Malley, R., & Lipsitch, M. (2006). Interference between Streptococcus pneumoniae and Staphylococcus aureus: in vitro hydrogen peroxide-mediated killing by Streptococcus pneumoniae. *Journal of Bacteriology*, *188*(13), 4996 LP – 5001. https://doi.org/10.1128/JB.00317-06

Slager, J., Aprianto, R., & Veening, J.-W. (2019). *Refining the Pneumococcal Competence Regulon by RNA Sequencing*. https://doi.org/10.1128/JB

Son, M. R., Shchepetov, M., Adrian, P. V., Madhi, S. A., de Gouveia, L., von Gottberg, A., Klugman, K. P., Weiser, J. N., & Dawid, S. (2011). Conserved mutations in the pneumococcal bacteriocin transporter gene, blpa, result in a complex population consisting of producers and cheaters. *MBio*, *2*(5). https://doi.org/10.1128/mBio.00179-11

Takagi, J., Aoki, K., Turner, B. S., Lamont, S., Lehoux, S., Kavanaugh, N., Gulati, M., Valle Arevalo, A., Lawrence, T. J., Kim, C. Y., Bakshi, B., Ishihara, M., Nobile, C. J., Cummings, R. D., Wozniak, D. J., Tiemeyer, M., Hevey, R., & Ribbeck, K. (2022). Mucin O-glycans are natural inhibitors of Candida albicans pathogenicity. *Nature Chemical Biology*, *18*(7), 762–773. https://doi.org/10.1038/s41589-022-01035-1

Van Den Broek, M. F. L., De Boeck, I., Kiekens, F., Boudewyns, A., Vanderveken, O. M., & Lebeer, S. (2019). Translating recent microbiome insights in otitis media into probiotic strategies. *Clinical Microbiology Reviews*, *32*(4). https://doi.org/10.1128/CMR.00010-18

Wagner, C. E., Wheeler, K. M., & Ribbeck, K. (2018). Mucins and Their Role in Shaping the Functions of Mucus Barriers. *Annual Review of Cell and Developmental Biology*, *34*(1), 189–215. https://doi.org/10.1146/annurev-cellbio-100617-062818

Wang, B. X., Takagi, J., McShane, A., Park, J. H., Aoki, K., Griffin, C., Teschler, J., Kitts, G., Minzer, G., Tiemeyer, M., Hevey, R., Yildiz, F., & Ribbeck, K. (2023). Host-derived O -glycans inhibit toxigenic conversion by a virulence-encoding phage in Vibrio cholerae. *The EMBO Journal*, *42*(3). https://doi.org/10.15252/embj.2022111562

Wang, B. X., Wheeler, K. M., Cady, K. C., Lehoux, S., Cummings, R. D., Laub, M. T., & Ribbeck, K. (2021). Mucin Glycans Signal through the Sensor Kinase RetS to Inhibit Virulence-Associated Traits in Pseudomonas aeruginosa. *Current Biology*, *31*(1), 90-102.e7. https://doi.org/10.1016/j.cub.2020.09.088

Wang, C. Y., Patel, N., Wholey, W. Y., & Dawid, S. (2018). ABC transporter content diversity in Streptococcus pneumoniae impacts competence regulation and bacteriocin production. *Proceedings of the National Academy of Sciences of the United States of America*, *115*(25), E5776–E5785. https://doi.org/10.1073/pnas.1804668115

Werlang, C. A., Chen, W. G., Aoki, K., Wheeler, K. M., Tymm, C., Mileti, C. J., Burgos, A. C., Kim, K., Tiemeyer, M., & Ribbeck, K. (2021). Mucin O-glycans suppress quorum-sensing pathways and genetic transformation in Streptococcus mutans. *Nature Microbiology*. https://doi.org/10.1038/s41564-021-00876-1

Wholey, W. Y., Abu-Khdeir, M., Yu, E. A., Siddiqui, S., Esimai, O., & Dawid, S. (2019). Characterization of the competitive pneumocin peptides of streptococcus pneumoniae. *Frontiers in Cellular and Infection Microbiology*, *9*(MAR). https://doi.org/10.3389/fcimb.2019.00055

Wholey, W. Y., Kochan, T. J., Storck, D. N., & Dawid, S. (2016). Coordinated Bacteriocin Expression and Competence in Streptococcus pneumoniae Contributes to Genetic Adaptation through Neighbor Predation. *PLoS Pathogens*, *12*(2). https://doi.org/10.1371/journal.ppat.1005413

Acknowledgements

This research was supported by the NIH NIBIB award R01EB017755-04 (OSP 6940725; to K.R.), the Bill and Melinda Gates Foundation award INV-041182 (to K.R.), the National Science Foundation MIM grant EF-2125118 (to K.R.), the US Army Research Office under cooperative agreement W911NF-19-2-0026 for the Institute for Collaborative Biotechnologies (to K.R.), and the Toxicology Training Grant support T32-ES007020 (to J.B.). We acknowledge additional support from the MIT BioMicro Center and the National Institute of Environmental Health Sciences of the NIH (no. P30-ES002109). We thank the MIT BioMicro Center for maintaining the RT-qPCR machine facility, Gerardo Cácrarmo-Oyarce for sharing his expertise in designing co-culture experiments, and Justin Thornton for providing genetically modified *S. pneumoniae* strains. Biorender was used to create Figure 3.1a.

Figures

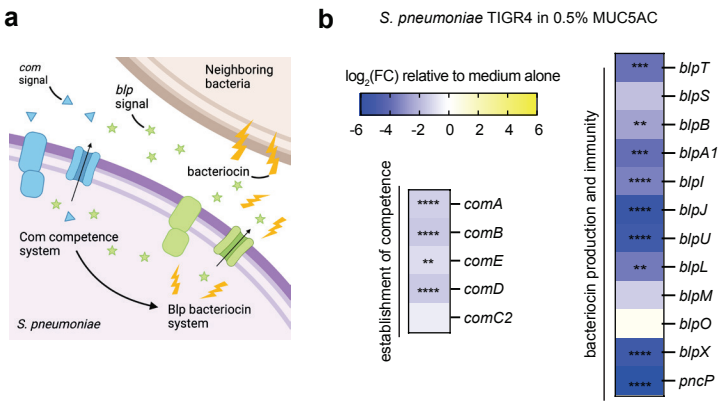

Figure 3.1: The interconnected *com* QS and *blp* bacteriocin system are regulated by MUC5AC.

(A) The *S. pneumoniae* competence system positively regulates the Blp bacteriocin system, which can antagonize neighboring microbes. **(B)** FC data from RNA-sequencing of TIGR4 after exposure to 0.5% MUC5AC. Data are average measurements from n = 4 biological replicates. FDR-adjusted *P* values were determined using the Benjamini-Hochberg *P*-value adjustment method (FDR-adjusted $P < 0.05$). FC values are mean of n = 4 biological replicates. * $P < 0.05$; ** $P < 0.01$; *** $P < 0.001$; **** $P<0.0001$.

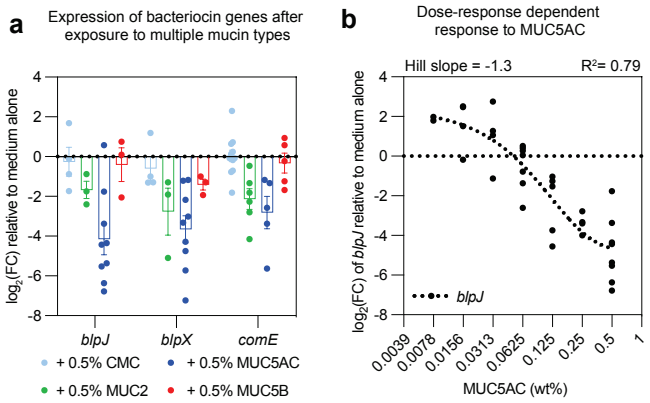

Figure 3.2: Mucins downregulate bacteriocin expression.

(A) Multiple mucin types downregulate genes in the Blp bacteriocin operon and major competence regulator *comE*. Gene expression was measured by RT-qPCR and normalized to *gyrB*. Bars indicate mean ± s.e.m. with individual biological replicates shown. **(B)** MUC5AC regulates *blp* expression in a dose-dependent manner. Gene expression was measured by RT-qPCR and normalized to a control gene *gyrB*. Individual biological replicates and a nonlinear agonist binding best-fit curve are shown ($R^2 = 0.79$, hill slope = -1.3).

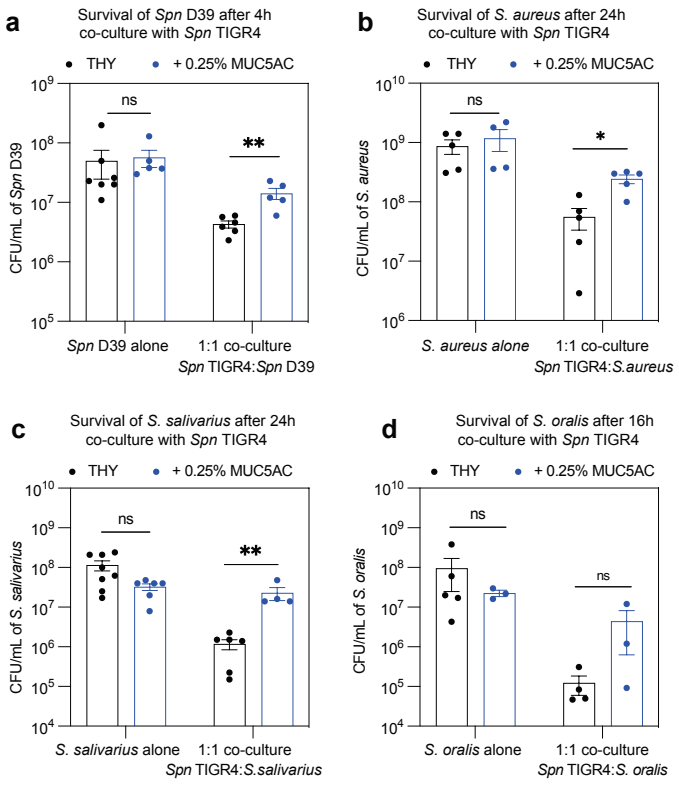

Figure 3.3: Mucins reduce antagonism of *S. pneumoniae* TIGR4 against nasopharyngeal microbes. (A) MUC5AC enhances survival of *S. pneumoniae* D39-GFP during co-culture with *S. pneumoniae* TIGR4 and *S. pneumoniae* D39-GFP were added in a 1:1 co-culture to THY broth with or without 0.25% MUC5AC and co-cultured at 37 °C for 24 h. *S. pneumoniae* D39-GFP survival was determined by CFU plating on TSB + cam plates at 0 and 4 h. **(B)** MUC5AC enhances survival of *S. aureus*. *S. pneumoniae* and *S. aureus* were added in a 1:1 co-culture to THY broth with or without 0.25% MUC5AC and co-cultured at 37 °C for 24 h. *S. aureus* survival was determined by CFU plating on mannitol-salt agar plates at 0, 4, and 24 h. **(C)** MUC5AC enhances survival of *S. salivarius*. *S. pneumoniae* and *S. salivarius* were added in a 1:1 co-culture to THY broth with or without 0.25% MUC5AC and co-cultured at 37 °C for 24 h. *S. salivarius* survival was determined by CFU plating on mitis-salivarius agar plates at 0, 4, and 24 h. **(D)** MUC5AC enhances survival of *S. oralis*. *S. pneumoniae* and *S. oralis* were added in a 1:1 co-culture to THY broth with or without 0.25% MUC5AC and co-cultured at 37 °C for 24 h. *S. oralis* survival was determined by CFU plating on mitis-salivarius agar plates at 0, 4, and 24 h. **(A-D)** Bars show mean ± s.e.m. with biological replicates shown. Significance was assessed using the Mann-Whitney U-test. ns: not significant; * $P < 0.05$; ** $P < 0.01$; *** $P < 0.001$; **** $P<0.0001$.

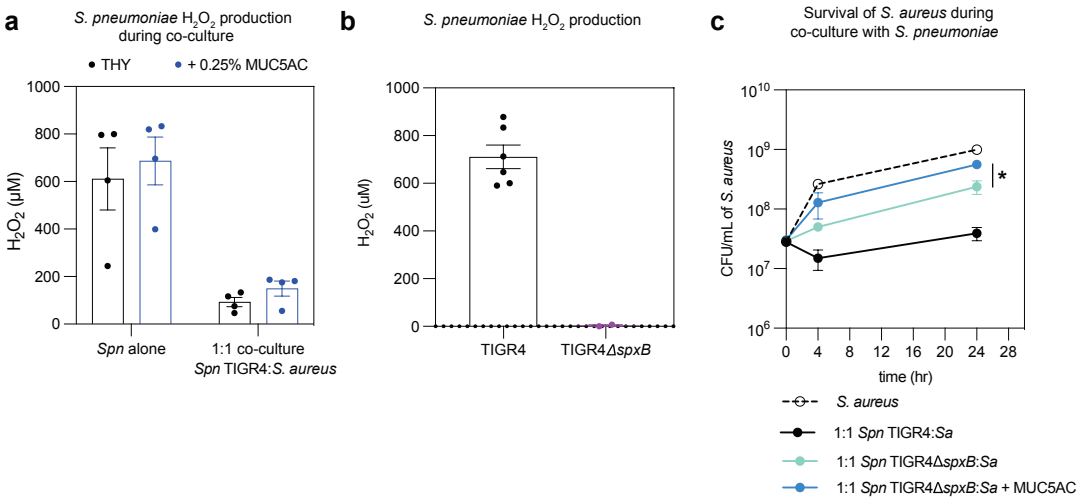

Figure 3.4: H_2O_2 production does not explain mucin-mediated microbial coexistence.

(A) H_2O_2 production of *S. pneumoniae* TIGR4 alone, and *S. pneumoniae* TIGR4 co-cultured with *S. aureus* with and without MUC5AC. Bacteria were added to either a mono or 1:1 co-culture in THY broth with or without 0.25% MUC5AC and co-cultured at 37 °C for 4h. H_2O_2 in the culture supernatant was measured. **(B)** H_2O_2 production of TIGR4 and TIGR4Δ*spxB*. Bacteria were grown to mid-log phase and H_2O_2 was measured. **(A-B)** Bars show mean ± s.e.m. with biological replicates shown. **(C)** MUC5AC enhances survival of *S. aureus* in the absence of H_2O_2 production. *S. pneumoniae* TIGR4Δ*spxB* and *S. aureus* were added in a 1:1 co-culture to THY broth with or without 0.25% MUC5AC and co-cultured at 37 °C for 24h. *S. aureus* survival was determined by CFU plating on mannitol salt agar plates at 0, 4, and 24h.

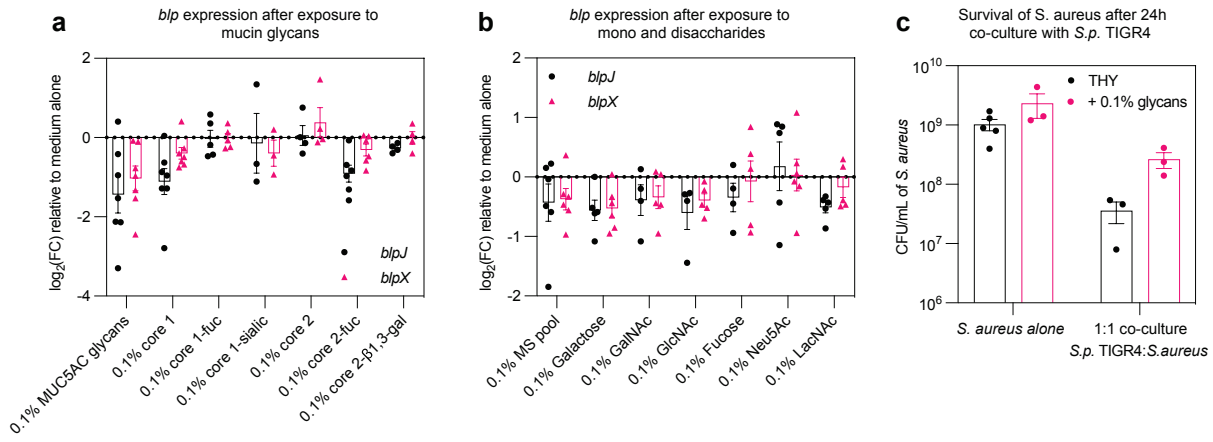

Figure 3.5: Mucin glycans downregulate *blp* and reduce *S. pneumoniae* antagonism.

(A) Gene expression was measured during growth with mucin glycans after 5 h in the indicated strain and medium condition by RT-qPCR and normalized to *gyrB*. **(B)** Gene expression was measured during growth with mono and disaccharides after 5 h in the indicated strain and medium condition by RT-qPCR and normalized to *gyrB*. **(C)** MUC5AC glycans enhance survival of *S. aureus*. *S. pneumoniae* and *S. aureus* were added in a 1:1 co-culture to THY broth with or without 0.1% MUC5AC glycans and co-cultured at 37 °C for 24 h. *S. aureus* survival was determined by CFU plating on mannitol-salt agar plates at 0, 4, and 24 h. **(A-C)** Bars indicate mean ± s.e.m. with individual biological replicates shown.

Supplementary Figures

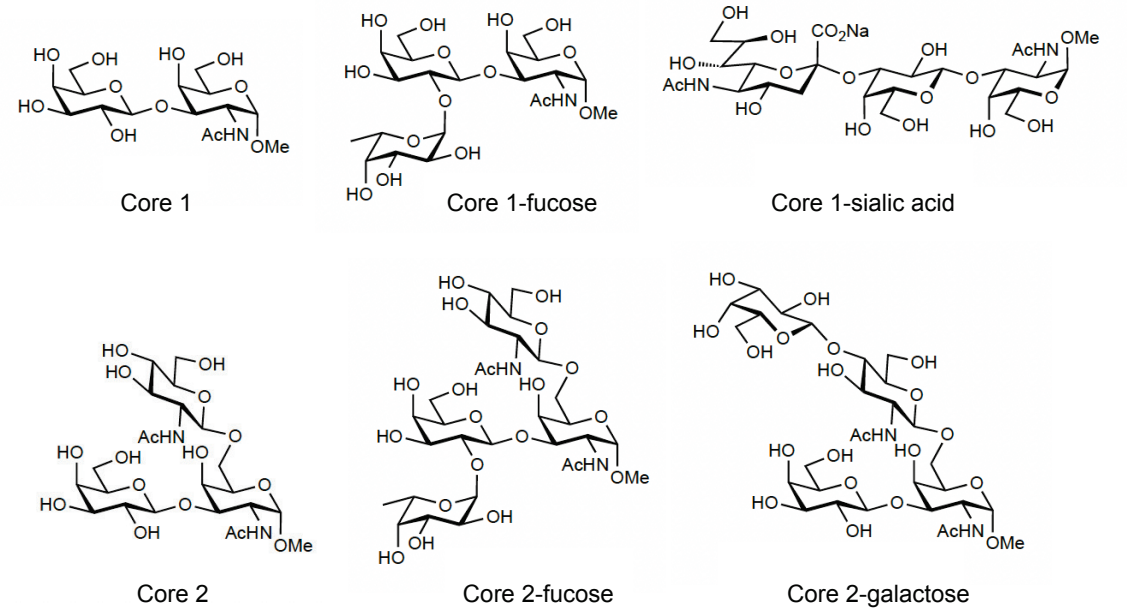

Supplementary Figure 3.1: Synthetic mucin glycan structures.

Depiction of synthesized mucin glycans that are abundant in the full mucin glycan pool. AcHN, acetamido; OMe, methoxy.

Supplementary Tables

Strain	Species	Description	Source
TIGR4	*S. pneumoniae*	Serotype 4, WT	Tettelin et al. 2001
TIGR4Δ*spxB*	*S. pneumoniae*	ΔspxB-EryR	Bryant et al. 2016
D39V	*S. pneumoniae*	Serotype 2, WT	Kjos et al. 2015
JWV500	*S. pneumoniae*	D39V PhlpA-hlpA-gfp_CamR	Kjos et al. 2015
Newman	*S. aureus*	WT	NCTC 8178
ATCC 13419	*S. salivarius*	WT	ATCC 13419
ATCC 6249	*S. oralis*	WT	ATCC 6249

Supplementary Table 3.1: Strains of bacteria used in this study.

Primer name	Purpose	Primer Sequence 5'>3'
blpJ-F	RT-qPCR blpJ	ATGCTTGCGAAAGTTGAAGGG
blpJ-R	RT-qPCR blpJ	CTGCTCCAGTTCCACCAGTT
blpX-F	RT-qPCR blpX	ACAGTGGTTTGTTTGAAGCAGG
blpX-R	RT-qPCR blpX	GCGATTTCGAATATCTACTTCCTTG
16S-F	RT-qPCR 16S	CTGCGTTGTATTAGCTAGTTGGTG
16S-R	RT-qPCR 16S	TCCGTCCATTGCCGAAGATTC
gyrB-F	RT-qPCR gyrB	CCAATCCTAGAAGCTGGTTATGT
gyrB-R	RT-qPCR gyrB	CACCCGGCTGGATATATTCTTT

Supplementary Table 3.2: List of primers used in this study.

Chapter 4: Conclusions and Future Directions

Conclusions

In this thesis, I focused on the interaction of *S. pneumoniae* with mucin glycoproteins which are abundant in the mucus environment. In Chapter 2, I identified that mucins and their associated glycans broadly and potently downregulate the critical virulence factor, pneumolysin (PLY). Further, I show that through this regulation of PLY, mucins protect host cells from toxin-mediated killing, calibrate host neutrophils to remain active against the bacterium, and attenuate infection in an *in vivo* model. In Chapter 3, I discovered that mucins downregulate the *com* and *blp* systems of *S. pneumoniae*, and modulate microbe-microbe competition. I show that individual glycan and monosaccharide components of mucin glycans are sufficient to regulate gene expression. Together, the projects presented in my thesis show that mucins are powerful regulators of *S. pneumoniae* physiology, generating new hypotheses that merit further exploration. In this chapter, I will detail future areas of research to extend the projects presented here.

Future directions

Screening extended mucin glycan libraries and mucin mimetics for *ply* regulation

In Chapter 3, I show that individual mucin glycans and individual sugars are sufficient to regulate *blp* genes, however the individual structures are not sufficient to regulate *ply* (Fig 4.1a-b). This creates a major gap as to which structures in the mucin glycan pool are important for *ply* regulation, or indicates that substantially higher concentrations are needed. In addition, mucin is more effective than the glycan pool (Fig. 2.1d), leaving open the possibility that synergistic effects of glycans or multivalent binding is an important factor. Continued efforts to synthesize mucin glycans, modify native mucins, or engineer mucin mimetic materials may reveal the specific mucin structures that regulate *ply*.

The synthesized mucin glycans presented in Chapter 3 represent 33-51% of the mucin glycan pool isolated from MUC5AC. These glycans are relatively small with a maximum of four monosaccharides and do not contain many of the terminal epitopes or sulfation present in larger structures (Takagi et al., 2022; Wheeler et al., 2019). It is possible that sulfated or larger glycans present in the full pool are important for regulation of *ply*. Generating sulfated mucin glycans is

an active area of research. However, generating longer glycans structures at preparatory scales through *de novo* synthesis is time consuming and technically difficult. Advancements in glycan synthesis such as leveraging chemoenzymatic strategies to generate *O*-glycans may allow us to screen a larger library of glycans (Wang et al., 2021).

An alternative approach could optimize fractionating our existing glycan pool using a combination of techniques. Hydrophilic interaction liquid chromatography (HILIC) separates polar compounds (including *O*-glycans) by size and hydrophilicity. Porous graphitized carbon liquid chromatography (PGC-LC) utilizes the polar retention effect on graphite which separates glycan isomers that may not be separated by HILIC (Saldova & Wilkinson, 2020). After separation, glycan fractions could be tested for regulatory activity through multiple assays such as RT-qPCR or hemolysis. While these glycan fractions may not have single glycan resolution, smaller pools could further define feature of active glycans, potentially clarifying target glycans for synthesis.

In addition to probing additional mucin glycan structures, we can also leverage natural differences between intact mucins to understand glycan activity. In Chapter 2, we showed that MUC5B does not regulate *ply* as strongly as MUC2 or MUC5AC (Fig. 2.1d), potentially due to differences in glycosylation patterns. Previous work in the Ribbeck lab has profiled glycans from MUC2, MUC5B, and MUC5AC (Takagi et al., 2022). One key difference between mucin isomers is the level of fucosylation. In isolated mucin glycan pools, 76% of MUC5B glycans were fucosylated, while only 52% and 44% of glycans were fucosylated in MUC2 and MUC5AC respectively. In addition, glycans in MUC5AC, which is the strongest regulator of *ply*, has long afucosylated LacNAc repeats that are not present in MUC2 and MUC5B glycans. Enzymatic treatment of mucins with glycosidases to remove specific glycans may reveal underlying differences in activity. For example, treatment of MUC5B with commercially available fucosidases may alter its regulatory activity of *ply*. One challenge of this approach would be to optimize and validate the removal of glycans from the mucin backbone. However, understanding the differences in activity of native mucins may clarify which glycan structures are important in regulating *ply*, and why some mucins are more potent than others.

Finally, the presentation of glycans on the mucin backbone may enhance activity through synergistic effects of glycans or multivalent binding. Testing engineered mucin mimetic materials will enable further understanding of the importance of glycan presentation in regulating *ply*. There

are several different platforms for mucin mimetics, each with its own advantages and disadvantages which have been reviewed extensively (Donahue et al., 2023; Kohout et al., 2022; Werlang et al., 2019). Depending on the model, mucin mimetics allow us to vary the polymer length and stiffness, glycosylation density, and glycan identity. Recent work has shown that galactose-functionalized cis-poly(norbornene) polymers are able to form linear polymers that recapitulate native mucin binding of cholera toxin (Kruger et al., 2021). Similarly, silk fibroin polymers functionalized with GalNAc sugars were able to prevent *S. mutans* biofilm formation, and the potency varied with polymer concentration and glycan density (Werlang, 2022). Although mono and disaccharides do not regulate *ply* (Fig 4.1b), it is possible that grafting sugars to a polymer may increase activity through multivalent binding. There are other mucin mimetics that include longer mucin glycans including cell-based methods to produce defined glycosylated peptides (Nason et al., 2021), and synthetic mucin (synMUC) polypeptides based on glycosylated α-amino acid *N*-carboxy-anhydrides (NCAs) that bear core glycan structures (Detwiler et al., 2023; Kohout et al., 2022). Overall, testing expanded mucin glycan libraries or mucin mimetic materials for their ability to regulate *ply* will clarify the active structure in mucin, and potentially inform the design of mucin inspired therapeutics.

Impact of mucin regulation of *S. pneumoniae in vivo*

In Chapter 2, I show that pre-treatment with mucins and mucin glycans attenuate lung infection in an intratracheal mouse infection model. This pilot experiment has several levers that could be adjusted to optimize the attenuation of infection, and additional readouts may overall strengthen our findings. First, we could test additional concentrations of mucin and mucin glycans, both in the pre-treatment step and as an additional treatment 8 h post infection. We could also test additional infection readouts such as the bacterial burden in the broncho-alveolar lavage fluid and spleen. We could directly test changes in the immune response by measuring cytokine levels in the blood, and histological analysis of lung tissue as PLY causes inflammatory cell infiltration. In addition. These experiments may further reveal the protective effect of mucin in dampening *in vivo* infection.

While the intratracheal model of infection is convenient to look at the impact of changes in PLY expression, *Spn* does not infect humans through the intratracheal route, and this model does not offer an opportunity to look at changes in colonization dynamics. Mucin downregulates

com and *blp* genes that impact colonization, thus mucin may impact *Spn* colonization in an *in vivo* colonization model. One option to test colonization fitness could be to generate *Spn* strains with different fluorophores (like GFP or mCherry) or antibiotic markers, and to grow the bacteria with and without mucin. These bacteria could then be mixed and used to infect *Spn* using an intranasal infection route. After several days, *Spn* survival could be enumerated through analysis of nasal lavage fluid by flow cytometry, or by CFU counts on selective plates.

An alternative route of investigating the impact of mucins *in vivo* during *S. pneumoniae* infection could leverage genetic knockouts of secreted mucins to deplete mucins from host mucus. *Muc1*$^{-/-}$, *Muc2*$^{-/-}$, *Muc5ac*$^{-/-}$, and *Muc5b*$^{-/-}$ knockout mice have been generated and used with a variety of infection models. While these mice are generally unhealthy with increased risk of infection and colitis depending on the specific knockout, they still represent a viable model system. For example, previous work in a *Muc1*$^{-/-}$ mouse model has shown that membrane-bound mucin MUC1 protects against progression to severe *S. pneumoniae* disease (Dhar et al., 2017). In addition, *Muc5b*$^{-/-}$ mice spontaneously developed Streptococcal *spp*. infection (Roy et al., 2014). We have shown that MUC5AC is the most potent secreted mucin in regulating *ply* (Fig 2.1). In addition, *blp* bacteriocins, which are downregulated by mucins, are known to enhance colonization in vivo (Dawid et al., 2007). Future work could test murine models of *S. pneumoniae* infection in a *Muc5ac*$^{-/-}$ mouse. I would be particularly interested in understanding whether MUC5AC protects against the transition to invasive disease following intranasal or intratracheal infection, as observed with MUC1. It would also be important to note whether *S. pneumoniae* is more able to colonize the existing microbiota of a *Muc5ac*$^{-/-}$ mouse after intranasal infection. These experiments would enable an understanding of the importance of host mucin *in vivo* in protecting against *S. pneumoniae* colonization and infection.

Mechanism and conservation of mucin-dependent regulation of *ply*

The regulation of *ply* in *S. pneumoniae* is not well understood. In Appendix A, I review what is currently known about the regulation of *ply* and test several hypotheses, however the mechanism of mucin regulation of *ply* is still unknown. Identifying a strain of *S. pneumoniae* that does not downregulate *ply* in response to mucin may illuminate the mechanism of action. In Chapter 2, I established that mucin downregulates *ply* in multiple strain backgrounds representing five different serotypes, however over 90 serotypes of *S. pneumoniae* have been identified.

Recently, a strain-specific mechanism of *ply* regulation has been described in clinical isolates of serotype 23F (Stevens et al., 2022). Profiling the ability of mucin to reduce *ply* expression in additional serotypes and clinical isolates may reveal strains that do not respond to mucin. Genomic analysis or genetic analysis of putative *ply* regulators may reveal differences between strains, potentially exposing the mechanism of mucin regulation.

In addition, PLY is part of a family of 28 cholesterol dependent cytolysins (CDCs) that are encoded by other Gram-positive opportunistic pathogens including *Listeria monocytogenes*, *Streptococcus pyogenes*, *Clostridium perfringens*, and *Gardnerella vaginalis*. Preliminary data suggests mucin reduces the expression of vaginolysin (*vly*), a CDC encoded by the bacterial vaginosis-causing bacterium *G. vaginalis* (Werlang, 2022). However, it is not known whether mucin regulates CDC expressed in other organisms, or if the mechanisms that control mucin regulation of *ply* is conserved in other organisms. The regulation of CDCs in other organisms is complex, but in some cases more defined than the regulation of PLY in *S. pneumoniae*. For example, in *C. perfringens*, CDC perfringolysin O is regulated by multiple quorum sensing systems and a two-component system (Verherstraeten et al., 2015). Additionally, it has recently been shown that the expression of CDC streptolysin O in *S. pyogenes* is regulated by carbon source in addition to feedback from two-component system *covR/S* (Hirose et al., 2023). Identifying additional CDCs regulated by mucin may suggest a mechanism in that organism, which could in turn enable the detangling of the regulatory pathway of PLY in *S. pneumoniae* both in the context of mucin-regulation and more generally.

Impact of mucin on *S. pneumoniae* and microbial communities of the URT

In Chapter 3, I show that mucin and mucin glycans downregulate *blp* bacteriocins, reducing microbial competition between *S. pneumoniae* and nasopharyngeal microbes in defined co-culture models. However, this model was limited to an interaction between a few microbes. The ability of *S. pneumoniae* to colonize the microbiota of the URT is the first step of invasive disease. Thus, understanding how mucin may modulate the interaction between *S. pneumoniae* and microbial communities may point to therapeutic strategies to prevent colonization.

Ex vivo models of salivary microbial communities have leveraged *16S* sequencing to show that mucins and mucin glycans support greater microbial diversity (Wu et al., 2023), and bolster the community against the invasion of pathogens such as *Streptococcus mutans* (Chloe Wu, 2023).

A similar approach could profile the impact of mucins on *ex vivo* communities from the URT, and the ability to resist invasion of *S. pneumoniae*. It is known that the presence of *S. pneumoniae* is inversely correlated with different species such as *Prevotella* spp. or *Corynebacterium* spp. depending on age (De Steenhuijsen Piters et al., 2016; Edouard et al., 2018; Xu et al., 2021). Profiling communities from healthy individuals of different ages, as well as individuals with dysbiotic communities that are associated with pneumonia, may reveal how mucin supports the growth of health promoting species, or species that prevent the outgrowth of *S. pneumoniae*.

References

Chiavolini, D., Pozzi, G., & Ricci, S. (2008). Animal models of Streptococcus pneumoniae disease. In *Clinical Microbiology Reviews* (Vol. 21, Issue 4, pp. 666–685). https://doi.org/10.1128/CMR.00012-08

Chloe Wu. (2023). *Examining how mucins and their associated O-glycans shape oral microbial communities*. Massachusetts Institute of Technology.

Dawid, S., Roche, A. M., & Weiser, J. N. (2007). The blp bacteriocins of Streptococcus pneumoniae mediate intraspecies competition both in vitro and in vivo. *Infection and Immunity*, *75*(1), 443–451. https://doi.org/10.1128/IAI.01775-05

De Steenhuijsen Piters, W. A. A., Huijskens, E. G. W., Wyllie, A. L., Biesbroek, G., Van Den Bergh, M. R., Veenhoven, R. H., Wang, X., Trzcinski, K., Bonten, M. J., Rossen, J. W. A., Sanders, E. A. M., & Bogaert, D. (2016). Dysbiosis of upper respiratory tract microbiota in elderly pneumonia patients. *ISME Journal*, *10*(1), 97–108. https://doi.org/10.1038/ismej.2015.99

Detwiler, R. E., McPartlon, T. J., Coffey, C. S., & Kramer, J. R. (2023). Clickable Polyprolines from Azido-proline N-Carboxyanhydride. *ACS Polymers Au*, *3*(5), 383–393. https://doi.org/10.1021/acspolymersau.3c00011

Dhar, P., Ng, G. Z., Dunne, E. M., & Sutton, P. (2017). Mucin 1 protects against severe Streptococcus pneumoniae infection. *Virulence*, *8*(8), 1631–1642. https://doi.org/10.1080/21505594.2017.1341021

Donahue, R., Sahoo, J. K., Rudolph, S., Chen, Y., & Kaplan, D. L. (2023). Mucosa-Mimetic Materials for the Study of Intestinal Homeostasis and Disease. In *Advanced Healthcare Materials* (Vol. 12, Issue 25). John Wiley and Sons Inc. https://doi.org/10.1002/adhm.202300301

Edouard, S., Million, M., Bachar, D., Dubourg, G., Michelle, C., Ninove, L., Charrel, R., & Raoult, D. (2018). The nasopharyngeal microbiota in patients with viral respiratory tract infections is enriched in bacterial pathogens. *European Journal of Clinical Microbiology and Infectious Diseases*, *37*(9), 1725–1733. https://doi.org/10.1007/s10096-018-3305-8

Hirose, Y., Poudel, S., Sastry, A. V., Rychel, K., Lamoureux, C. R., Szubin, R., Zielinski, D. C., Lim, H. G., Menon, N. D., Bergsten, H., Uchiyama, S., Hanada, T., Kawabata, S., Palsson, B. O., & Nizet, V. (2023). Elucidation of independently modulated genes in Streptococcus

pyogenes reveals carbon sources that control its expression of hemolytic toxins. *MSystems*, *8*(3). https://doi.org/10.1128/msystems.00247-23

Kohout, V. R., Wardzala, C. L., & Kramer, J. R. (2022). Synthesis and biomedical applications of mucin mimic materials. In *Advanced Drug Delivery Reviews* (Vol. 191). Elsevier B.V. https://doi.org/10.1016/j.addr.2022.114540

Kruger, A. G., Brucks, S. D., Yan, T., Cárcarmo-Oyarce, G., Wei, Y., Wen, D. H., Carvalho, D. R., Hore, M. J. A., Ribbeck, K., Schrock, R. R., & Kiessling, L. L. (2021). Stereochemical Control Yields Mucin Mimetic Polymers. *ACS Central Science*, *7*(4), 624–630. https://doi.org/10.1021/acscentsci.0c01569

Li, H., Zhao, X., Wang, J., Dong, Y., Meng, S., Li, R., Niu, X., & Deng, X. (2015). β-sitosterol interacts with pneumolysin to prevent Streptococcus pneumoniae infection. *Scientific Reports*, *5*. https://doi.org/10.1038/srep17668

Lv, Q., Zhang, P., Quan, P., Cui, M., Liu, T., Yin, Y., & Chi, G. (2020). Quercetin, a pneumolysin inhibitor, protects mice against Streptococcus pneumoniae infection. *Microbial Pathogenesis*, *140*, 103934. https://doi.org/https://doi.org/10.1016/j.micpath.2019.103934

Nason, R., Büll, C., Konstantinidi, A., Sun, L., Ye, Z., Halim, A., Du, W., Sørensen, D. M., Durbesson, F., Furukawa, S., Mandel, U., Joshi, H. J., Dworkin, L. A., Hansen, L., David, L., Iverson, T. M., Bensing, B. A., Sullam, P. M., Varki, A., … Narimatsu, Y. (2021). Display of the human mucinome with defined O-glycans by gene engineered cells. *Nature Communications*, *12*(1). https://doi.org/10.1038/s41467-021-24366-4

Orihuela, C. J., Gao, G., Francis, K. P., Yu, J., & Tuomanen, E. I. (2004). Tissue-specific contributions of pneumococcal virulence factors to pathogenesis. *The Journal of Infectious Diseases*, *190*(9), 1661–1669. https://doi.org/10.1086/424596

Roy, M. G., Livraghi-Butrico, A., Fletcher, A. A., McElwee, M. M., Evans, S. E., Boerner, R. M., Alexander, S. N., Bellinghausen, L. K., Song, A. S., Petrova, Y. M., Tuvim, M. J., Adachi, R., Romo, I., Bordt, A. S., Bowden, M. G., Sisson, J. H., Woodruff, P. G., Thornton, D. J., Rousseau, K., … Evans, C. M. (2014). Muc5b is required for airway defence. *Nature*, *505*(7483), 412–416. https://doi.org/10.1038/nature12807

Saldova, R., & Wilkinson, H. (2020). Current methods for the characterization of o-glycans. In *Journal of Proteome Research* (Vol. 19, Issue 10, pp. 3890–3905). American Chemical Society. https://doi.org/10.1021/acs.jproteome.0c00435

Stevens, E. J., Morse, D. J., Bonini, D., Duggan, S., Brignoli, T., Recker, M., Lees, J. A., Croucher, N. J., Bentley, S., Wilson, D. J., Earle, S. G., Dixon, R., Nobbs, A., Jenkinson, H., van Opijnen, T., Thibault, D., Wilkinson, O. J., Dillingham, M. S., Carlile, S., … Massey, R. C. (2022). Targeted control of pneumolysin production by a mobile genetic element in Streptococcus pneumoniae. *Microbial Genomics*, *8*(4). https://doi.org/10.1099/mgen.0.000784

Takagi, J., Aoki, K., Turner, B. S., Lamont, S., Lehoux, S., Kavanaugh, N., Gulati, M., Valle Arevalo, A., Lawrence, T. J., Kim, C. Y., Bakshi, B., Ishihara, M., Nobile, C. J., Cummings, R. D., Wozniak, D. J., Tiemeyer, M., Hevey, R., & Ribbeck, K. (2022). Mucin O-glycans are natural inhibitors of Candida albicans pathogenicity. *Nature Chemical Biology*, *18*(7), 762–773. https://doi.org/10.1038/s41589-022-01035-1

Verherstraeten, S., Goossens, E., Valgaeren, B., Pardon, B., Timbermont, L., Haesebrouck, F., Ducatelle, R., Deprez, P., Wade, K. R., Tweten, R., & Immerseel, F. Van. (2015). Perfringolysin o: The underrated clostridium perfringens toxin? *Toxins*, *7*(5), 1702–1721. https://doi.org/10.3390/toxins7051702

Wang, S., Chen, C., Gadi, M. R., Saikam, V., Liu, D., Zhu, H., Bollag, R., Liu, K., Chen, X., Wang, F., Wang, P. G., Ling, P., Guan, W., & Li, L. (2021). Chemoenzymatic modular assembly of O-GalNAc glycans for functional glycomics. *Nature Communications*, *12*(1). https://doi.org/10.1038/s41467-021-23428-x

Werlang, C. (2022). *The regulation of bacterial virulence by mucin glycans*. Massachusetts Institute of Technology.

Werlang, C., Cárcarmo-Oyarce, G., & Ribbeck, K. (2019). Engineering mucus to study and influence the microbiome. *Nature Reviews Materials*, *4*(February). https://doi.org/10.1038/s41578-018-0079-7

Wheeler, K. M., Cárcamo-Oyarce, G., Turner, B. S., Dellos-Nolan, S., Co, J. Y., Lehoux, S., Cummings, R. D., Wozniak, D. J., & Ribbeck, K. (2019). Mucin glycans attenuate the virulence of Pseudomonas aeruginosa in infection. In *Nature Microbiology* (Vol. 4, Issue 12, pp. 2146–2154). Nature Research. https://doi.org/10.1038/s41564-019-0581-8

Wu, C. M., Wheeler, K. M., Cárcamo-Oyarce, G., Aoki, K., McShane, A., Datta, S. S., Mark Welch, J. L., Tiemeyer, M., Griffen, A. L., & Ribbeck, K. (2023). Mucin glycans drive oral microbial community composition and function. *Npj Biofilms and Microbiomes*, *9*(1). https://doi.org/10.1038/s41522-023-00378-4

Xu, L., Earl, J., & Pichichero, M. E. (2021). Nasopharyngeal microbiome composition associated with Streptococcus pneumoniae colonization suggests a protective role of Corynebacterium in young children. *PLoS ONE*, *16*(9 September). https://doi.org/10.1371/journal.pone.0257207

Figures

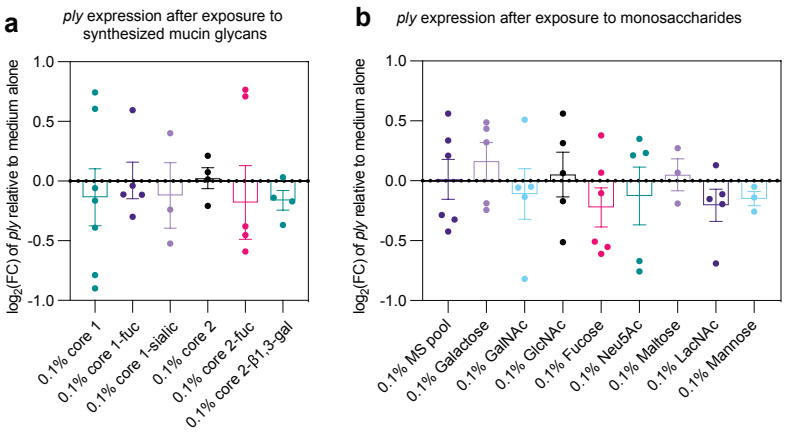

Figure 4.1: Individual mucin glycans and monosaccharides do not regulate *ply*.

(A, B) Gene expression was measured during growth with mucin glycans **(A)** or mono and disaccharides **(B)** after 5 h in the indicated strain and medium condition by RT-qPCR and normalized to *gyrB*. **(A-B)** Bars indicate mean ± s.e.m. with individual biological replicates shown.

Appendix A: Mucins do not regulate ply through characterized mechanisms

Deniz Uzun contributed to experimental work presented in this section.

Introduction

Pneumolysin (PLY) is a critical virulence factor in *S. pneumoniae* and is produced by virtually all sequenced clinical isolates (Paton et al., 1993). PLY enhances transmission, damages host tissue and is a potent immune stimulant (Weiser et al., 2018). Despite being first identified over a century ago (Cole, 1914), the regulation of PLY is not well understood (Stevens et al., 2022). As the threat of antibiotic resistance increases, PLY has been investigated as a therapeutic target, and many inhibitors of PLY oligomerization and host-cell binding have been described (Cabal et al., 2023). Improving the understanding of the regulation of *ply* may enhance the development of therapeutic agents.

In Chapter 2, I demonstrated that mucins downregulate *ply* in *S. pneumoniae*. Among PLY inhibitors, acting as a regulator is a unique feature and opens a viable channel for us to further define *ply* regulation. In this Appendix, I explore potential mechanisms for mucin regulation of *ply* by exploring mucin binding and gene deletions based on putative regulators identified in forward genetic screens.

Results

S. pneumoniae does not regulate *ply* by sensing extracellular PLY

We first explored whether mucin binding of PLY could control regulation. Feedback loops are a common regulatory mechanism in *S. pneumoniae* (Slager et al., 2019b), and one model for regulation of PLY could depend on a feedback loop in which *S. pneumoniae* senses the toxin to activate its own transcription. If mucin bound PLY sequestering the toxin, it would disrupt this mechanism.

Rather than purify PLY protein, we leveraged our PLY knockout strain TIGR4Δ*ply* to test whether *S. pneumoniae* responds to soluble PLY. By hemolysis assay, the supernatant of TIGR4 contains active PLY, while the supernatant of TIGR4Δ*ply* does not. We exposed *S. pneumoniae* TIGR4 to spent medium from TIGR4 and TIGR4Δ*ply*, and measured gene expression by RT-

qPCR after 30 m of exposure (Fig. A.1). In Chapter 2 of this thesis, we demonstrated mucin is effective at reducing the expression of *ply* after 30 m of exposure (Fig 2.2e). In contrast, we found that the expression of *ply* does not change after 30 m exposure to spent medium from different strains. These data suggest that *S. pneumoniae* does not regulate *ply* through sensing extracellular PLY concentration. Thus, mucin likely does not bind PLY to disrupt regulation.

FruA and LuxS do not regulate *ply* in TIGR4

One of the few genes that has been described as a *ply* regulator is *luxS* (Vidal et al., 2011), an enzyme required to produce the quorum sensing molecule autoinducer 2 (AI-2). In D39Δ*luxS*, expression of *ply* was reduced relative to WT, suggesting LuxS, and potentially AI-2, is an activator of *ply*. In addition, it was described that FruA is a receptor for AI-2 (Trappetti et al., 2017), suggesting FruA may be involved in LuxS signal transduction, and thus regulation of PLY.

We generated marked gene deletion strains to test whether *luxS* regulates *ply* in TIGR4, and whether *fruA* senses this signal. We measured the release of PLY by measuring hemolytic activity but did not observe a significant difference in both TIGR4Δ*luxS* and TIGR4Δ*fruA* (Fig. A.2a). We next measured the expression of *ply* by RT-qPCR. Interestingly, we did not observe changes in *ply* expression in TIGR4Δ*luxS* or TIGR4Δ*fruA* (Fig. A.2b), suggesting LuxS/AI-2 regulation of *ply* may differ depending on genetic background based on the existing literature. We also exposed TIGR4Δ*luxS* and TIGR4Δ*fruA* to MUC2 and MUC5AC and observed robust down-regulation of *ply* by RT-qPCR (Fig. A.2b). Together, these data show LuxS does not regulate *ply* in TIGR4, and importantly, mucin does not regulate *ply* through this pathway.

Transposon screens, mutagenesis screens, and genome-wide association studies identify genes that regulate *ply*

Given the interest in PLY, multiple screens have been described to identify PLY regulators, each with their own drawbacks. We analyzed these screens for candidate genes that may be involved with mucin-regulation of *ply*. In one example, authors leveraged a transposon insertion library to identify mutants with defects in PLY release using hemolytic activity as a readout (Price, 2011). This screen identified several genes, notably two genes of unknown function that are co-transcribed in the same operon as *ply*. However, it was also hampered by incomplete coverage of the genome. In addition, transposon insertion screens cannot identify the contribution of essential

genes.

Another approach to screening for *ply* regulators utilized *Bacillus subtilis*, a Gram-positive model organism (Greene, 2015). The author noted that when *ply* is expressed in *B. subtilis*, the resulting colonies are distinguishable from WT through a zone of α-hemolysis when plated on blood agar. The authors performed a mutagenesis screen using N-ethyl-N-nitrosourea to identify mutants with defects in PLY production. The authors sequenced 20 mutants and found mutations in genes with homologues in *S. pneumoniae* that impacted PLY release.

Recently, a genome-wide association study (GWAS) analyzing hemolytic activity as a proxy for PLY release in clinical isolates of the PMEN1 lineage was published (Stevens et al., 2022). This study identified a mobile genetic element that encoded machinery that specifically modulated *ply* transcription. While this element is not widely conserved in *S. pneumoniae*, there are several other genes of interest their study identified as *ply* regulators. A key feature of the screens mentioned is that they assay PLY release rather than transcriptional changes to *ply* as observed with mucin.

By analyzing the results of these studies, we created a panel of genes (Table A.1) that may be involved in mucin regulation of *ply*. In total, nine genes were selected based on their annotation in the screens presented, annotation in the Carbohydrate-Active enZYmes (CAZY) database as mucin-binding genes, and whether they are regulated by MUC5AC. Each of these features suggest involvement in mucin-regulation of *ply*.

We generated several marked gene deletions to test the involvement of genes in PLY release and the mucin-regulation of PLY. One gene of interest, *pbp2x*, is annotated as essential thus could not be deleted gene. We generated ten knockouts, TIGR4Δ*SP_1925*, TIGR4Δ*SP_1926*, TIGR4Δ*lytN*, TIGR4Δ*eng*, TIGR4Δ*mucB*, TIGR4Δ*psrP*, TIGR4Δ*gtfA*, TIGR4Δ*xylS*, TIGR4Δ*adhE*, and TIGR4Δ*clpL*. We first measured whether these genes are involved in PLY release through a standard hemolysis assay. We found that deletion of these genes did not significantly alter hemolytic activity relative to TIGR4 (Fig. A.3a). This result was expected for TIGR4Δ*lytN* where the role in altering PLY release was shown to be dose dependent (Greene, 2015). The genes identified through GWAS were validated as PLY regulators, and this data suggests that those genes may have been false positives or that the genetic background matters for the contribution of these genes to PLY release.

We next measured the expression of *ply* in each strain by RT-qPCR. Interestingly, we did

not observe changes in *ply* expression in any of the strains tested, which makes sense with our hemolysis result (Fig. A.3b). Interestingly, we found that disrupting these genes did not prevent MUC2-regulation of *ply*. In each case, transcription of *ply* was lower after exposure to 0.5% MUC2 (Fig. A.3b). For a few genes, we also tested the transcription of *ply* after exposure to 0.1% MUC5AC, and again found mucin was still able to regulate *ply*. Thus, deleting these genes was not sufficient to alter the response to MUC2 or MUC5AC. Together, these data show these genes do not regulate *ply* in TIGR4, and importantly, are not important for mucin-regulation of *ply*.

Discussion

This work did not reveal the mechanism through which mucin regulates *ply*, we were able to narrow down likely models. While mucin may bind PLY, it is unlikely this binding is responsible for mucin regulation of *ply* expression. Similarly, our brute force exploration of genetic knockouts failed to identify genes involved in mucin-regulation of *ply*, we have clarified single genes that are not involved. This study did not test for the possibility that these genes act together to suppress *ply* transcription or are otherwise redundant. For example, both *xylS* and *eng* encode putative glycosidases that could be redundant such that knocking each gene out separately did not alter mucin regulation of *ply*.

Identifying general regulators of *ply* is an active area of research. PLY is one member of a family of cholesterol-dependent cytolysins (CDCs) where the regulation of these toxins in other species is similarly murky and an open que. For example, *Streptococcus pyogenes* encodes CDC streptolysin O (SLO), and regulation of this toxin is similarly murky. A recent study demonstrated that carbon source regulates expression of SLO (Hirose et al., 2023). Interestingly, they showed that when supplied as a carbon source, glucose, dextrin and maltose (all of which are composed of glucose), differentially regulated SLO expression. Similar breakthroughs on the regulation of PLY will likely lead to clarifying the mechanism of mucin regulation.

Materials and methods

Strains and reagents

The bacterial strain *S. pneumoniae* TIGR4 was a gift from Marc Lipsitch (Harvard T.H. Chan School of Public Health). TIGR4 was originally isolated from the blood of a 30-year-old male and is highly virulent in a mouse infection model. The bacterial strain *S. pneumoniae* TIGR4Δ*ply* was a gift from Justin Thornton (Bryant et al., 2016b) (Mississippi State University). For general propagation and storage, bacteria were grown on tryptic soy with 5% sheep blood (TSB) agar plates overnight at 37 °C with 5% CO_2. Bacteria were cultured and maintained in THY broth. Erythromycin (Ery; 0.5 μg/mL) was added to the medium for strains with antibiotic-resistance.

Mutant strain construction

Marked deletions were generated by amplifying up and downstream regions of the gene of interest followed by overlap extension PCR to insert the *ermB* gene. A list of primers used is available in Table A.2. The DNA fragment was amplified by PCR (Roche KAPA HiFi HotStart ReadyMix) and purified. *S. pneumoniae* was transformed via stimulation with 100ng CSP-2 (AnaSpec) before adding purified DNA fragments. Transformed mutants that incorporated *ermB* were isolated on TSB agar supplemented with Ery.

Hemolysis assay

PLY release into the supernatant was quantified by a standard hemolytic assay. Briefly, after 5 hours, the OD of *S. pneumoniae* cultures was measured. The supernatants from cultures were isolated and serially diluted in PBS + 0.1% dithiothreitol. Washed 1% sheep red blood cells in PBS were added to the wells and were incubated at 37 °C for 1 hour. Water and PBS alone were added for a 100% and 0% hemolysis control, respectively. After incubation, the sheep erythrocytes were pelleted, the supernatant was removed, and the absorbance was measured at 540nm. The hemolytic activity was normalized to total growth of each strain.

RNA preparation for gene expression analysis

In brief, *S. pneumoniae* was grown on TSB agar overnight and liquid pre-cultures were inoculated in THY broth. After growth to OD ~0.4, cultures were diluted to OD 0.01 (approximately 10^7 colony-forming units (CFU)/mL) into THY broth supplemented with or without 0.5% mucin. After

5 h (unless otherwise noted) of growth at 37 °C with 5% CO_2, the samples were collected mid-log phase and pelleted at 16,000*g*. For spent medium experiments, cultures were grown for 4.5 h and then spent medium was added. After an additional 30 m incubation, samples were pelleted. The supernatant was then removed, and the pellets were flash-cooled in liquid nitrogen and stored at −80 °C. Pellets were thawed on ice and resuspended in 25µL lysozyme buffer. Ready-Lyse Lysozyme (Biosearch Technologies) was added, and the samples were incubated at room temperature (RT) for 15 min. Total RNA was then extracted using the MasterPure Complete RNA Purification kit (Biosearch Technologies). Genomic DNA was removed using the Turbo DNA-free kit (Invitrogen). The samples were stored at -20 °C.

RT–qPCR analysis

A list of the primers used for RT-qPCR are listed in Table A.2. First-strand complementary DNA (cDNA) was synthesized using the Protoscript II First-Strand cDNA Synthesis kit (New England Biolabs). The elimination of genomic DNA was confirmed by qPCR amplification on negative control samples that did not have reverse transcriptase during cDNA synthesis. 8 ng of cDNA was used as a template for RT-qPCR using the SYBR Green Master Mix (Thermo Fisher Scientific) and performed in a Cycler 480 II Real-time PCR Machine (Roche). Forward and reverse primers were added at 3 µM each. Melting-curve analyses verified amplification of a single product. Gene expression changes were calculated based on mean change in the qPCR cycle threshold compared to *gyrB* or *16S* (ΔC_t) and are reported as $\log_2[\text{FC}] = \Delta C_t\_\text{CM} - \Delta C_t\_\text{sample}$. Each sample was analyzed with at least three technical replicates.

References

Bryant, J. C., Dabbs, R. C., Oswalt, K. L., Brown, L. R., Rosch, J. W., Seo, K. S., Donaldson, J. R., McDaniel, L. S., & Thornton, J. A. (2016). Pyruvate oxidase of Streptococcus pneumoniae contributes to pneumolysin release. *BMC Microbiology*, *16*(1), 1–12. https://doi.org/10.1186/s12866-016-0881-6

Cabal, M. D. C., Molina, F., López-Sánchez, J. I., Pérez-Santín, E., & del Mar García-Suárez, M. (2023). Pneumolysin as a target for new therapies against pneumococcal infections: A systematic review. *PLoS ONE*, *18*(3 March). https://doi.org/10.1371/journal.pone.0282970

Cole, R. (1914). Pneumococcus hemotoxin. *Journal of Experimental Medicine*, *20*(4), 346–362. https://doi.org/https://doi.org/10.1084/jem.20.4.346

Greene, Neil. G. (2015). *An investigation of the role that peptidoglycan composition and remodeling plays in the release of pneumolysin from Streptococcus pneumoniae*. Tufts University.

Hirose, Y., Poudel, S., Sastry, A. V., Rychel, K., Lamoureux, C. R., Szubin, R., Zielinski, D. C., Lim, H. G., Menon, N. D., Bergsten, H., Uchiyama, S., Hanada, T., Kawabata, S., Palsson, B. O., & Nizet, V. (2023). Elucidation of independently modulated genes in Streptococcus pyogenes reveals carbon sources that control its expression of hemolytic toxins. *MSystems*, *8*(3). https://doi.org/10.1128/msystems.00247-23

Paton, J. C., Andrew, P. W., Boulnois, G. J., & Timothy Mitchell, K. J. (1993). Molecular analysis of the pathogenicity of Streptococcus pneumoniae: the role of pneumococcal proteins. In *Annu. Rev. Microbial* (Vol. 47). www.annualreviews.org

Price, Katherine. E. (2011). *Characterization of the Cell Wall Localization of Pneumolysin in Streptococcus pneumoniae*. Tufts University.

Slager, J., Aprianto, R., & Veening, J.-W. (2019). *Refining the Pneumococcal Competence Regulon by RNA Sequencing*. https://doi.org/10.1128/JB

Stevens, E. J., Morse, D. J., Bonini, D., Duggan, S., Brignoli, T., Recker, M., Lees, J. A., Croucher, N. J., Bentley, S., Wilson, D. J., Earle, S. G., Dixon, R., Nobbs, A., Jenkinson, H., van Opijnen, T., Thibault, D., Wilkinson, O. J., Dillingham, M. S., Carlile, S., … Massey, R. C. (2022). Targeted control of pneumolysin production by a mobile genetic element in Streptococcus pneumoniae. *Microbial Genomics*, *8*(4). https://doi.org/10.1099/mgen.0.000784

Trappetti, C., McAllister, L. J., Chen, A., Wang, H., Paton, A. W., Oggioni, M. R., McDevitt, C. A., & Paton, J. C. (2017). Autoinducer 2 signaling via the phosphotransferase FruA drives galactose utilization by streptococcus pneumoniae, resulting in hypervirulence. *MBio*, *8*(1). https://doi.org/10.1128/mBio.02269-16

Vidal, J. E., Ludewick, H. P., Kunkel, R. M., Zähner, D., & Klugman, K. P. (2011). The luxs-dependent quorum-sensing system regulates early biofilm formation by streptococcus pneumoniae strain D39. *Infection and Immunity*, *79*(10), 4050–4060. https://doi.org/10.1128/IAI.05186-11

Weiser, J. N., Ferreira, D. M., & Paton, J. C. (2018). Streptococcus pneumoniae: Transmission, colonization and invasion. In *Nature Reviews Microbiology* (Vol. 16, Issue 6, pp. 355–367). Nature Publishing Group. https://doi.org/10.1038/s41579-018-0001-8

Acknowledgements

This work was supported by the Toxicology Training Grant T32-ES007020 (to J.B.), the NIH NIBIB under award R01-EB017755-07 (to K.R.), the Bill and Melinda Gates Foundation under award INV-041182 (to K.R.), and the National Institute of Environmental Health Sciences of the NIH under award P30-ES002109 (to the MIT Center for Environmental Health Science). We thank the MIT BioMicro Center for maintaining the RT-qPCR machine facility. We thank Deniz Uzun for generating several of the strains tested.

Figures

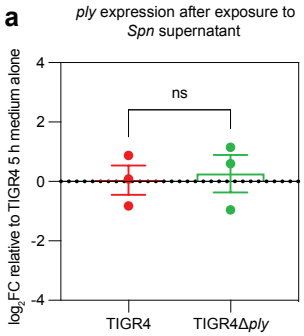

Figure A.1: *S. pneumoniae* does regulate *ply* in response to extracellular PLY

(A) Expression of *ply* was measured after 30 m exposure to spent medium from the indicated strain by RT-qPCR and normalized to *gyrB*. Bars indicate mean ± s.e.m. with individual biological replicates shown. Significance was assessed using the Mann-Whitney U-test. ns: not significant.

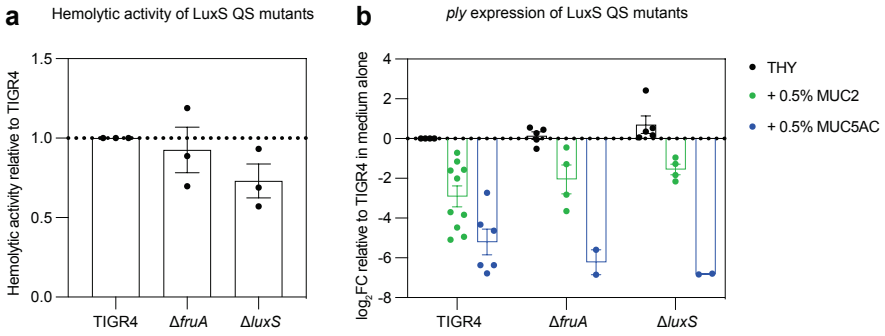

Figure A.2: *S. pneumoniae* does not regulate *ply* through a *luxS*-dependent mechanism.

(A) Hemolytic activity of the culture supernatant of each strain was assessed by absorbance at 540 nm and normalized to the activity of TIGR4. **(B)** Expression of *ply* was measured after 5 h in the indicated strain and medium condition by RT-qPCR and normalized to *gyrB*. Bars indicate mean ± s.e.m. with individual biological replicates shown.

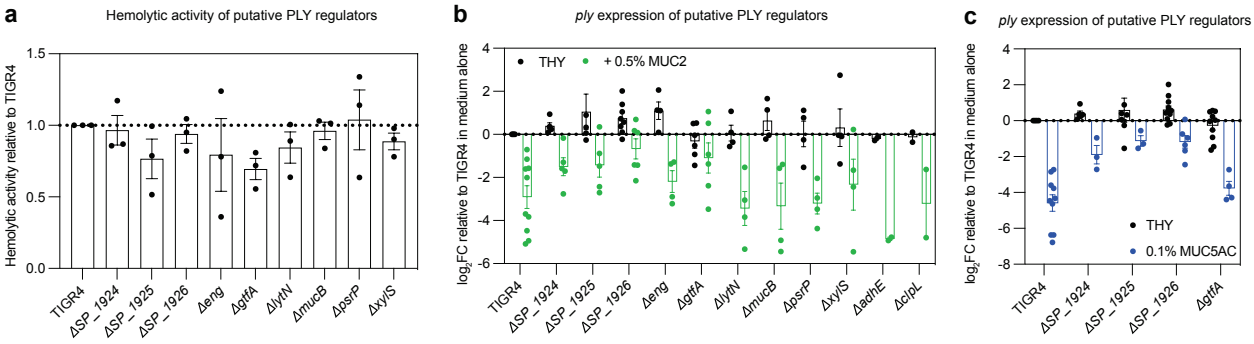

Figure A.3: *S. pneumoniae* does not regulate *ply* through genes identified in genetic screens. **(A)** Hemolytic activity of the culture supernatant of each strain was assessed by absorbance at 540 nm and normalized to the activity of TIGR4. **(B)** Expression of *ply* was measured after 5 h in the indicated strain and THY ± 0.5% MUC2 by RT-qPCR and normalized to *gyrB*. **(C)** Expression of *ply* was measured after 5 h in the indicated strain and THY ± 0.1% MUC5AC by by RT-qPCR and normalized to *gyrB*. Bars indicate mean ± s.e.m. with individual biological replicates shown.

Supplementary Tables

Gene	Transposon screen	*B. subtilis* screen	GWAS	CAZY	Mucin binding	Log2FC of DEG from MUC5AC RNA-seq
SP_1925	X					-5.42
SP_1926	X					-5.48
lytN		X		X		-1.10
eng			X	X		
mucB					X	
psrP				X	X	
gtfA			X	X		
xylS			X	X		+0.27
pbp2X		X	X	X		
adhE			X			+1.24
clpL			X			+2.41

Supplementary Table A.1: Genes identified as *ply* regulators through forward genetic screens.

Table shows each gene selected and relevant features including the screen where it was identified, presence in the CAZY database, mucin binding features, and the log2FC after exposure to MUC5AC, as identified with RT-qPCR. DEG: differentially expressed gene.

Primer name	Purpose	Primer sequence 5'>3'
ply-F	RT-qPCR	GAGAGGAATTTCTGCAGAGC
ply-R	RT-qPCR	CTTCATCACTCTTACTCGTGG
gyrB-F	RT-qPCR	CCAATCCTAGAAGCTGGTTATGT
gyrB-F	RT-qPCR	CACCCGGCTGGATATATTCTTT
ermB-F	amplify ermB	GGAAATAAGACTTAGAAGCAAAC
ermB-R	amplify ermB	CCAAATTTACAAAAGCGACTC
luxS_up_F	SP0340 luxS KO	CGTAAGGTTGCTGTCGTTGC
luxS_up_R_ermB	SP0340 luxS KO	GTTTGCTTCTAAGTCTTATTTCCATAAAGGTTGCTCCTGAGAC
luxS_down_F_ermB	SP0340 luxS KO	GAGTCGCTTTTGTAAATTTGGGATGCCTTTGAACGTCATGTG
luxS_down_R	SP0340 luxS KO	GACTTGGTAGTCAGTCAAGC
fruA_up_F	SP0877 fruA KO	CCAGGTGGCAGAAGATACTC
fruA_up_R_ermB	SP0877 fruA KO	GTTTGCTTCTAAGTCTTATTTCCGCCTGCAAATCTAGCAACATG
fruA_down_F_ermB	SP0877 fruA KO	GAGTCGCTTTTGTAAATTTGGGTTACCTACGCAAACCACAAG
fruA_down_R	SP0877 fruA KO	CTGACTAGGAGAGAACCCAC
1926_up_F	SP1926 KO	CCGTCGCATCAATCATTAC
1926_up_R_ermB	SP1926 KO	GTTTGCTTCTAAGTCTTATTTCCCTTTGATAATCATAGTATAACATATTTG
1926_down_F_ermB	SP1926 KO	GAGTCGCTTTTGTAAATTTGGGGTAGAGGAAATGTCTCAATC
1926_down_R	SP1926 KO	GCTGTCAATTTAGTAGCATCTTG
1925_up_F	SP1925 KO	GTTTCGCAGGAAGTCTAATAAG
1925_up_R_ermB	SP1925 KO	GTTTGCTTCTAAGTCTTATTTCCGACAGGTAGCTGGATTGAG
1925_down_F_ermB	SP1925 KO	GAGTCGCTTTTGTAAATTTGGGATTAAGAGAGGAGATGTTGTAG
1925_down_R	SP1925 KO	CAATACTTTCTCCCTGATGG
LytN_up_F	SP0107 LytN KO	GTCCAGACAATCTTGATACC
LytN_up_R_ermB	SP0107 LytN KO	GTTTGCTTCTAAGTCTTATTTCCCTCCTTCTTTCTATAGTTCTATCATAC
LytN_down_F_ermB	SP0107 LytN KO	GAGTCGCTTTTGTAAATTTGGGTAAAGAGTCGAGGAAATCC

LytN_down_R	SP0107 LytN KO	GAACAACCAGAGTAGTATTAAGC
eng_up_F	SP0368 eng KO	CTTGGTTGACAGATAGTGC
eng_up_R_ermB	SP0368 eng KO	GTTTGCTTCTAAGTCTTATTTCCCTCCTT CCTCTGAAAGTGC
eng_down_F_ermB	SP0368 eng KO	GAGTCGCTTTTGTAAATTTGGCTCTTAA CAAGATTACGGAAGC
eng_down_R	SP0368 eng KO	CTAACCGTCTGACACCAC
MucB_up_F	SP1492 MucB KO	GTGAAAGTTCGCTATGTTGATG
MucB_up_R_ermB	SP1492 MucB KO	GTTTGCTTCTAAGTCTTATTTCCCCTCAA CATTCTCACGGTAG
MucB_down_F_ermB	SP1492 MucB KO	GAGTCGCTTTTGTAAATTTGGCAGGAAA AGCTCACAGATG
MucB_down_R	SP1492 MucB KO	GTATGTTGCCACAACTAAGG
SpsrP_up_F	SP1772 PsrP KO	GTCCTATATATTGACGAAACGG
psrP_up_R_ermB	SP1772 PsrP KO	GTTTGCTTCTAAGTCTTATTTCCCGCAAG ACCTTAAACAAGC
psrP_down_F_ermB	SP1772 PsrP KO	GAGTCGCTTTTGTAAATTTGGAGTTAGG CTAAACTAACTCGC
psrP_down_R	SP1772 PsrP KO	TCTTGAGTTTCATACAAGTTCTC
xylS_up_F	SP0312 xylS KO	GATCCGGGTTCTTCAGTT
xylS_up_R_ermB	SP0312 xylS KO	GTTTGCTTCTAAGTCTTATTTCCTCTAGTA CGTTTGATGTCTCG
xylS_down_F_ermB	SP0312 xylS KO	GAGTCGCTTTTGTAAATTTGGTAGTGTAT ATGAAGATTCTGTATGG
xylS_down_R	SP0312 xylS KO	GGATTTCCCTTGCAATCAG
gtfA_up_F	SP1894 gtfA KO	ACACCTGCATATTGGGTG
gtfA_up_R_ermB	SP1894 gtfA KO	GTTTGCTTCTAAGTCTTATTTCCTGAAGC CTTGATATGGTGG
gtfA_down_F_ermB	SP1894 gtfA KO	GAGTCGCTTTTGTAAATTTGGAGTCTCA TATGATCTGGCTTC
gtfA_down_R	SP1894 gtfA KO	TTGTCTTGAACCGGGATTC
adhE_up_F	SP2026 adhE KO	CCAAGGTACCATTACCTTCC
adhE_up_R_ermB	SP2026 adhE KO	GTTTGCTTCTAAGTCTTATTTCCGCTTTC AAGGAACGATATCC
adhE_down_F_ermB	SP2026 adhE KO	GAGTCGCTTTTGTAAATTTGGGTTTATCA GTCTAGAAGCAAGAC
adhE_down_R	SP2026 adhE KO	CAACACACCTTGTCATCG
clpL_up_F	SP0338 clpL KO	ATGTAAGAATGGCACCCTG

clpL_up_R_ermB	SP0338 clpL KO	GTTTGCTTCTAAGTCTTATTTCCGATTACTGATATTGACTATCTTTGACC
clpL_down_F_ermB	SP0338 clpL KO	GAGTCGCTTTTGTAAATTTGGTCGTGAGAAAGTCTAAGACAG
clpL_down_R	SP0338 clpL KO	GGCTTCCACATGATTATGTG

Supplementary Table A.2: Primers used to generate marked gene deletions.

Sequences for each primer are shown. For ermB overlap primers used in overlap extension PCR, the segment in black binds to the *ermB* gene and the segment in blue binds to the gene of interest.

Appendix B: Mucins sensitize *S. pneumoniae* to cell wall-targeting antibiotics

Introduction

Cell wall-targeting antibiotics are important and effective tools for the treatment of *S. pneumoniae* infections. However, the spread of antibiotic resistance is a constant threat (CDC, 2019). *S. pneumoniae* is naturally competent and can take up and integrate extracellular DNA from the environment, leading to remarkable genomic plasticity and rapid evolution, including the development of antibiotic resistance (Slager et al., 2019a). Thus, the mechanisms of antibiotic action and resistance in *S. pneumoniae* is an active area of research.

Many antibiotics target the bacterial cell wall; the Gram-positive cell wall is composed of a thick outer layer of peptidoglycan and an inner plasma membrane (Vollmer et al., 2008). The cell wall of *S. pneumoniae* also contains a large proportion of teichoic acids (Vollmer et al., 2019). Peptidoglycan is composed of polysaccharides cross-linked to short peptides creating a mesh like structure. The biosynthesis is a complex process with several key steps that are vulnerable to disruption. For example, beta-lactam antibiotics inhibit transpeptidase enzymes that link nascent peptidoglycan components to the existing structure by competing with peptide components (Vollmer et al., 2008). In many cases, cell wall-targeting antibiotics interfere with peptidoglycan biosynthesis, weakening the scaffold such that the structural integrity eventually fails, lysing the cell (Kohanski et al., 2010).

In *S. pneumoniae*, the two-component system CiaRH is involved in the response to antibiotic stress, and mutations in these genes can alter sensitivity to cell wall inhibitors (Haas et al., 2005; Mascher et al., 2006; Peters et al., 2021; Rogers et al., 2007). In the RNA-seq presented in Chapter 2 of this thesis, we identified that MUC5AC downregulates CiaRH. Given this result, we explored whether mucin modulates sensitivity to antibiotics and if this occurs through CiaRH-mediated signaling.

Results

To evaluate the sensitivity of *S. pneumoniae* TIGR4 to antibiotics after exposure to mucin, we exposed mid-log phase bacteria after growth in mucin to a panel of antibiotics for 2 h at a concentration of 1-5x the minimum inhibitory concentration (MIC) and evaluated survival by plating for CFUs (Fig. B.1; Fig SB.1). We selected three different cell wall inhibitors representing

different mechanisms of action including vancomycin, bacitracin, and piperacillin. As a comparison, we also tested ciprofloxacin that inhibits DNA replication, and tetracycline that inhibits protein translation. We found that mucins MUC2 and MUC5AC increased sensitivity to cell wall inhibitors by a factor of 3-60x, but not to other types of antibiotics (Fig B.2). The effect was strongest with piperacillin which is a beta-lactam and clinically relevant for *S. pneumoniae* treatment (C. T. Huang et al., 2022; Speich et al., 1998). Of note, vancomycin and ciprofloxacin do not bind mucins, and non-charged antibiotics would not be expected to bind mucins (Witten, 2019).

Because *S. pneumoniae* downregulates *ciaRH* in response to mucin, we hypothesized this two-component system may be involved in mediating cell wall inhibitor sensitization. CiaRH is a classic two-component system in which *ciaH* encodes a transmembrane histidine kinase that upon activation, phosphorylates the response regulator ciaR, which acts as a transcription factor and directs changes in gene expression. Thus, CiaH could sense and respond to extracellular mucin. We generated a signal blind mutant JB01 to test whether CiaRH regulates genes in response to mucin or sensitizes *S. pneumoniae* to antibiotics. Specifically, we deleted *ciaH* and placed *ciaR* under the control of the isopropyl β-D-1-thiogalactopyranoside (IPTG)-inducible P_{lac} promoter (Keller et al., 2019). We validated our approach by measuring *ciaR* expression after exposure to multiple concentrations of IPTG and saw that as expected, the expression of *ciaR* increased with increasing concentrations of IPTG (Fig B.3).

We used this strain to test if mucin signals through CiaRH to sensitize *S. pneumoniae* to cell wall inhibitors. We grew TIGR4 and JB01 with or without mucin, and with or without IPTG and exposed the bacterium to 1μg/mL piperacillin. Bacteria were evaluated for survival by CFU after 2 h of antibiotic exposure (Fig B.3). We found that as expected, when CiaR was not induced without the addition of IPTG, JB01 was more sensitive to piperacillin compared to TIGR4. When IPTG was added, JB01 was less sensitive to piperacillin, on par with TIGR4. However, regardless of the addition of IPTG, the addition of MUC2 enhanced sensitivity in both cases, suggesting mucin does not signal through CiaH to regulate CiaR and mediate this phenotype. However, it leaves open the possibility that mucin-regulation of CiaR contributes to this phenotype through a CiaH-independent mechanism.

Discussion

In this work, we demonstrated that mucin sensitizes *S. pneumoniae* to cell wall-targeting antibiotics. However, CiaH does not sense mucin to mediate this phenotype through signaling. While this work did not decipher the mechanism of this phenotype, it leaves room for further exploration as CiaRH is not the only locus associated with antibiotic resistance. There are many characterized pathways of antibiotic resistance in *S. pneumoniae* beyond CiaRH activity that could be explored. For example, changes in penicillin binding proteins (PBP), including at the level of post-transcriptional regulation, can lead to resistance to cell wall inhibitors (Hakenbeck et al., 1999; Peters et al., 2021). *S. pneumoniae* encodes six PBPs but none were significantly differentially regulated at the transcript level in our RNA-seq after exposure to MUC5AC. Future work to elucidate antibiotic sensitivity could explore changes in protein levels through a variety of methods including Western blot or proteomics.

Despite decades of work, defining alternative mechanisms of antibiotic resistance is an active area of research. Recent work leveraging transposon insertion sequencing (Tn-Seq) defined the *S. pneumoniae* regulon after exposure to 20 different antibiotics (Leshchiner et al., 2022). Comparing the regulon of cell wall-targeting antibiotics and MUC5AC may illuminate other mechanisms at play. For example, disruption of *fabT*, which controls fatty acid biosynthesis, is strongly downregulated by mucin and was identified as part of the regulon of every cell wall inhibitor tested (Leshchiner et al., 2022). Thus, new methods of defining antibiotic resistance mechanisms will generate new hypotheses for how mucin sensitizes *S. pneumoniae* to cell wall inhibitors.

Materials and methods

Strains and reagents

The bacterial strain *S. pneumoniae* TIGR4 was a gift from Marc Lipsitch (Harvard T.H. Chan School of Public Health). TIGR4 was originally isolated from the blood of a 30-year-old male and is highly virulent in a mouse infection model. The bacterial strain *S. pneumoniae* TIGR4Δ*ply* was a gift from Justin Thornton (Bryant et al., 2016b) (Mississippi State University). For general propagation and storage, bacteria were grown on tryptic soy with 5% sheep blood (TSB) agar plates overnight at 37 °C with 5% CO_2. Bacteria were cultured and maintained in THY broth. Erythromycin (Ery; 0.5 μg/mL), spectinomycin (Spc; 200 μg/mL), kanamycin (Kan; 50 μg/mL) and gentamycin (Gm; 40 μg/ml) was added to the medium for plasmids and strains with antibiotic resistance.

Minimum inhibitory concentration (MIC) assay

S. pneumoniae TIGR4 was grown on TSB agar overnight and liquid pre-cultures were inoculated in THY broth. After growth to OD ~0.4, the culture was diluted to OD 0.01 (approximately 10^7 colony-forming units (CFU)/mL) into THY broth supplemented with serially diluted antibiotic. The cultures were incubated at 37 °C with 5% CO_2 and the optical density was measured every 30 min in a Synergy H1 microplate reader (BioTek) for 12 h. The MIC was defined as the lowest concentration that prevented growth.

Antibiotic sensitivity assay

S. pneumoniae was grown on TSB agar overnight and liquid pre-cultures were inoculated in THY broth. After growth to OD ~0.4, cultures were diluted to OD 0.01 (approximately 10^7 colony-forming units (CFU)/mL) into THY broth supplemented with or without 0.25% mucin or 1mM IPTG. After 3 h of growth at 37 °C with 5% CO_2, antibiotic was added at the indicated concentration and samples were incubated for an additional 2 h. After 5 h of total growth, surviving CFU of *S. pneumoniae* were plated on TSB agar and enumerated the following day.

Mutant strain construction

To generate JB01, we first generated a marked deletion of *ciaH*. The up and downstream regions of *ciaH* and the *ermB* gene were amplified and followed by overlap extension PCR to create a

fusion gene product. The DNA fragment was amplified by PCR (Roche KAPA HiFi HotStart ReadyMix) and purified before transforming into *S. pneumoniae* to replace the *ciaH* gene with *ermB*.

We utilized published plasmids pPEPY-PF6-lacI and pPEPZ-Plac to place *ciaR* under an IPTG-inducible lac promoter (Keller et al., 2019). First, we amplified a region from pPEPY-PF6-lacI to insert *lacI*-gmR in the *prs1* locus of the Δ*ciaH* background. We then inserted *ciaR* into the pPEPZ-Plac plasmid behind the lac promoter and amplified this region to insert Plac-*ciaR-specR* into a region near SP_1935 that is transcriptionally silent (Keller et al., 2019). This yielded strain JB01 with the genotype lacI-gmR, Δ*ciaH*, Plac-ciaR-specR.

A full list of primers used is available in Table B.2. In each case, *S. pneumoniae* was transformed via stimulation with 100 ng CSP-2 (AnaSpec) before adding 1 ug of purified DNA fragments. Transformed mutants were isolated on TSB agar supplemented with the appropriate antibiotic.

RNA preparation for gene expression analysis

In brief, *S. pneumoniae* was grown on TSB agar overnight and liquid pre-cultures were inoculated in THY broth. After growth to OD ~0.4, cultures were diluted to OD 0.01 (approximately 10^7 colony-forming units (CFU)/mL) into THY broth supplemented with or without IPTG. After 5 h (unless otherwise noted) of growth at 37 °C with 5% CO_2, the samples were collected mid-log phase and pelleted at 16,000*g*. The supernatant was then removed, and the pellets were flash-cooled in liquid nitrogen and stored at −80 °C. Pellets were thawed on ice and resuspended in 25µL lysozyme buffer. Ready-Lyse Lysozyme (Biosearch Technologies) was added, and the samples were incubated at room temperature (RT) for 15 min. Total RNA was then extracted using the MasterPure Complete RNA Purification kit (Biosearch Technologies). Genomic DNA was removed using the Turbo DNA-free kit (Invitrogen). The samples were stored at -20 °C.

RT–qPCR analysis

A list of the primers used for RT-qPCR are listed in Supplementary Table B.1. First-strand complementary DNA (cDNA) was synthesized using the Protoscript II First-Strand cDNA Synthesis kit (New England Biolabs). The elimination of genomic DNA was confirmed by qPCR amplification on negative control samples that did not have reverse transcriptase during cDNA synthesis. 8 ng of cDNA was used as a template for RT-qPCR using the SYBR Green Master Mix

(Thermo Fisher Scientific) and performed in a Cycler 480 II Real-time PCR Machine (Roche). Forward and reverse primers were added at 3 µM each. Melting-curve analyses verified amplification of a single product. Gene expression changes were calculated based on mean change in the qPCR cycle threshold compared to *gyrB* or *16S* (ΔC_t) and are reported as $\log_2[FC] = \Delta C_t\_CM - \Delta C_t\_sample$. Each sample was analyzed with at least three technical replicates.

References

Bryant, J. C., Dabbs, R. C., Oswalt, K. L., Brown, L. R., Rosch, J. W., Seo, K. S., Donaldson, J. R., McDaniel, L. S., & Thornton, J. A. (2016). Pyruvate oxidase of Streptococcus pneumoniae contributes to pneumolysin release. *BMC Microbiology*, *16*(1), 1–12. https://doi.org/10.1186/s12866-016-0881-6

CDC. (2019). *Antibiotic resistance threats in the United States, 2019*. https://doi.org/10.15620/cdc:82532

Haas, W., Kaushal, D., Sublett, J., Obert, C., & Tuomanen, E. I. (2005). Vancomycin stress response in a sensitive and a tolerant strain of Streptococcus pneumoniae. *Journal of Bacteriology*, *187*(23), 8205–8210. https://doi.org/10.1128/JB.187.23.8205-8210.2005

Hakenbeck, R., Grebe, T., Zähner, D., & Stock, J. B. (1999). β-lactam resistance in Streptococcus pneumoniae: Penicillin-binding proteins and non-penicillin-binding proteins. *Molecular Microbiology*, *33*(4), 673–678. https://doi.org/10.1046/j.1365-2958.1999.01521.x

Huang, C. T., Chen, C. H., Chen, W. C., Wang, Y. T., Lai, C. C., Fu, P. K., Kuo, L. K., Chen, C. M., Fang, W. F., Tu, C. Y., & Ku, S. C. (2022). Clinical effectiveness of cefoperazone-sulbactam vs. piperacillin-tazobactam for the treatment of pneumonia in elderly patients. *International Journal of Antimicrobial Agents*, *59*(1). https://doi.org/10.1016/j.ijantimicag.2021.106491

Keller, L. E., Rueff, A. S., Kurushima, J., & Veening, J. W. (2019). Three new integration vectors and fluorescent proteins for use in the opportunistic human pathogen Streptococcus pneumoniae. *Genes*, *10*(5). https://doi.org/10.3390/genes10050394

Kohanski, M. A., Dwyer, D. J., & Collins, J. J. (2010). How antibiotics kill bacteria: From targets to networks. In *Nature Reviews Microbiology* (Vol. 8, Issue 6, pp. 423–435). https://doi.org/10.1038/nrmicro2333

Leshchiner, D., Rosconi, F., Sundaresh, B., Rudmann, E., Ramirez, L. M. N., Nishimoto, A. T., Wood, S. J., Jana, B., Buján, N., Li, K., Gao, J., Frank, M., Reeve, S. M., Lee, R. E., Rock, C. O., Rosch, J. W., & van Opijnen, T. (2022). A genome-wide atlas of antibiotic susceptibility targets and pathways to tolerance. *Nature Communications*, *13*(1). https://doi.org/10.1038/s41467-022-30967-4

Mascher, T., Heintz, M., Zähner, D., Merai, M., & Hakenbeck, R. (2006). The CiaRH system of Streptococcus pneumoniae prevents lysis during stress induced by treatment with cell wall inhibitors and by mutations in pbp2x involved in β-lactam resistance. *Journal of Bacteriology*, *188*(5), 1959–1968. https://doi.org/10.1128/JB.188.5.1959-1968.2006

Peters, K., Schweizer, I., Hakenbeck, R., & Denapaite, D. (2021). New insights into beta-lactam resistance of streptococcus pneumoniae: Serine protease htra degrades altered penicillin-binding protein 2x. *Microorganisms*, *9*(8). https://doi.org/10.3390/microorganisms9081685

Rogers, P. D., Liu, T. T., Barker, K. S., Hilliard, G. M., English, B. K., Thornton, J., Swiatlo, E., & McDaniel, L. S. (2007). Gene expression profiling of the response of Streptococcus pneumoniae to penicillin. *Journal of Antimicrobial Chemotherapy*, *59*(4), 616–626. https://doi.org/10.1093/jac/dkl560

Slager, J., Aprianto, R., & Veening, J.-W. (2019). *Refining the Pneumococcal Competence Regulon by RNA Sequencing*. https://doi.org/10.1128/JB

Speich, R., Imhof, E., Vogt, M., Grossenbacher, M., & Zimmerli, W. (1998). Efficacy, Safety, and Tolerance of Piperacillin/Tazobactam Compared to Co-Amoxiclav plus an Aminoglycoside in the Treatment of Severe Pneumonia. In *Eur J Ctin Microbiol Infect Dis* (Vol. 17). Springer-Verlag.

Vollmer, W., Blanot, D., & De Pedro, M. A. (2008). Peptidoglycan structure and architecture. In *FEMS Microbiology Reviews* (Vol. 32, Issue 2, pp. 149–167). https://doi.org/10.1111/j.1574-6976.2007.00094.x

Vollmer, W., Massidda, O., & Tomasz, A. (2019). The Cell Wall of Streptococcus pneumoniae. *Microbiology Spectrum*, *7*(3). https://doi.org/10.1128/microbiolspec.gpp3-0018-2018

Witten, J. (2019). *Understanding the selective permeability of biological hydrogels*. Massachusetts

Institute of Technology.

Acknowledgements

This work was supported by the Toxicology Training Grant T32-ES007020 (to J.B.), the NIH NIBIB under award R01-EB017755-07 (to K.R.), the Bill and Melinda Gates Foundation under award INV-041182 (to K.R.), and the National Institute of Environmental Health Sciences of the NIH under award P30-ES002109 (to the MIT Center for Environmental Health Science). We thank the MIT BioMicro Center for maintaining the RT-qPCR machine facility. We thank Ben Wang and Julie Takagi for feedback on the cloning experiments.

Figures

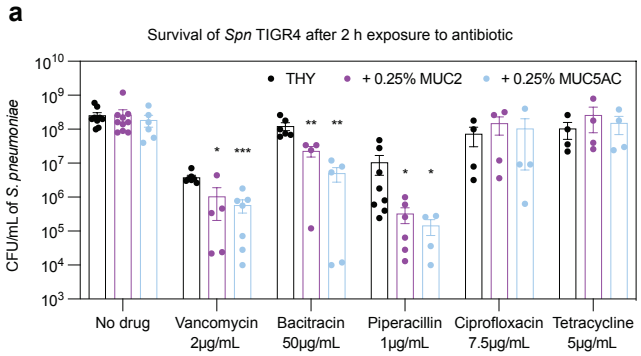

Figure B.1: Mucin sensitizes *S. pneumoniae* to cell wall-targeting antibiotics.

S. pneumoniae was grown for 3 h with or without 0.25% MUC2 or MUC5AC or until mid-log phase. *S. pneumoniae* was then treated with antibiotics at the concentration shown and survival was evaluated by plating CFUs after 2 h of treatment. Bars indicate mean ± s.e.m. with individual biological replicates shown.

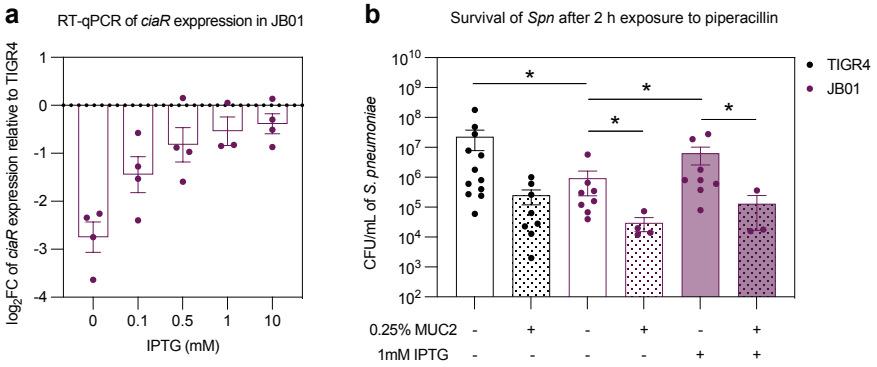

Figure B.2: Signaling through ciaRH does not mediate changes in piperacillin sensitivity after exposure to mucin.

(A) Expression of *ciaR* was measured after 5 h in TIGR4 and JB01 after exposure to different concentrations of IPTG by RT-qPCR and normalized to *gyrB*. Bars indicate mean ± s.e.m. with individual biological replicates shown. **(B)** *S. pneumoniae* was grown for 3 h with or without 0.25 % MUC2 or 1mM IPTG until mid-log phase. *S. pneumoniae* was then treated with piperacillin at 1µg/mL and survival was evaluated by plating CFUs after 2 h of treatment. **(A, B)** Bars indicate mean ± s.e.m. with individual biological replicates shown.

Supplementary Figures

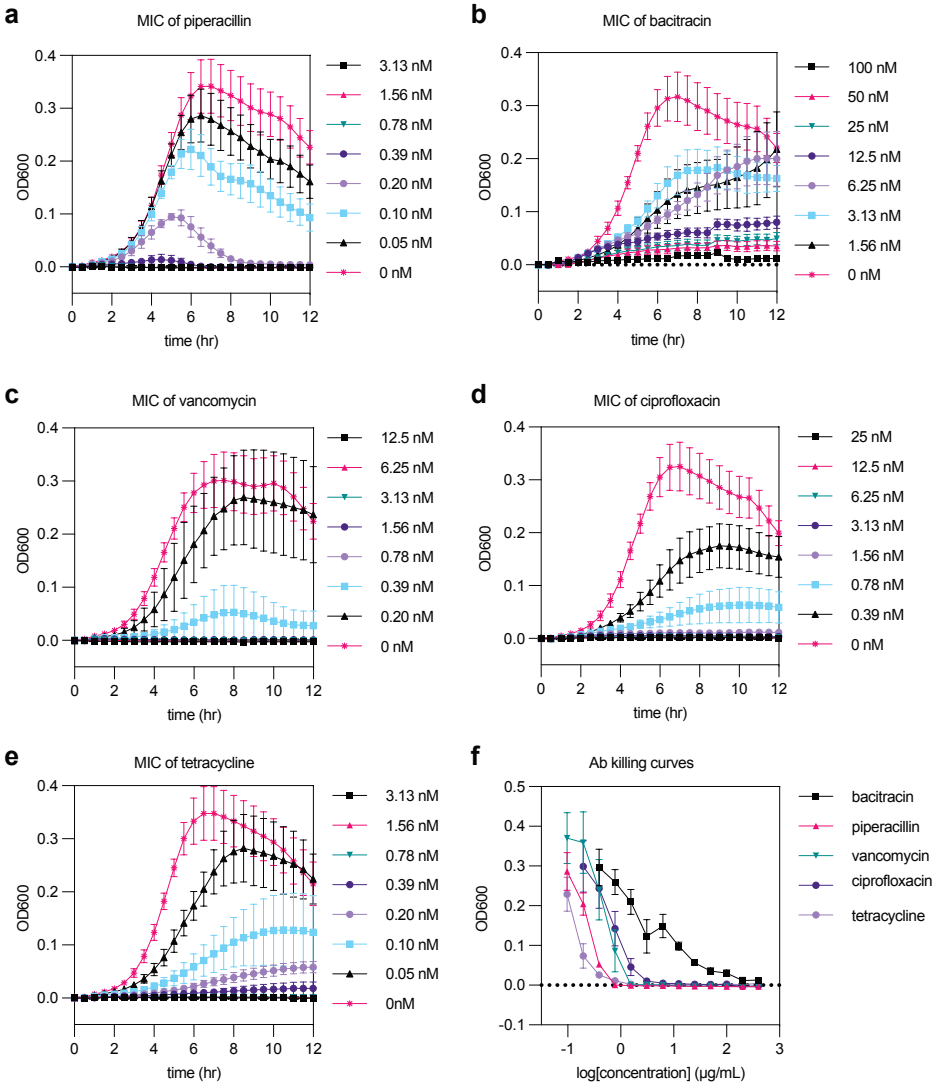

Supplementary Figure SB.1: Determination of minimum inhibitory concentration (MIC) of antibiotics representing multiple classes.

(A-E) The MIC of each antibiotic was determined by measuring the growth after exposure to a 7-point dilution series of the antibiotic indicated. Data are the mean OD value at 600 nm ± s.e.m. for n ≥ 4 biological replicates**. (F)** Antibiotic killing curves at a 6 h timepoint reveal differences in potency and killing dynamics.

Supplementary Tables

Primer name	Purpose	Primer sequence 5'>3'
ermB_F	ciaH KO	GGAAATAAGACTTAGAAGCAAAC
ermB_R	ciaH KO	CCAAATTTACAAAAGCGACTC
ciaH_up_F	ciaH KO	CCAATTCCTAGCTCATCAAGCAACT
ciaH_up_ermB_R	ciaH KO	GTTTGCTTCTAAGTCTTATTTCCACTAAAGTCATC CGCATACCATGTT
ermB_ciaH_down_F	ciaH KO	GAGTCGCTTTTGTAAATTTGGGTGAAGATTG CCATTCAGACACCAT
ciaH_down_R	ciaH KO	GAATGATGGATGACGCTAGCACC
prs1_F	check integration of pPEPY	GAAACAGATTTTATCTGCTTTATATCG
prs1_R	check integration of pPEPY	ATCAGAAAGCAAACTAGAAAGTTATG
ciaR_for_BglII	amplify ciaR with BglII site	GCGCAGATCTAGGAGGCAAATATGATAAAAAT CTTATTGGTTGAGG
ciaR_rev_BamHI	amplify ciaR with BamHI site	GAGCGGATCCCTGAACATCTTTTAAAAGATACC
pPEPZ_seq_F	check integration of pPEPZ	TGATAGGGTGGTCTCCGATCG
pPEPZ_seq_R	check integration of pPEPZ	CCAGATATGATTGCCCTCTTGTTC
ciaR-F	RT-qPCR	TGACTGCCAAGGAAAGTTTG
ciaR-R	RT-qPCR	GTTTGAGAAGGGCCTGAATC
gyrB-F	RT-qPCR	CCAATCCTAGAAGCTGGTTATGT
gyrB-F	RT-qPCR	CACCCGGCTGGATATATTCTTT

Supplementary Table B.1: Primers used in this study.

Sequences for each primer are shown. Sequences shown in blue overlap with the gene of interest and sequences that are underlined represent a restriction site.